University of Alberta

Characterization of the Bicarbonate Transport Metabolon: Interaction Between Carbonic Anhydrase II and Bicarbonate Transporters

By

Heather Lynn McMurtrietrie ©

A thesis submitted to the Faculty of Graduate Studies and Research in partial fulfilment of the requirements for the degree of

Master of Science

Department of Biochemistry

Edmonton, Alberta, Canada
Fall 2006

Your file Votre référence
ISBN: 978-0-494-22320-8
Our file Notre référence
ISBN: 978-0-494-22320-8

Abstract

We examined the role of glutamate in regulating CAII/bicarbonate transporter (BT) interaction, a complex that has been called the bicarbonate transport metabolon. Binding of CAII, the enzyme that catalyzes the conversion of CO_2 into HCO_3^-, to the C-terminus of a BT enhances bicarbonate transport. We expressed the C-terminal cytoplasmic tails of the BTs AE1 and SLC26A6 as GST fusion proteins. Using a microtitre dish binding assay we measured CAII binding to AE1Ct and SLC26A6Ct. Glutamate disrupted the interaction between CAII and BTs. The affinity of CAII for AE1 and SLC26A6 was decreased by 110 ± 17% and 85 ± 2%, respectively. The glutamate effect was specific as gluconate, leucine and aspartate did not affect CAII/BT binding affinity. Glutamate did not affect CAII catalytic activity. This thesis describes a novel mechanism for regulation of the bicarbonate transport metabolon and an approach for identifying more sites of regulation.

Acknowledgements

I would like to thank Dr. Joe Casey for his guidance, support and interest in my professional and personal development. I entered the University of Alberta as a Chemist from a small university with small hopes and dreams. I now leave the university as a Biochemist with a wide-open future.

Also, I would like to sincerely thank all of the members of the Casey lab who day after day provided me with joy and laughter. In particular, Dr. Bernardo Alvarez and Dr. Patricio Morgan have served as wonderful mentors both in the lab and in life. I appreciate all of the extra time they took to teach me how to work at the bench. Danielle Johnson, Daniel Sowah, Anita Quon and Carmen Rieder have been great companions and lab mates. Thank you especially to Haley Shandro, my lab twin who has stuck by me through thick and thin. I will never forget the time that we have shared together both in the lab and out.

Beyond my lab there have been many people who have helped me in my project. My committee members, Dr. Marek Michalak and Dr. Howard Young, have been very supportive of my progress throughout my degree. Dr. Marek Duszyk who not only acted as my external committee member but also collaborated with us on a project. Also, thank you to all those people around the department that helped me with new techniques or the use of a piece of equipment.

I would like to acknowledge the Canadian Institute of Health Research Strategic Training Initiative in Membrane Proteins and Cardiovascular Disease for their financial support.

I am so grateful for the endless support of my family, especially Mom, Dad and Ian, and my wonderful boyfriend, Andrew.

Your constant love and encouragement has been my guiding light.

Table of Contents

List of Figures

List of Equations

Abbreviations

ACTZ, Acetazolamide

AE, anion exchanger

ATP, adenosine triphosphate

BSA, bovine serum albumin

BT, bicarbonate transporter

CA, carbonic anhydrase

CAB, CAII consensus binding motif

CD, circular dichroism spectroscopy

CF, cystic fibrosis

CFTR, cystic fibrosis transmembrane conductance regulator

CFTR-g_{Cl-}, CFTR Cl^- conductance

CFTR-g_{HCO3-}, CFTR HCO_3^- conductance

Ct or C-terminus, carboxyl-terminal

dRTA, distal renal tubular acidosis

EAAT, excitatory amino acid transporter

E. coli, Escherichia coli

ELISA, enzyme-linked immunosorbent assay

GSH, reduced glutathione

GST, glutathione-*S*-transferase

GST.AE1Ct, GST fusion of AE1Ct

GST.NBC3Ct, GST fusion of NBC3Ct

GST.SLC26A6Ct, GST fusion of NBC3Ct

HEK, human embryonic kidney

HPLC, high performance liquid chromatography

HRP, horseradish peroxidase

IBD, Institute for Biomolecular Design

IPTG, isopropylthiogalactoside

Kd, dissociation constant

kDa, kiloDalton

LB, Luria-Bertani

MS, mass spectrometry

NBC, sodium bicarbonate co-transporter

NBC3Ct, Ct domain of NBC3

NHE, sodium proton exchanger

Nt or N-terminus, amino-terminal

pI, isoelectric point

PVDF, polyvinylidene difluoride

SDS, sodium dodecyl sulfate

SDS-PAGE, SDS-polyacrylamide gel electrophoresis

SLC, solute carrier family

STAS, sulfate transporters and bacterial anti-sigma factor antagonists

TFA, trifluoroacetic acid

TMs, transmembrane segments

Chapter 1

Introduction

1.1 Maintenance of pH homeostasis

1.1.1 Balance of acids and bases to maintain intracellular pH

The maintenance of physiological intracellular pH (pH_i) is critical for sustaining cellular life. Cellular proteins are pH dependent for maintenance of structure and activity [1-3]. Not only will large changes in pH alter the structure of a protein due to a shift in amino acid interactions, but also smaller shifts in pH_i can regulate cellular functions [1]. Most mammalian cells maintain a steady-state pH_i of 7.1 - 7.2 despite the negative resting membrane potential and the generation of H^+ through metabolic activity [1].

pH can be regulated by the removal of H^+ from the cell or alternatively, the influx of a natural buffer into the cell to neutralize the pH. There are transporters and channels located in the plasma membrane involved in both processes. The removal of H^+ from the cytosol is mediated by the Na^+/H^+ exchanger proteins (NHE) [4, 5], and the addition of the intracellular buffer, the alkaline molecule HCO_3^-, is mediated by the family of bicarbonate transporters. When HCO_3^- is moved into the cytosol it interacts with free H^+ and through the activity of the enzyme carbonic anhydrase will reversibly convert to CO_2 and H_2O thereby effectively removing free H^+ and increasing cytosolic pH.

The NHEs and the bicarbonate transporters work together in multiple tissues throughout the body, in particular in cardiomyocytes [6], the pancreas [7], and the kidney [8, 9]. However, it is the process by which the bicarbonate transporters neutralize cytosolic pH that is important to this study.

Although there is evidence to suggest that bicarbonate transporters are sensitive to pH changes [10], there is speculation that another membrane protein,

the cystic fibrosis transmembrane conductance transport regulator (CFTR), aids in the regulation of bicarbonate transporter activity. As inhibition of CFTR is often linked to a dysfunction in pH regulation, CFTR may regulate the other pH equilibrating proteins.

1.1.2 Bicarbonate transport and CFTR

CFTR and bicarbonate transporters are located in many of the same tissues, and there is overlap between their substrates. CFTR is predominantly a Cl^- channel, but many of the mutations in CFTR affect HCO_3^- conductance with no effect on Cl^- conductance [11]. CFTR does play a role in pH homeostasis, although typically in the extracellular environment [12]. HCO_3^- secretion from epithelial cells can reach a concentration as high as 140 mM in the lumen [13]. This extracellular secretion of HCO_3^- is critical for protecting the epithelial cells that constitute the alveoli, where gas exchange occurs. For protection, a moist mucosal layer covers the airway tissue and filters the air before reaching the epithelial cells [14].

Since CFTR is not conventionally known as a HCO_3^- channel, it is logical that another bicarbonate transporter could associate with CFTR and work in concert to maintain proper HCO_3^- secretion. Preliminary studies of the sweat gland and small airways suggest that CFTR is the only protein conducting HCO_3^- because HCO_3^- conductance is cAMP and ATP dependent [11, 14], which are characteristics of CFTR and not bicarbonate transporters. However, the flux ratio of HCO_3^-/Cl^- through CFTR is not high enough to account for the total HCO_3^- flux [15] since Cl^- permeability is between four to eight times higher than HCO_3^- [16]. Furthermore, HCO_3^- transport is disulfonic stilbene (DIDS) sensitive [11],

which is a known inhibitor of SLC26A6 [15] and not CFTR. It is more likely that the bicarbonate transporter in sweat gland has yet to be identified since many other CFTR expressing cells often express bicarbonate transporters. Although the sweat gland is a good model experimental system for studying cystic fibrosis (CF), it is the pancreas that has shed the most insight into the regulation of HCO_3^- transport in CF patients.

It is the role that bicarbonate transporters and CFTR play in maintaining the pH of pancreatic juice by HCO_3^- secretion that is most important for CF research [7, 17]. pH regulation in the lumen of the pancreas is extremely important for regulating the digestive enzymes secreted from the pancreas. These enzymes are activated in alkaline pH. At time of digestion there is an increase in HCO_3^- secretion, while at rest there is reabsorption of HCO_3^- to acidify the pancreatic juice thereby deactivating the digestive enzymes [7]. There are a number of transporters and channels that work together to regulate the pH in the pancreas. The bicarbonate transporter, pNBC1, located in the basolateral membrane of secretory duct cells assures an influx of HCO_3^- into the pancreatic duct cells to maintain a constant store of HCO_3^- available for secretion into the lumen [7]. Secretion of HCO_3^- into the pancreatic lumen occurs via CFTR and/or the bicarbonate transporters SLC26A6 and SLC26A3 [7, 15] (Fig 1.1).

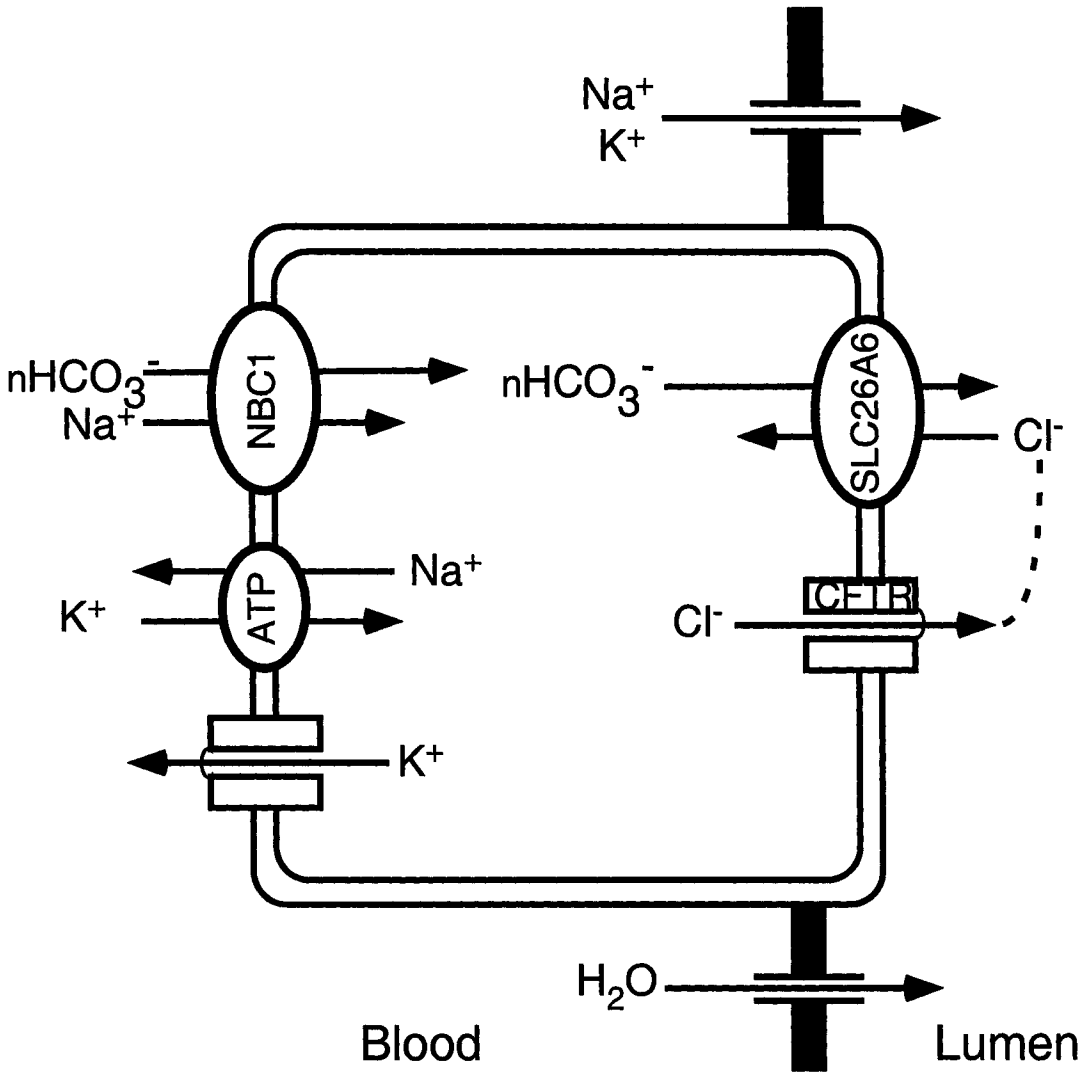

Figure 1.1: Model of HCO_3^- secretion by the pancreatic duct cell.
HCO_3^- is recruited from the blood into the pancreatic duct cell by pNBC1, which is located in the basolateral membrane [7]. It is then secreted into the lumen of the pancreatic duct via SLCA26A6 (or SLC26A3) [7, 15, 16]. The Cl^- channel CFTR aids in HCO_3^- secretion by providing the Cl^- used for HCO_3^- exchange through SLC26A6. Many other transporters and channels work to maintain ionic concentrations within the cell [16]. Figure is a modified version of that prepared by Hug and Bridges [16].

1.1.3 Role of bicarbonate transporters

Bicarbonate transporters are essential for maintaining whole body and cellular pH homeostasis [18]. Bicarbonate is a natural pH buffer and it is the responsibility of the bicarbonate transporters to regulate the amount of buffer available to the cell [18]. Bicarbonate transporters are ubiquitously expressed throughout the body. Their function can be categorized into two essential functions, HCO_3^- reabsorption and maintenance of pH_i homeostasis. Our body needs to reabsorb HCO_3^- to maintain the body's pH balance and most HCO_3^- reabsorption occurs in the kidney. The overall pH balance of the body is maintained by balancing the pH levels in cells and body fluid. This leads to the second function of bicarbonate transporters, maintaining pH_i homeostasis. Tissues such as heart, lung, eye, intestine, pancreas, and stomach are of interest to bicarbonate transport research since there are detrimental effects associated with bicarbonate transport dysfunction in these tissues.

1.2 Bicarbonate transporter family

1.2.1 Anion exchangers; role and regulation

Bicarbonate transporters are divided into three separate families: the classical Cl^-/HCO_3^- exchangers (AE), Na^+-coupled transporters (NBC), and the novel SLC26A family [19] (Fig. 1.2). AEs exchange bicarbonate for chloride with a 1:1 stoichiometry, resulting in an electroneutral transfer of anions across the plasma membrane [19]. The well-known Cl^-/HCO_3^- exchanger, anion exchanger 1 (AE1, SLC4A1 or band 3) serves as a model bicarbonate transporter to study

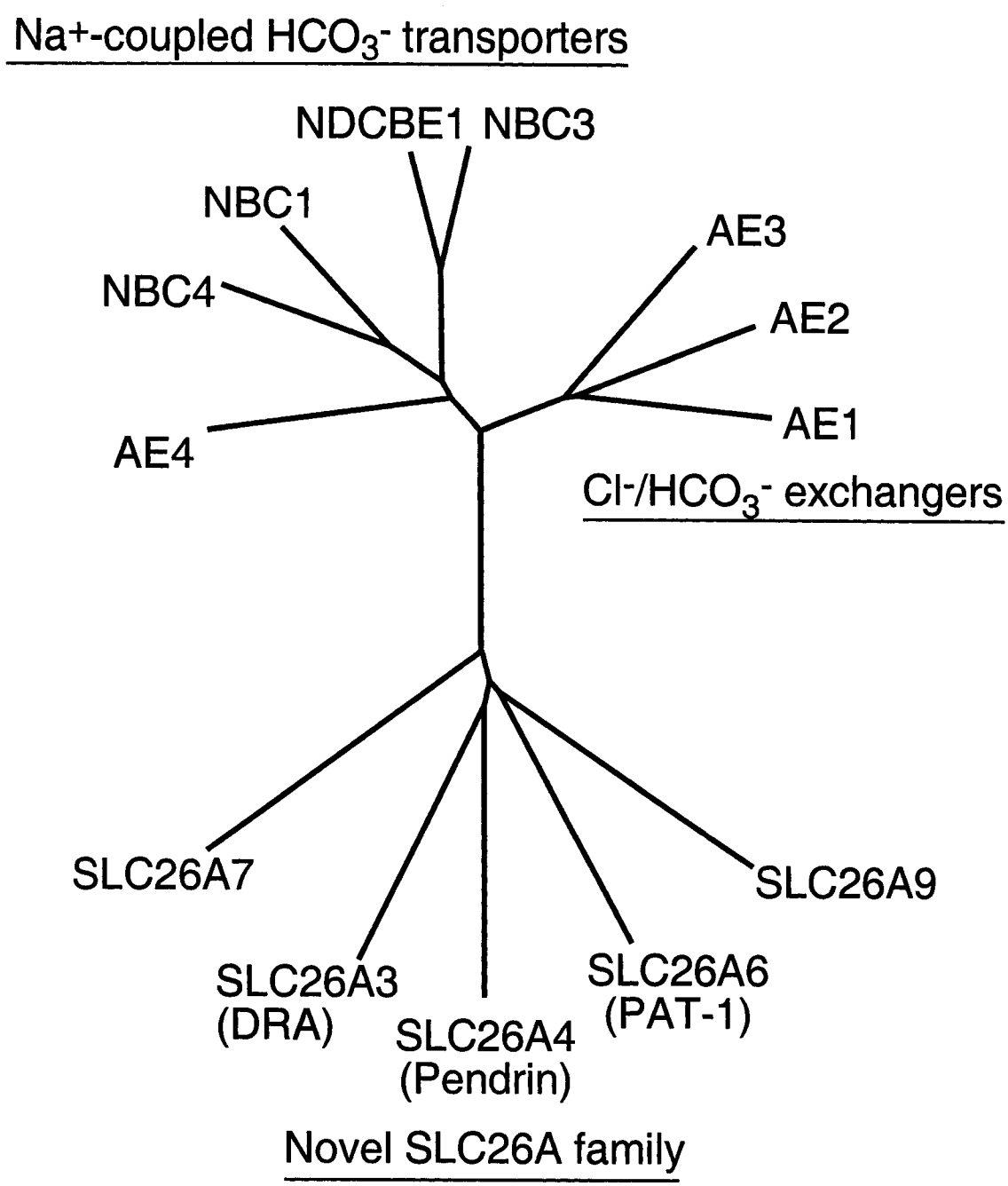

Figure 1.2: Phylogenetic relationships of human bicarbonate transport proteins.

Amino acid sequences for human bicarbonate transporters were analysed with the program Phylip on the ClustalW website [20]. Plotted are evolutionary relationships for the transporters, where the length of the line is proportional to the degree of sequence similarity between the proteins. Separate lines represent divergence from common ancestors. The names of the three individual families of the human bicarbonate transporter superfamily are underlined (Cl^-/HCO_3^- exchangers: AE1 [21]; AE2 [22]; AE3 [23], Na^+-coupled bicarbonate transporters: NBC1 [24, 25]; NBC3 [26]; NBC4 [26]; AE4 [27]; and NDCBE1 [28], and Novel SLC26A transporters: SLC26A3 [29]; SLC26A4 [30]; SLC26A6 [31]; SLC26A7 [32, 33]; and SLC26A9 [32]).

general trends across the larger family of bicarbonate transporters.

The AE family (Fig. 1.2) has three isoforms that share 65% amino acid sequence identity [19, 34]. AEs exchange bicarbonate for chloride with a 1:1 stoichiometry, resulting in an electroneutral transfer of anions across the cell membrane. AE1 is found in plasma membrane of erythrocytes and a truncated version of AE1 is found on the basolateral surface of renal α-intercalated cells [35]. Intercalated cells are located in the distal convoluted tubule, connecting tubule, cortical collecting duct and the medullary collecting duct [36]. Intercalated cells are loosely subclassified based on their acid secretion (α-intercalated) or acid absorption (β-intercalated) properties. More specifically, localization of the H^+-ATPase at the apical surface promotes acid secretion [36]. Bicarbonate transporters aid the intercalated H^+-ATPase in maintaining acid/base levels by controlling the HCO_3^- concentration in the human body.

AE2 is the most widely expressed AE isoform, present in nearly all human tissues [18]. AE3 is found in the brain [37], heart [38], retina [39] and other excitable tissues [18]. Although located in different tissues, all of the AE proteins share a similar structure consisting of three major domains [19] (Fig. 1.3). A topology model of AE1 has been proposed and has served as a reference for the predicted topology models of other members of the bicarbonate transporter superfamily [40] (Fig. 1.3). The amino-terminal cytosolic domain is important for protein-protein interactions with cytosolic proteins, metabolic enzymes, and cytoskeletal elements [41]. The carboxyl-terminal membrane domain consists of 12 transmembrane segments [42] and is responsible for anion transport [43]. The C-terminal cytosolic tail can be considered a third domain as it folds

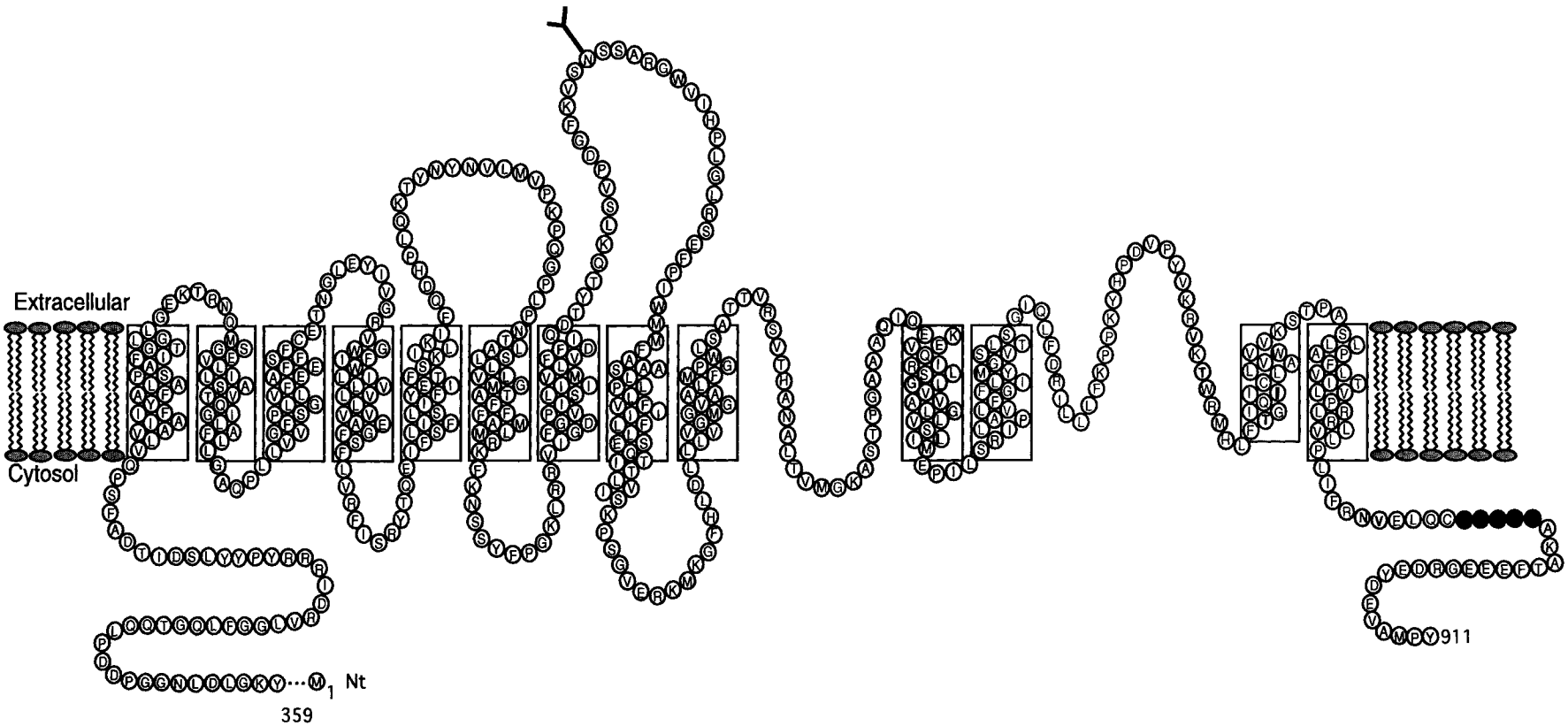

Figure 1.3: Topology model of AE1, an example of a bicarbonate transporter.
The AE1 topology model previously reported [40] shows three domains. The N-terminus and C-terminus are cytosolic and the transmembrane domain contains 12 – 14 TMs, with possible re-entrant loops between TMs 9 and 10 and TMs 11 and 12. The topology model was created from cysteine-scanning mutagenesis [40, 44, 45] and sulfhydryl-specific chemistry analysis data [40] combined with proteolytic mapping [46] and glycosylation-scanning mutagenesis [42, 47]. Surface accessible residues were detected by labelling of cysteine mutants with biotin maleimide. Biotin maleimide labelling revealed two large aqueous-accessible regions separated by two transmembrane segments and an intervening extracellular loop [40]. The identified carbonic anhydrase II binding motif [48] is highlighted in red.

independently and has a separable function. The C-terminal tail contains the binding site for CAII [48, 49], forming the basis for the intracellular bicarbonate transport metabolon.

1.2.2 Na^+/HCO_3^- co-transporters; role and regulation

The second family of the bicarbonate transporter superfamily contains the sodium-coupled bicarbonate transporters (Fig. 1.2) [19]. Na^+/HCO_3^- co-transporters (NBC) co-transport sodium and bicarbonate across the plasma membrane with either an electroneutral (NBC3) or electrogenic (NBC1, NBC4) mechanism (2/3 HCO_3^-:1 Na^+). All NBC isoforms are expressed in the kidney indicating they play a key role in whole body pH homeostasis [18]. NBCs are also located in heart, skeletal muscle, and parts of the intestinal tract. Phylogenetic analysis groups AE4, which is less genetically similar to the AE family than to the NBC family, with the NBCs [27], and suggests that it acts through a Na^+-dependent mechanism.

The NBC1 (SLC4A4, NBCe1) has wide tissue distribution. Splicing variants are located in the basolateral membranes of proximal tubules, pancreas, heart, eye, lung, testis, and the digestive system [50]. Splicing variant NBC1a mediates HCO_3^- efflux into the blood resulting in 80% of renal HCO_3^- reabsorption [51]. Defects in human NBC1a are associated with proximal renal tubular acidosis [52], a deficiency in HCO_3^- re-uptake in the proximal tubule leading to deficient urinary acidosis. The mRNA of splicing variant NBC1b, which varies from NBC1a only in the sequence of 61 amino acids in the C-terminus, was first identified in the pancreas [53, 54]. NBC1b has greater tissue

distribution and is likely the NBC variant that affects vision and cardiac hypertrophy [18].

The electroneutral NBC3 (SLC4A7, NBCn1) has tissue specific distribution. It is most commonly located in apical membrane of α–intercalated cells [55, 56] however it is also located in the basolateral membrane of β–intercalated cells [56-58] of the thick ascending limb of the loop of Henle in the kidney. The location of NBC3 shows its importance in HCO_3^- reabsorption in the kidney. Its location in the distal part of the nephron indicates that the HCO_3^- reabsorption by NBC3 is likely very precise. As the bulk of HCO_3^- absorption occurs in the proximal tubule, NBC3 is present in the distal tubule to tweak the final body pH, alkalinizing the body by reabsorbing HCO_3^- in the α-intercalating cells and acidifying when necessary by secreting HCO_3^- through the β-intercalating cells. The fine-tuning of body pH would require specific regulation of NBC3. NBC3 is upregulated by chronic metabolic acidosis [59], the depletion of K^+ [60] and the presence of NH_4^+ [61]. Multiple modes of NBC3 regulation likely exist because of the role that NBC3 plays in fine-tuning HCO_3^- levels.

NBC3 is also located in the heart [62], eye [63], and skeletal muscle [64]. The main role of NBC3 in tissues other than the kidney is pH_i regulation. For instance, half of the pH recovery in sarcolemmal vesicles produced from rat muscle is mediated by a HCO_3^- -dependent pathway (NBC3) [64]. Cells in the body use HCO_3^- transport as a means of ensuring intracellular pH homeostasis [51], emphasizing the importance for studying bicarbonate transporters.

1.2.3 Novel bicarbonate transporters (SLC26A family); role and regulation

The third branch of the bicarbonate transporter phylogenetic tree shows members of the SLC26A family that are known to transport bicarbonate (Fig. 1.2) [19]. The SLC26A anion transport gene family [65], also mediates anion exchange at the plasma membrane of mammalian cells. The family is comprised of eleven genes, SLC26A1-A11, which transport Cl^-, SO_4^{2-}, OH^-, HCO_3^-, I^-, oxalate and formate anions with different preferences [66-71]. Thus far SLC26A3 [69], SLC26A4 [66], SLC26A6 [31], SLC26A7 [32, 33] and SLC26A9 [32] have been reported as Cl^-/base (HCO_3^- and OH^-) exchangers (Fig. 1.2). Due to sequence similarity, SLC26A8 could also be a Cl^-/base exchanger in the testis [32, 72].

The novel SLC26A6 (PAT-1), however, is most physiologically relevant to the present study. SLC26A6 is a Cl^-/base (HCO_3^- or OH^-) exchanger [73, 74]. The stoichiometry by which the exchange occurs is still under debate, however initial reports indicate an electrogenic exchange of 2 HCO_3^- to 1 Cl^- [15, 71]. SLC26A6 is expressed in the heart [74], lung [31], duodenum [73], pancreas [75], stomach [76], kidney [77-79], brain and liver [79]. CFTR is located in many of the same tissues and physically interacts with the STAS domain of SLC26A6 through the CFTR R domain[80]. The STAS domain is a conserved region in the C-terminal tail of SLC26A bicarbonate transporters [81]. Interestingly the STAS domain is also found in bacterial anti-sigma factor antagonists and was thus named for sulfate transporters and bacterial anti-sigma factor antagonists [81, 82]. CFTR and SLCA26A6 also interact functionally [75, 80, 83-85] with speculation that

CFTR activates Cl^-/OH^- exchange in SLC26A6 [80] and activation of CFTR by the SLC26A6 STAS domain [80, 81].

Research has already begun into the regulation of SLC26A6. PKC stimulation decreases anion secretion in pancreatic cells [86], which corresponds to a decrease in SLC26A6-mediated HCO_3^- secretion upon PKC stimulation in HEK293 cells [81]. Given that CFTR and SLC26A6 co-localize in many tissues and functionally interact, it is likely that there is some feedback mechanism by which CFTR regulates SLC26A6 or vice-versa. However, the exact mechanism for this regulation remains unclear. The activity of SLC26A6 is also regulated by the HCO_3^- catalyzing enzyme CAII [81].

1.3 Carbonic anhydrase family

1.3.1 Role of carbonic anhydrase

Carbonic anhydrases (CA) are zinc metalloenzymes that catalyze the reversible reaction of: $CO_2 + H_2O \leftrightarrows HCO_3^- + H^+$ [87]. There are currently 14 CA isoforms identified [88-90]. CAII, one of the most efficient biological catalysts (turnover rate of 10^6 s^{-1} at 37°C [91]), uses a zinc-activated hydroxide ion in the active site. The metal ion stabilizes the highly reactive hydroxide ion, thereby ensuring that the nucleophile (the zinc-hydroxide complex) is available for rapid catalysis.

CA isoforms differ in their cellular localization. For example, CAI and II are cytosolic while CAV localizes to mitochondria [18, 92, 93]. Uniquely, CAIV is anchored to the extracellular surface via a glycosyl phophatidyl inositol (GPI) anchor. Similarly, CAIX, XII, and CAXIV are anchored to the extracellular

surface, but via a transmembrane protein anchor. CA isoforms are broadly expressed throughout the body, with similarity to the broad BT expression [94]. As for bicarbonate transporters, tissues tend to have multiple isoforms of CA [94]. For example, in erythrocytes CAI and CAII are both present in the cytosol and CAIV is bound to the extracellular membrane [49, 95]. Interestingly, in the heart only extracellular CA isoforms CAIV [96, 97], CAIX and CAXIV [98] have been identified.

Although CAI is the dominant isoform in the erythrocyte, the more catalytically active isoform, CAII, accounts for the majority of activity in erythrocytes. CAII and CAIV also work in concert in the kidney to regulate acid-base balance [88]. CAII catalyzes the hydration of carbon dioxide in the cytoplasm and CAIV catalyzes the reverse reaction on the extracellular surface of the plasma membrane. Cytosolic CAII comprises about 95% of carbonic anhydrase activity in kidney cells. The remaining 5% is largely due to the activity of the membrane bound CAIV [99]. CAII and CAIV are the focus for this discussion since they have been identified to be a part of one or more metabolons. The remaining CA isoforms are still under investigation for their role in bicarbonate transport metabolons.

1.3.2 Regulation of carbonic anhydrase

The Zn(II) ion located at the base of the carbonic anhydrase active site is essential for catalytic activity [100-104] (Fig. 1.4 A). This creates a target for inhibition of the enzyme. Currently there are two types of CA inhibitors, the metallo-complexing anions and the unsubstituted sulfonamides, which both bind to the Zn(II) ion [105]. Sulfonamide inhibitors are more potent than the

A

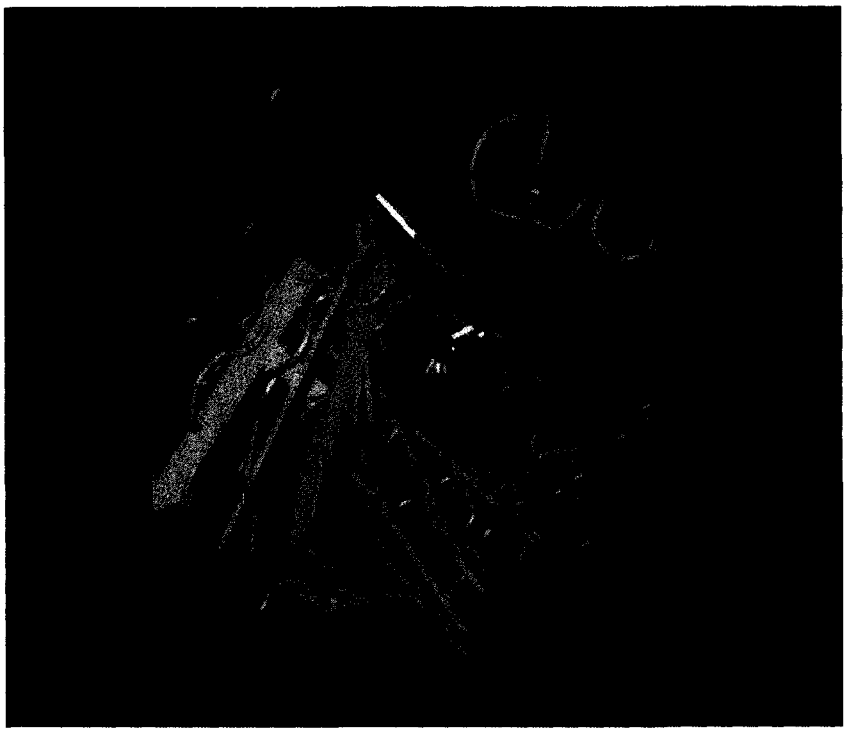

B

NBC3:	$_{1126}$TKRELSWLDDLMPESKKKKEDDKKKKEKEEAERMLQ
AE1:	$_{878}$RNVELQCLDADDAKATFDEEEGR----------DEYDEVA
SLC26A6:	$_{538}$ALKQRCGVDVDFLISQKKKLLKKQEQLKLKQLQKEEK

Figure 1.4: X-ray crystal structure of CAII and the CAII binding motif in the bicarbonate transporters C-terminal tail.
A, An X-ray crystal structure that was previously published [106] was rendered by CND3 version 4.1 program produced by the National Centre for Biotechnology Information. The N-terminal sequence (highlighted in yellow) is exposed to the surface and contains five essential histidine molecules for bicarbonate transporter binding [107]. B, The C-terminal sequences of human NBC3, AE1 and SLC26A6 contain the CAII binding (CAB) motif (underlined). The CAB motif is one hydrophobic amino acid followed by four amino acids, two of which are acidic [108], and is conserved in most bicarbonate transporters.

metallocomplexing anions as there are several points of contact within the active site [105]. The relationship between the Zn(II) atom in the active site of CAs and sulfonamide-containing compounds can prove useful in designing drugs, and also for purification of CAs by immobilizing the enzyme on the resin.

Much information is available regarding CA inhibition, while little is known about CA activation. Initially there does not appear to be a need for CA activators since CAII is one of the most active enzymes known [100, 102, 103, 109] and several other isoforms (CAIV, CAV, CAVII and CAIX) demonstrate extremely high activity [105]. However, among the 14 known isoforms two display moderate catalytic activity, three isoforms display low catalytic activity and three isoforms are acatalytic [105]. In addition, there are severe physiological and pathophysiological disorders associated with the underactiviation of CAs [105, 110-114]. X-ray crystallographic data aided in identifying CA activators and solved the issue of how they interact with the enzyme. CA activators are molecules that bind to the entrance of the enzyme active site and aid in the rate limiting step of electron transfer from the H^+ to the OH^- in a water molecule sitting at the active site [105]. Understanding the process by which these small molecules can enhance CA activity may provide evidence for natural activators existing in mammalian cells.

Interestingly, evidence suggests that CAII is also activated *in vivo* by association with AE1. This was demonstrated when di-/tri- and tetrapeptides expressing the C-terminal AE1 amino acid sequence improved CAII activity [115]. However, binding of the peptides did not affect CAI or CAIV activity. This would be expected since CAI does not bind to AE1 [48] and CAIV is extracellular and would not have access to the C-terminus of AE1. These results

indicated that AE1 was both a bicarbonate transporter and a CAII activator [115] and perhaps could activate other CAs. It would be interesting to study the effect of the extracellular loop of AE1 on CAIV because they also physically interact [94]. This evidence is important for validating the functional relationship between CAII and bicarbonate transporters in what is referred to as the bicarbonate transport metabolon.

1.4 The bicarbonate transport metabolon

1.4.1 A metabolon

Bicarbonate transporters are limited by how quickly they are able to transport substrate and also by the amount of available substrate. The enzyme family of carbonic anhydrases (CA) catalyzes the hydration of CO_2 to yield HCO_3^- and one proton and thus provides the substrate for bicarbonate transporters. To channel HCO_3^- more efficiently from the transporter to the enzyme, or vice-versa, the bicarbonate transporter and CA are located in close proximity to one another by a physical interaction [108, 116, 117]. This complex of transporter and enzyme has been termed a transport metabolon. The classic example of the bicarbonate transport metabolon is the interaction between the C-terminus of AE1 and the N-terminus of CAII [48, 49, 107]. Upon disruption of this interaction there is a 60% reduction in transporter activity [108]. An interaction between SLC26A6 and CAII has also been reported [81].

1.4.2 Discovery of the bicarbonate transport metabolon

The first HCO_3^- transport metabolon reported was between CAII and AE1 [49, 117]. Several lines of evidence demonstrated an association of the two proteins. Firstly, tomato lectin will bind the carbohydrate on AE1 and cause clustering of the protein in the plane of the erythrocyte membrane. Interestingly, in tomato lectin treated erythrocyte membranes, immunofluorescence showed that CAII clustered on the cytosolic surface in a pattern very similar to AE1, indicating co-localization [49]. More direct evidence for an AE1/CAII association was the coimmunoprecipitation of CAII with AE1, when solubilized from erythrocyte membranes [49]. Finally, a glutathione-*S*-transferase (GST) fusion protein of the terminal 33 amino acids of the C-terminus of AE1, but not GST alone, interacted with CAII with high affinity in both GST pull-down assays and in a solid phase microtitre dish binding assay [49]. Taken together this data showed that CAII and AE1 interact with high affinity in the erythrocyte membrane.

Further studies revealed the nature of the CAII/AE1 interaction. The pH dependence of CAII/AE1 interaction suggested a requirement for electrostatic interactions [49]. Acidic regions of the AE1 C-terminal region were the likely candidates for the CAII binding site (Fig. 1.4 B). This hypothesis was borne out by peptide competition assays, a sensitive microtitre binding assay, and functional assays that tested the activity of AE1 mutated by truncation or point mutations at the Carboxyl-terminal binding sequence [48]. When the acidic region D887ADD was removed from the C-terminal region, binding of CAII was lost [48]. When mutating the motif to DANE, the analogous motif from AE2, binding of CAII was retained indicating that AE2 was also capable of CAII binding [48]. Further analysis demonstrated that AE3 also bound CAII [118].

The motif for CAII binding was thus identified as a hydrophobic residue followed by four residues, at least two of which are acidic (Fig. 1.4 B). This motif has been found in the C-terminus of all examined bicarbonate transporter sequences, except SLC26A3 (DRA) [108].

Since AE1, AE2 and AE3 have an acidic CAII binding site it was reasoned that CAII would contain a corresponding basic region that binds AE. Truncation mutations of the amino-terminal region of CAII localized the binding region to a basic patch in the first 17 amino acids [107]. Point mutation analysis confirmed that CAI, which lacks five histidine (His) residues in the first 17 amino acids of the N-terminus, did not bind AE1 [107]. These five His residues are the major differences between CAI and CAII. X-ray crystallography revealed that the N-terminus of CAII is found on the surface of the protein [119] (Fig. 1.4 A). Thus, CAII mutations outside the N-terminus can impair catalytic activity, without effect on AE1 binding capacity. For example, V143Y CAII mutant can still bind to AE1 but is catalytically inactive [108]. The suggestion of a metabolon came with the structural basis for CAII/AE1 binding [116], but a functional significance for this interaction was also required to support this theory.

Evidence for the functional significance of the CAII/AE1 interaction did emerge, supporting the theory of a metabolon. When AE1-transfected HEK293 cells were treated with acetazolamide, a carbonic anhydrase inhibitor, bicarbonate transport was nearly completely inhibited [117]. This indicated that endogenous CAII was essential for efficient AE1 activity [117], identifying an intracellular component of the bicarbonate transport metabolon (Fig. 1.5 A & B) [19]. To assess the functional importance of the CAII/AE1 interaction, a dominant negative approach was used. HEK293 cells, which endogenously

Figure 1.5: Model of the bicarbonate transport metabolon.
Bicarbonate transporters (BT) transport bicarbonate across cell membranes. Carbonic anhydrases (CA) catalyze the reversible hydration of CO_2 to HCO_3^- and H^+. The CAIV isoform associates with the extracellular leaflet of the plasma membrane via a glycosyl phosphatidyl inositol (GPI) linkage. Although CAIV binds both AE proteins and NBC1, the reversibility of the process in the membrane has not been studied. BTs bind CAII at their cytosolic carboxyl terminus; CAII can also exist free in the cytosol. When CAII and CAIV are bound to BT the transport rate is maximized (A). When CAII is not bound to BT and CAIV is not expressed the transport rate is reduced, but not abolished (B). The physical complex between the BT and the CAs facilitates efficient transport by minimizing the distances the substrates must diffuse, thereby maximizing the local concentration of substrate both for the transporter and the enzyme.

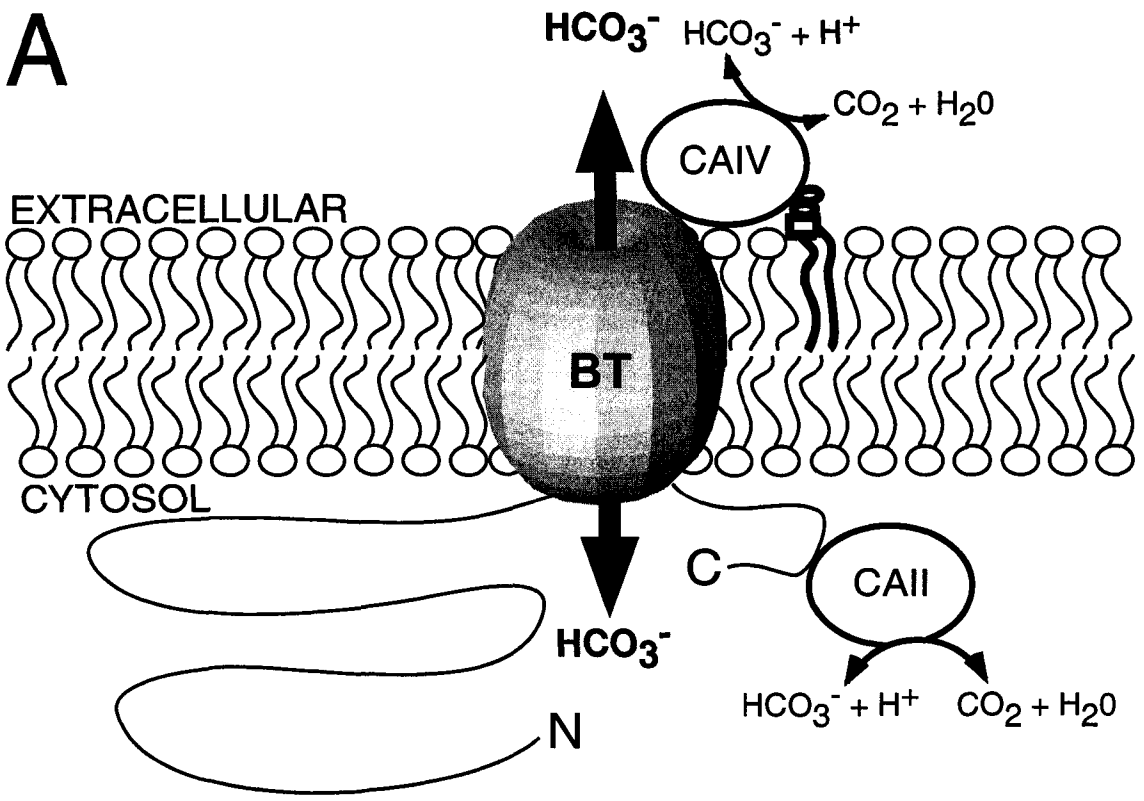

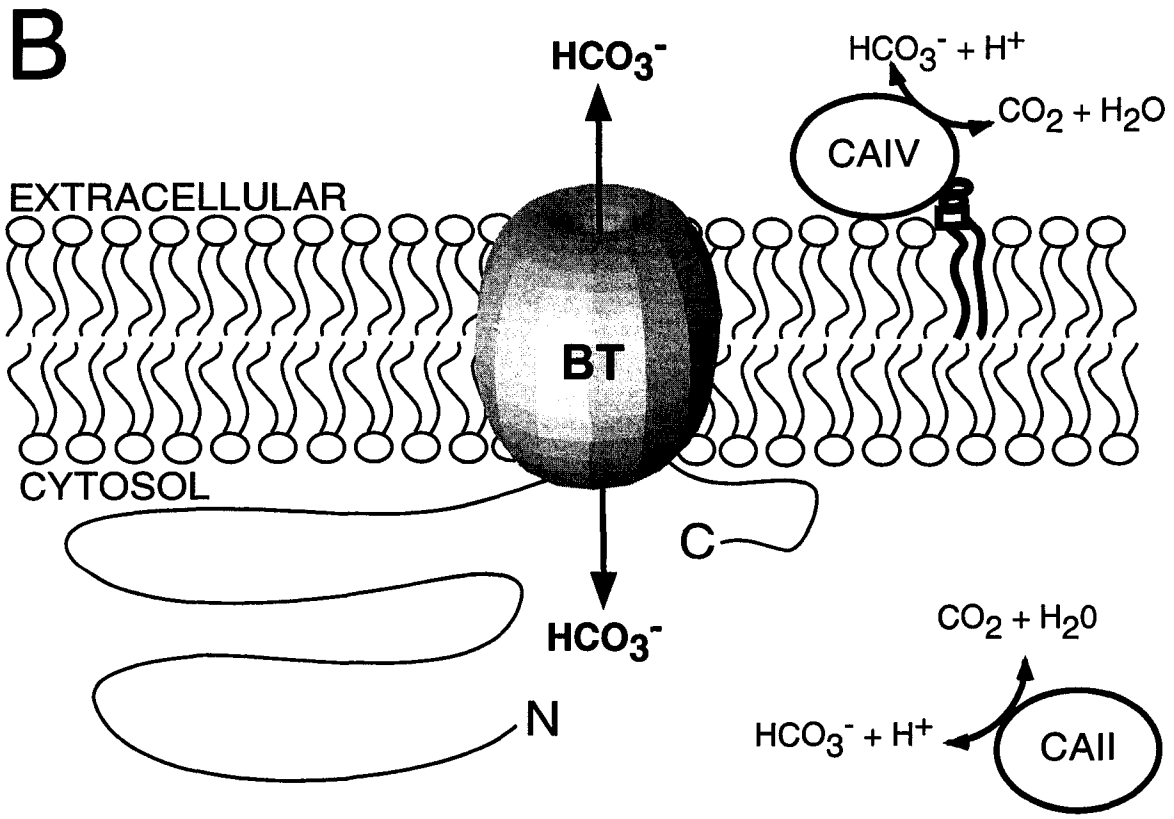

express CAII, were co-transfected with cDNA encoding AE1 and CAII or the functionally inactive human CAII mutant, V143Y. V143Y CAII was expressed at levels 20-fold higher than the endogenous wild type CAII in the cells and could thus compete with endogenous CAII for the CAII binding site on the AE1 C-terminus. Since the V143Y CAII-expressing cells still expressed wild type CAII, the expression of V143Y CAII would not affect total CA activity in the cells; V143Y CAII would affect only the location of functional CAII. AE1 activity was inhibited by 39% when HEK293 cells were co-transfected with functionally inactive V143Y CAII [108]. This indicates that displacement of endogenous CAII from the AE1 C-terminus into the cytosol greatly reduced AE1 HCO_3^- transport activity. In another set of experiments, the CAII binding site of AE1 was mutated so that it could not bind CAII. HCO_3^- transport activity was reduced by 90% relative to wild type AE1 activity [108]. This indicated that binding of CAII was necessary for full HCO_3^- transport activity.

CAII/AE1 interaction was also demonstrated when the proteins were expressed in *Xenopus* oocytes. The bicarbonate transport activities of supposedly inactive AE1 mutants were monitored with the expression of CAII [120]. As expected, inhibition of CAII inhibited AE1 transport activity in *Xenopus* oocytes, similar to overexpression of V143Y CAII in HEK293 cells [120]. CAII affected Cl^-/HCO_3^- exchange activity but had no effect on Cl^-/Cl^- exchange activity of AE1, consistent with the bicarbonate transport metabolon model [120]. Although there are differences between transport assays in *Xenopus* oocyte and HEK293 cells, these findings support the role of CAII as a bicarbonate channelling activator.

Since the discovery of the HCO_3^- transport metabolon in the AEs, physical and functional relationships between CAII and NBC1 [121, 122], NBC3 [123], and human putative anion transporter 1 (SLC26A6/PAT-1) [74, 81] have been identified. Considering this is a conserved relationship across most, but not all transporters, it is important to gain a better understanding of the interaction itself. Extracellular CA isoforms also associate with the extracellular surface of bicarbonate transporters, creating two classes of HCO_3^- transport metabolon, the intracellular and the extracellular metabolon.

1.4.3 Intracellular metabolon

The intracellular metabolon is the interaction of CAII with a bicarbonate transporter. To date CAII is the only intracellular CA isoform that has been identified in an intracellular metabolon. There are more cytosolic CA isoforms, two of which have moderate or high activity, the rest have either low or nil catalytic activity. CAVII and CAXIII display high and moderate catalytic activity, respectively, [105] however their interaction with bicarbonate transporters has yet to be explored. The remaining cytosolic isoforms likely do not interact with bicarbonate transporters since they would not increase the concentration of HCO_3^- at the opening of the transporter quickly enough to facilitate increased flux across the membrane. For instance, CAI, which shares 60% sequence identity to CAII, but has low catalytic activity does not have the bicarbonate transporter binding site and therefore does not physically interact with AE1 [107].

CAII is tethered to the C-terminus of a bicarbonate transporter via an electrostatic interaction. This brings CAII into close proximity of the bicarbonate

transporter (Fig. 1.5 A). The acidic CAII binding motif (CAB) on the C-terminus of the bicarbonate transporter, is composed of a hydrophobic amino acid followed by 4 amino acids, 2 of which are acidic [19]. For example the CAB on AE1 is LDADD [48], for NBC3 it is LDDLM [123, 124] and for SLC26A6 it is VDVDF [81] (Fig. 1.4 A). CAII binds bicarbonate transporters through a basic region located in the N-terminal 17 amino acids of CAII, containing five essential His residues [107].

This electrostatic interaction is of great interest to us since it is a relatively weak type of interaction although there is a strong association of CAII and bicarbonate transporters. The Kd for the interaction is around 100 nM [49, 81, 123], which is well in the range for protein-protein interactions [123]. This type of interaction is easily regulated. It is pH dependent and salt dependent [49, 123], both factors that can be altered in the vicinity of the interaction.

1.4.4 Extracellular metabolon

The extracellular metabolon has similar criteria as the intracellular component. A membrane linked CA interacts both physically and functionally with the extracellular surface of bicarbonate transporters.

Since the first report of an extracellular component of the metabolon, there have been multiple examples of this phenomenon. The extracellular metabolon was first demonstrated with CAIV, which is the extracellular isoform that is bound through a GPI linkage to the extracellular surface, interacting with the extracellular loop 4 of AE1 (Fig. 1.5 A & B) [19, 94]. This interaction was suspected when CAIV was recruited to the fraction containing AE1 in Triton X-100 HEK293 extracts resolved by sucrose gradient ultracentrifugation [94]. Gel

overlay assays demonstrated a specific physical interaction between CAIV and AE1, AE2, and AE3 [94]. This interaction is functionally significant since the inhibition of AE HCO_3^- transport activity by CAII V143Y is counteracted by CAIV [94]. Glutathione-*S*-transferase pull-down assays localized the physical interaction of CAIV to extracellular loop 4 of AE1, in a region conserved between bicarbonate transporters [94].

The extracellular metabolon also exists between NBC1 and CAIV resulting in a physical and functional relationship [121]. Like AE1, CAIV binds the fourth extracellular loop of NBC1 [121].

These experiments identified the extracellular component of the bicarbonate transport metabolon (Fig. 1.5 A & B) [19]. The intracellular and the extracellular components can work together to generate a HCO_3^- gradient across the plasma membrane. In the case of HCO_3^- efflux, CAII catalyzes the hydration of CO_2 generating a region of high HCO_3^- concentration at the intracellular surface. At the extracellular surface, CAIV will rapidly convert HCO_3^- to CO_2, thereby decreasing the local concentration. The action of the two CAs generates a HCO_3^- gradient across the plasma membrane where CAII pushes HCO_3^- across the membrane and CAIV effectively pulls HCO_3^- across the membrane (Fig. 1.6) [19].

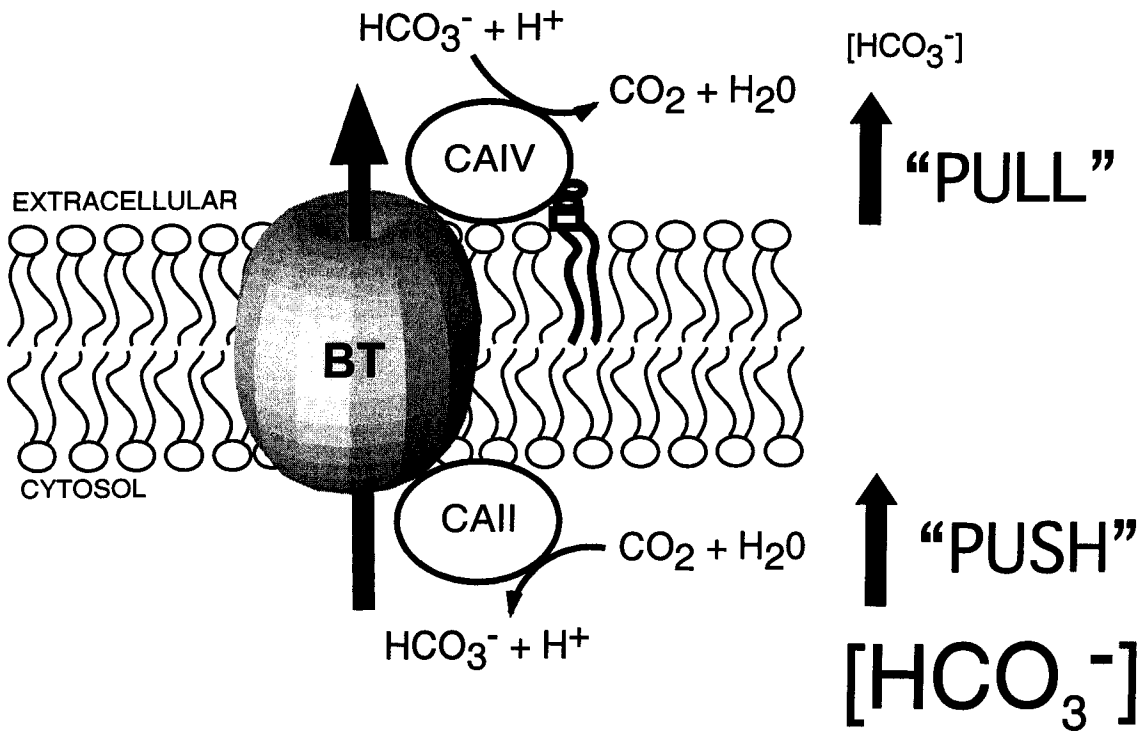

Figure 1.6: The metabolon maximizes the size of the transmembrane bicarbonate gradient.
The carbonic anhydrases that interact with the bicarbonate transporter are responsible for the generation of a concentration gradient of HCO_3^- via a "push-pull" mechanism. In HCO_3^- efflux mode, CAII rapidly converts CO_2 to HCO_3^- establishing a local high concentration of HCO_3^- to "push" transport of bicarbonate out of the cell. At the extracellular face, CAIV rapidly converts HCO_3^- to CO_2, which depletes the local extracellular HCO_3^- concentration, thereby "pulling" bicarbonate into the extracellular space. Combined, these effects drive bicarbonate transport out of the cell. The reverse of this process also occurs to drive bicarbonate transport into the cell.

1.5 Disease and dysfunction related to the impairment of bicarbonate transport

1.5.1 Renal Tubular Acidosis

There are multiple pathophysiologies related to the impairment of AE1, although no other AE isoform has yet been linked to a human disease. Such pathophysiologies include hereditary spherocytosis, hereditary stomatocytosis, haemolytic anemia, southern asian ovalocytosis, and distal renal tubular acidosis (dRTA) [125]. dRTA is most related to the subject of pH_i homeostasis as it is characterized by impaired urinary acid secretion due to the loss of Cl^-/HCO_3^- exchange activity in α-intercalated cells of the renal distal tubule [125].

Mutations in the kidney isoform of AE1 (kAE1) resulting in dRTA affect the targeting of kAE1 to the basolateral membrane of α-intercalated cells [126]. Autosomal dominant dRTA has a dominant-negative effect on wild type AE1 because of the oligomerization of AE1 by mistargeting wild type AE1 to the basolateral membrane [126]. Autosomal recessive dRTA patients tend to have more severe symptoms that have longer lasting effects [126-129]. Recessive dRTA arises from multiple different missense mutations; heterozygous combinations often consist of different mutations on both alleles [126]. These mutations often result in the targeting of AE1 to the proteosome for degradation and as a result there is a loss of functional AE1 in α-intercalated cells [130]. Interestingly, neither dominant nor recessive dRTA result in a red blood cell phenotype [126]. This is likely because glycophorin A will aid in the targeting of AE1 to the plasma membrane in red blood cells, while glycophorin A is not present in α-intercalated cells [131]. However, the severity of the condition in

patients with the recessive disorder is illustrated by the occurrence of severe anemia in human neonates [132].

The loss of functional AE1 or the mistargeting of AE1 results in a decrease of HCO_3^- reuptake in the kidney. A decrease in blood HCO_3^- levels impairs the ability of bicarbonate transporters throughout the body to regulate pH_i, resulting in whole body acidosis. Acidic conditions in the body result in the leaching of Ca^{2+} from bones into the blood stream [133]. Increases in Ca^{2+} levels results in skeletal deformities, impaired growth of children, muscle weakness, and an increased incidence of kidney stones and nephrocalcinosis [133]. Fortunately, ingestion of sodium bicarbonate can reverse the symptoms by alkalinizing the blood to reach normal pH levels [133].

Proximal renal tubular acidosis (pRTA) is similar to dRTA in that an impairment of a bicarbonate transporter results in acidosis. The affected bicarbonate transporter is NBC1, which is located in the basolateral membrane of the proximal tubule. Recessive pRTA is often associated with ocular disease due to mutations in NBC1, while heterozygous recessive pRTA is associated with osteopetrosis and mental retardation is due to mutations in CAII [110]. Both types of pRTA are a result of deficient NBC activity. Beyond pRTA, deficient NBC activity dramatically alters eye and ear function.

1.5.2 Auditory and visual impairment

NBCs located in the kidney carry out a different function than NBCs in other epithelial cells. In the kidney, NBC acts as an acid loader by moving HCO_3^- out of the cell and into the blood while in other epithelial tissues, such as the eye,

it acts to alkalinize the cell by moving HCO_3^- from the blood into the cell [134]. In this manner, NBCs are responsible for maintaining pH_i in extrarenal cells.

NBCs are abundant in the human eye and the auditory system and not surprisingly are associated with many acid-base diseases in these systems. NBC1 is expressed in multiple cell types within the eye and thus there is still speculation about which mutations in NBC1 are associated or attributed to each specific ocular disease since there appears to be overlap between symptoms [126]. These diseases are the result of either mistargeting of NBC1 or of decreased NBC1 activity [135]. In both cases, the cellular tissue cannot adequately regulate pH_i resulting in tissue degeneration.

NBC3 plays an important role in the eye and in the ear that cannot be compensated for by other mechanisms [136]. NBC3 knock-out mice display hearing loss and blindness due to degeneration of sensory receptors [137]. The loss of both hearing and vision is characteristic of the human disease Usher syndrome, the most frequent cause for the dual sensory impairment [138]. In Usher syndrome, blindness due to *retinitis pigmentosa* (a degeneration of the rod and cones) is a late onset symptom, while bilateral deafness is congenital [138]. NBC3 is located at the synapse in both the cochlear hair cells of the inner ear [139] and the retinal neurons [137, 139]. The function of NBC3 is to transport HCO_3^- into the cell to buffer the large H^+ load generated by the highly metabolic tissue. NBC3 is expressed in multiple inner ear cells in addition to the cochlear hair cells [138], which could possibly explain why there is congenital hearing loss when there is late onset blindness.

Mutations in CAs can also result in visual impairment. Rods and cones regulate pH changes both extracellularly and intracellularly. A change in

extracellular pH stimulates retinal phototransduction, the loss of this pH sensitivity results in the loss of retinal stimulation [140]. Intracellular pH is highly regulated because the tissue has high metabolic activity and thus has a high rate of acid production [141]. NBC1 located in the choriocapillaries will ultimately aid in maintaining pH_i in the retina. NBC1 is associated with the extracellular, GPI anchored CA isoform, CAIV to form the extracellular bicarbonate transport metabolon [121, 141]. Two separate point mutations in CAIV have been associated with *retinitis pigmentosa*. The first CAIV mutation, R14W, disrupts the extracellular bicarbonate transport metabolon by preventing the association of the catalytically active CAIV with NBC1 [141]. The second mutation, R219S, disrupts the catalytic activity of CAIV while maintaining its association with NBC1 [141]. Although the mutation does not occur in the bicarbonate transporter, it is evident that a decrease in HCO_3^- flux has detrimental effects.

1.5.3 Cardiac diseases

Cardiac ischemia resulting from myocardial infarction, is an important area of research for bicarbonate transporters. Ischemia is the reduction of blood flow to a tissue, depriving the tissue of the essential necessities for life. This disruption in blood flow results in a decrease in pH due to the inability of the cell to remove metabolic waste. The process of re-establishing normal cellular pH upon reperfusion often leads to a more severe outcome due to hyperactivation of pH regulating proteins.

In addition to cardiac reperfusion, bicarbonate transporters have also been associated with cardiac hypertrophy. Cardiac hypertrophy, an enlargement of

the heart, results from prolonged pressure overload (stress) to the heart [142]. Hypertrophic hearts are therefore more susceptible to ischemic events, such as angina or myocardial infarction [142].

Post cardiac ischemia, there is an acid load and the pH regulating proteins, NHE and NBC1 are activated to both remove and buffer H^+, respectively [143]. The hyperactivity of NHE and NBC1 will in turn overload the cell with Na^+, which reverses the Na^+/Ca^{2+} exchanger. This in turn overloads the cell with Ca^{2+}, prolonging cellular contraction and Ca^{2+} overload signals cell death. Inhibition of NBC1 will protect the heart from the damaging effects due to Na^+ overload during reperfusion [144, 145].

During cardiac hypertrophy, AEs are activated to remove excess HCO_3^- that has been built up [146]. Removal of HCO_3^- via AE results in an increase in the concentration of cytosolic Cl^-. The increase in the ion results in a change of osmotic pressure and could trigger the swelling of the cardiomyocyte. Also, a decrease in cytosolic HCO_3^- is equivalent to an acid load and results in an outcome similar to ischemia [147]. The isoform that is primarily responsible for cardiac hypertrophy has not yet been identified. AE3 is a likely candidate as it is highly expressed in cardiac cells [148, 149] and displays increased activity upon Angiotensin II (a vasoconstrictor) stimulation [150]. Inhibition of AE3 transport prevented HCO_3^- removal from the cardiomyocyte and prevented negative effects from an acid load [151].

More recently, another anion exchanger has been identified in mouse hearts. SLC26A6 mRNA levels are seven fold higher than AE3 in adult mice hearts [74]. In addition to increased mRNA expression, SLC26A6 has a wider distribution in cardiac cells. Immunhistochemical analysis localized AE3 to the

ventricle while SLC26A6 was localized to the atrium as well as the ventricle [74]. Although SLC26A6 has not yet been identified in human heart, if it is expressed in human hearts it could follow the same expression pattern as in the mouse. Although SLC26A6 has not been directly linked to the cause of any human diseases, it has been implicated in many degenerative disorders. SLC26A6 has a similar tissue distribution to CFTR and has been identified as a key protein for cystic fibrosis research [15, 152].

1.5.4 Cystic fibrosis

Considerable evidence suggests that HCO_3^- plays an important role in CF. Cystic fibrosis, caused by mutations in a chloride channel CFTR, is characterized by epithelial high chloride and low bicarbonate secretion, particularly in the pancreatic juice [153-155]. The most prevalent mutation is ΔF508, which impairs proper processing of CFTR to the plasma membrane. The result of the poor processing of CFTR due to ΔF508 and other mutations that result in CF were originally believed to affect only Cl^- movement. Recent evidence, however, shows that the majority of CF-causing mutations impair epithelial HCO_3^- secretion in addition to causing Cl^- movement aberrations [156].

Although CFTR can transport HCO_3^- [157, 158], perhaps it is the regulatory effect that it has on other bicarbonate transporter that is affecting HCO_3^- transport. CFTR associates with bicarbonate transporters both *in vitro* and *in vivo* [80, 159]. Both CFTR and SLC26A6 are expressed in the pancreas [75] and transport the same substrates in an opposing manner [16] therefore supporting the possibility that the two proteins may functionally interact. As previously mentioned, the regulatory (R) domain of CFTR and the STAS domain of

SLC26A6 also physically interact [80]. Since SLC26A6 interacts with CAII it is quite possible that CAII is brought into the CFTR/SLC26A6 complex and could have an important regulatory role.

Glutamate receptors are also widely distributed in epithelial cells and for this reason the effect of glutamate on CFTR was studied [160]. Also, glutamate is a well-known ligand for ion channel regulation in neurons, particularly for Cl^- channels [161, 162]. It was discovered that the rate of Cl^- conductance through CFTR was stimulated not only by ATP and phosphorylation of the R domain but also by glutamate [160]. However, upon stimulation by glutamate there was an arrest of HCO_3^- conductance via CFTR. In homozygous ΔF508 duct cells harvested from CF patients there is no increase in Cl^- secretion upon glutamate stimulation [160]. This loss may be explained by a loss of HCO_3^- regulation [160]. It is this information in combination with the knowledge that CFTR and SLC26A6 interact in epithelial cells that led us to investigate the following question: is glutamate regulating the bicarbonate transport metabolon by disrupting the interaction between CAII and the bicarbonate transporter?

1.6 Glutamate; a regulatory biomolecule

Glutamate transporters are expressed in the apical membrane of the proximal tubule [163], similar to the expression of the SLC26A6 in the proximal tubule [51, 70, 78]. Glutamate transporters have also been located in the auditory system [164], eye [165], intestinal tract [166], stomach , kidney, liver [167], and pancreatic [168] tissues in which multiple bicarbonate transporters have been identified [22, 23, 65, 69]. There is likely more overlapping tissue distribution between the glutamate transporters and bicarbonate transporters that have yet to

be identified. Glutamate is largely regarded as a neurotransmitter. Consequently, the research emphasis has been on glutamate transport in neuronal cells and less in epithelial cells. As evidence to suggest that glutamate has a larger regulatory role than first thought grows, more effort can be placed on identifying all of the tissues that contain glutamate transporters.

1.7 Thesis objectives

The goal of this project is to better understand the interaction between bicarbonate transporters and CAII as an important area of regulation for bicarbonate transporter activity. It is our hope to also provide an explanation for why there is a loss of HCO_3^- conductance through CFTR in the presence of glutamate.

Two different projects were designed to study the interaction between CAII and the C-terminus of bicarbonate transporters. The first project had the overall goal of obtaining an X-ray crystal structure of the C-terminus of NBC3 (NBC3Ct) bound to the full length CAII enzyme. My role in this goal was to overproduce and purify NBC3Ct in preparation for crystallization by our collaborator, Dr. Claudiu Supuran (University of Florence, Italy). The goal of the second project was to identify the effects of glutamate on the bicarbonate transport metabolon. Our theory is that the decrease in HCO_3^- conductance via CFTR may be linked to a decrease in HCO_3^- conductance through adjacent bicarbonate transporters. The approach that we took looked at the effect that glutamate exhibited on the interaction between CAII and the C-terminus of both AE1 and SLC26A6. These two projects will identify more modes of regulation for bicarbonate transport activity.

Chapter 2

Materials and Methods

2.1 Materials

2.1.1 Materials for NBC3Ct project

E. coli, recombinant expression strain, BL21-CodonPlus ($BL21^+$) was from Stratagene. Glutathione sepharose 4B resin and PreScission Protease from Amersham Pharmacia Biotech Inc was used for GST purification. Protein concentrators were from Millipore. The Institute for Biomolecular Design (IBD) purified NBC3Ct by reverse-phase high performance liquid chromatography (HPLC) and performed mass spectroscopy (MS) analysis on the sample. Ion exchange chromatography using a Pharmacia Mono-Q sepharose column was also used to purify NBC3Ct. Protein quantification reagents were from Bio-Rad. Amino-acid analysis was provided by the Alberta Peptide Institute (API).

2.1.2 Materials for glutamate regulation project

P-aminomethylbenzene sulfonamide resin (p-AMBS) used to purify CAII, is from Sigma. 96 well EIA/RIA polystyrene plates, with high binding surface chemistry, are from VWR. 1-cyclohexy-3-(2-morpholino-ethyl) carbodiimide metho-*p*-toluenesulfonate (referred to in this text as carbodiimide) and *o*-phenylenediamine dihydrochloride (OPD) are from Sigma. Primary antibodies, rabbit polyclonal anti-GST and rabbit polyclonal anti-CAII, are from Santa Cruz. The secondary antibody, donkey anti-rabbit IgG biotinylated, and the peroxidase labelled streptavidin are from Amersham.

2.2 Plasmid DNA

2.2.1 DNA constructs

Members of the Casey lab constructed DNA constructs containing the GST fusion protein cassette. The GST fusion construct GST.NBC3Ct was constructed and described by Dr. Fred Loiselle [124], GST.SLC26A6Ct was constructed and described by Dr. Bernardo Alvarez [81]. The C-terminal tail of AE1 GST fusion construct, GST.AE1Ct, was constructed by Haley Shandro and has been described [169]. The CAII construct, pACA, is a generous gift from Dr. Carol Fierke [170]. Human NBC3 cDNA was a generous gift from Dr. Ira Kurtz (U.C.L.A.).

2.2.2 Plasmid DNA isolation

Plasmid DNA was transformed into DH5α cells via electroporation. Electroporated cells were grown in 600 μl of SOC media (20 g Bacto tryptone, 5 g Bacto yeast extract, 0.58 g NaCl, 0.186 g KCl in 1 l H_2O) for 1 h at 37 °C with shaking. Liquid culture (150 μl) was then plated on LB plates supplemented with ampicillin (100 μg/ml) and incubated overnight at 37 °C. A single colony was selected to inoculate 100 ml of LB media supplemented with ampicillin (100 μg/ml). Culture was grown overnight at 37 °C with shaking. Cells were harvested by centrifugation at 7 500 x g and plasmid DNA was prepared with Qiagen Hi-Speed columns (Qiagen Inc., Mississauga, Canada). Plasmid DNA was verified by restriction digestion.

2.2.3 Restriction Digests

Diagnostic restriction digests were performed on isolated plasmid DNA. DNA (1 μg) was cut with 10 units of restriction enzyme in a 10 μl reaction

mixture containing restriction digestion buffer and BSA (if required). Digestion was allowed to proceed for 1 h at the required temperature (dependent on restriction enzyme being used) before stopping the reaction by addition of DNA loading dye. DNA was resolved on 1% agarose gel to confirm proper DNA pattern.

2.3 Protein purification

2.3.1 GST-fusion protein purification

Purification commenced with the transformation of GST.NBC3Ct into *E. coli* $BL21^{+}$. A single colony was used to inoculate a 50 ml starter culture of Luria-Bertani, LB, medium. Following overnight growth at 37 °C with shaking, 1.2 litres of LB media was inoculated with 30 ml of the starter culture. Cultures were grown at 37 °C with shaking until A_{600} was 0.6 - 0.8. Isopropylthiogalactoside, IPTG, (1 mM final) was added and growth was allowed to continue for 3 hours at 37 °C with shaking. The culture was then centrifuged at 7 500 x g, 4 °C, for 10 min and bacterial pellets were resuspended in cold PBS buffer, pH 7.50, containing complete mini protease inhibitor cocktail. Suspended cells were sonicated (4 times 60 sec, power level 9.5 with model W185 probe sonifier (Heat systems-Ultrasonics Inc., Plainview, N.Y.)) and treated with 1% (v/v) Triton X-100, with slow stirring for 30 min. Following centrifugation (12 000 × g, 10 min at 4 °C) the supernatant was added to 1.2 ml GSH-sepharose (50% slurry washed with 5 ml PBS) and incubated at room temperature with gentle agitation for 1-2 hours. The sample was centrifuged (2 000 × g, 5 min) and the pellet washed three times with PBS.

Fusion proteins were eluted from the GSH-sepharose resin for use in the microtitre plate binding assay. Fusion proteins from a 200 ml bacterial cell culture were eluted with 3 times 100 μl glutathione elution buffer (10 mM reduced glutathione, 50 mM Tris-HCl, pH 8). Eluted proteins were quantified using the microtitre Bradford protein assay [171].

Purification of NBC3Ct did not require the fusion construct to be eluted from the glutathione sepharose resin. Instead, the fusion protein was then washed 3 times with cold PreScission cleavage buffer (150 mM NaCl, 1 mM EDTA, 1 mM dithiothreitol, 50 mM Tris-HCl, pH 7.0), and reduced to 50% slurry. PreScission Protease (80 units/ml resin) was then added and the sample incubated for forty-eight hours at 4 °C with rotation. Following cleavage, the resin was centrifuged at 2 000 × g for 5 minutes and the supernatant collected. The resin was washed once with an equal volume of cold cleavage buffer and the supernatants pooled. The cleaved fusion protein was then further purified by reverse-phase HPLC with an Agilent Zorbax 300 SB-C8 column (2.1 × 150 mm) on an Agilent 1100 HPLC system using a 1% H_2O/Acetonitrile gradient with 0.1% trifluoroacetic acid (TFA) and characterized by MS using a Voyageur–DE Pro mass spectrometer from Applied Biosystems at the Institute for Biomolecular Design.

A second approach for purification after the glutathione sepharose resin was explored. Ion exchange chromatography using a 10 ml Mono Q Sepharose column from Pharmacia was employed instead of HPLC. The sample was then concentrated with an Amicon Ultra centrifugal filter (threshold of 5 kDa) from Millipore to obtain a concentration of 200 μM.

2.3.2 Purification of CAII

The pACA vector, which contains human CAII cDNA, was transformed into BL21$^+$ *E. coli* cells [170]. A colony was used to inoculate a 25 ml starter culture of LB medium. Following overnight growth at 37 °C with shaking, 200 ml of LB medium was inoculated with 5 ml of the starter culture. LB growth medium was supplemented with 0.1 mM $ZnSO_4$ and 2 mM K_2HPO_4 and 1 mM of IPTG for induction of protein expression at an A_{600} of 0.5 - 0.6; growth was allowed to continue for 3 h. Subsequent lysis of bacterial cultures and collection of cell lysate was previously described in section 2.2.7. Before cell lysate was added to 500 μl of *p*-AMBS resin, the resin was washed three times 3 000 rpm for 30 seconds with 5 ml 4 °C wash buffer 0 (0.2 M K_2SO_4, 0.5 mM EDTA, 0.1 M Tris-SO_4, pH 7.5). Cell lysate was incubated with resin for 2 h with gentle agitation at room temperature. Resin was collected by centrifugation at 3 000 rpm for 5 min and the supernatant was removed. Resin was washed three times with 5 ml 4 °C wash buffer 1 (0.2 M K_2SO_4, 0.5 mM EDTA, 0.1 M Tris-SO_4, pH 9) in the same manner. Resin was loaded into a column and washed with 4 °C wash buffer 2 (0.2 M K_2SO_4, 0.1 M Tris-SO_4, pH 7) by gravity flow. CAII was eluted with 1.5 ml of 4 °C elution buffer (0.4 M KSCN, 0.5 mM EDTA, 0.1 M Tris-SO_4, pH 6.8). CAII was dialyzed twice against 2 l of 1 M NaCl, 100 mM Tris-HCl, pH 7.5 for 6 – 18 hours at 4 °C. Dialyzed samples were collected, checked for purity by Coomassie stained sodium dodecyl sulfate polyacrylamide gel electrophoresis (SDS-PAGE) and quantified with the microtitre Bradford protein assay [171]. Samples were then dispensed into aliquots and lyophilized for storage at –20 °C.

2.4 Qualification and quantification of purified protein

2.4.1 SDS-PAGE

Samples were prepared in 1 x sample buffer (10% (v/v) glycerol, 1% (v/v) 2-mercaptoethanol, 2% (w/v) SDS, 0.5% (w/v) bromophenol blue, 75 mM Tris, pH 6.8). Samples were heated for 5 min at 65 °C prior to centrifugation at 13 500 x g for 3.5 min. Samples were loaded on 1.5 mm 12.5% (w/v) polyacrylamide-gels [172] using Bio-Rad mini-protean II apparatus. Samples were resolved in the PAGE gel by running at 40 mA/gel until the dye front reaches the bottom of the gel.

2.4.2 Coomassie staining of SDS-PAGE gel

SDS-PAGE gels were stained with Coomassie Blue dye (0.05% Coomassie Blue R-250, 25% isopropanol, 10% acetic acid) for 1 h with gentle rocking at room temperature. Gel was destained with destaining buffer (5% methanol, 10% acetic acid) until gel was colourless. Gel image was collected on a Kodak Image Station 440CF and band quantification performed by Kodak 1D software available through Eastman Kodak Company.

2.4.3 Microtitre-dish protein quantification assay

Protein samples were quantified using a modified version of the Bradford protein quantification assay [171], as suggested by the Bio-Rad instruction manual. BSA standards were made up in 10 μl and samples (2 μl) were diluted in H_2O (8 μl) to the same volume and loaded into a well of a 96 well plate. Diluted Bio-Rad dye (1:4) (200 μl) was added directly to the sample and standards. Absorbance readings at wavelength 595 nm were taken following 30

s of shaking at 890 rpm with a Multiskan Ascent 100-120 V plate reader from Thermo Electron Corporation. Data was collected with Ascent Software version 2.6 from Thermo Electron and processed in MS Excel.

2.4.4 Circular dichroism spectroscopy

The structural integrity of NBC3Ct after being subjected to reverse-phase HPLC and lyophilization was assessed by CD. Lyophillized NBC3Ct was dissolved in cold CD buffer (100 mM KCl, 15 mM HEPES, pH 7.2) to a concentration of 0.2 mg/ml and stored at 4 °C; the concentration was verified by amino acid analysis. Experiments were performed with the following conditions: scan temperature of 25 °C, cell length 0.05 cm, scan range 194 nm to 255 nm, resolution 0.1 nm, sensitivity 20 mdeg, response 0.25 sec, speed, 10 nm/minute, and 8 accumulations per sample.

Data was collected on a JASCO J-720 spectropolarimeter using a JASCO spectropolarimeter power supply and analyzed with JASCO J700 analysis software. Data was formatted in Microsoft Excel and plotted in GraphPad Prism 4.0b.

2.5 Regulation of metabolon

2.5.1 Microtitre plate binding assay

The microtitre plate CAII-binding assay is modified from an assay previously reported [48, 49, 107]. 96 well microtitre dishes were coated with 200 ng of purified CAII by quickly adding CAII in ELISA Buffer (100 mM Na_2HPO_4, 150 Mm NaCl, pH 6.0) containing 1.25 mg/ml of carbodiimide to dishes and

incubating for 30 min at room temperature. CAII-coated wells were blocked with 2% BSA in PBS (140 mM NaCl, 3 mM KCl, 6.5 mM Na_2HPO_4, 1.5 mM KH_2PO_4, pH 7.5). After blocking, the dishes were incubated with varied concentrations (0 – 800 nM) of purified GST, GST.AE1Ct or GST.SLC26A6Ct (Fig. 2.1) in antibody buffer (100 mM NaCl, 5 mM EDTA, 0.25% gelatin, 0.05% Triton X-100, 50 mM Tris, pH 7.5) overnight at room temperature. The NaCl concentration in the antibody buffer was adjusted to accommodate the additions of ions (glutamate, gluconate, aspartate and leucine) with varying concentrations (0 – 40 mM). This allowed for the creation of binding curves in the presence of various ion compositions, with constant ionic strength. The plates were then washed, and bound fusion proteins were detected by sequential incubation with rabbit polyclonal anti-GST (1:5000 dilution) in antibody buffer at 4 °C overnight, biotinylated donkey anti-rabbit IgG (1:5000 dilution) in antibody buffer at room temperature for 2 h, and streptavidin-biotinylated horseradish peroxidase complex (1:5000 dilution) in antibody buffer at room temperature for 2 h. Plates were developed in the dark with OPD substrate in H_2O until sufficient colour had developed. The plates were shaken for 1 min in the dark at 840 rpm prior to reading the absorbance at 450 nm using a Multiskan Ascent 100-120 V plate reader from Thermo Electron Corporation. Data was collected with Ascent Software version 2.6 from Thermo Electron and processed in MS Excel and Prism Graphpad.

To estimate the affinity of the association between CAII and GST.AE1Ct or GST.SLC26A6Ct, the absorbance value, corrected for GST alone, was plotted versus the concentration of GST.AE1Ct or GST.SLC26A6Ct. The dissociation constant (Kd) for the interaction was determined using the Prism program from

GraphPad. The Kd was then plotted in relation to the concentration of ion present. From this curve a relationship could be formed between the ion present and the relative affinity of CAII for the bicarbonate transporters.

2.5.2 CAII activity assay

The CAII catalytic activity assay was modified from a previously described technique [141, 173-176]. Purified CAII was rehydrated to a concentration of 1 μg/100 μl in 5 mM Tris, pH 7.5. CAII was diluted in TI buffer (20 mM imidazole, 5 mM Tris, pH 7.5) for a final concentration of 1 μg CAII/3 ml of buffer. All assay reagents were chilled on ice for 30 min prior to commencement of the assay, and for the duration of the experiment. The pH electrode was calibrated with standards that had also been incubated on ice for 30 min. Assays were performed in glass test tubes in an ice-water bath on a magnetic stir plate with continuous stirring and CO_2-gassing throughout the experiment. In each assay 3 ml of H_2O was bubbled with CO_2 at a flow rate of 600 ml/min for 60 s. Recording of pH as a function of time was initiated upon addition of 3 ml of TI buffer, containing CAII; recording of pH continued for 90 s.

CAII activity is determined by the amount of H^+ production over a period of time (equation 3.1).

$$\text{CAII activity} = \frac{\text{amount } H^+ \text{ produced}}{\text{time}} \qquad \textbf{Equation 3.1}$$

The time over which H^+ are produced is determined by a linear regression of the rate of change of pH over the pH 7.0 - 6.5 range (equation 3.2), where the slope of the curve represents the rate of H^+ production over time (pH units/s).

$$\text{time} = \frac{0.5 \text{ pH units}}{\text{slope} \cdot (60 \text{ s/min})} \qquad \textbf{Equation 3.2}$$

The amount of protons produced between pH 7.0 and 6.5 is equivalent to the amount of base (B) in the sample (volume, v) consumed throughout the experiment (equation 3.3). To determine the amount of base consumed, determine the change in concentration of base at each pH (equation 3.4). The total base in the sample is derived from the amount of tris and imidazole present at the desired pH (equation 3.5).

$$\text{amount } H^+ \text{ produced} = v \cdot |\Delta[B]| \qquad \textbf{Equation 3.3}$$

$$\Delta[B] = [B]_{pH7.0} - [B]_{pH6.5} \qquad \textbf{Equation 3.4}$$

$$[B] = [\text{Tris base}] + [\text{Imidazole base}]^* \qquad \textbf{Equation 3.5}$$

**Determined from the Henderson-Hasselbach equation*

The rate of change of pH in blank samples (activity buffer without CAII) was subtracted from each of the rates. The activity for the different concentrations of ion (A_n) was then expressed as the percent of the activity with no ion present (A_o) (equation 3.5).

$$\% \text{ of the control} = \frac{A_n}{A_o} \times 100 \qquad \textbf{Equation 3.6}$$

Anions (glutamate, gluconate, aspartate, leucine) or the CAII inhibitor acetazolamide (ACTZ) were added to TI buffer to monitor their effect on the activity of CAII.

2.6 Statistics

All errors and error bars represent the standard error of the mean (SEM). Statistical significance was determined by paired t-test, and significant difference was defined as $p \leq 0.05$. Assays varied in n values, but they were all performed a minimum of three times.

Chapter 3

Large-Scale Purification and Analysis of the Human NBC3, Sodium/Bicarbonate Co-transporter, Carboxyl-Terminal Cytoplasmic Domain

3.1 Introduction

The Na^+/HCO_3^- cotransporter, NBC3, is important for maintaining pH_i. There are two ways that NBC3 accomplishes this goal, one is by aiding in the reabsorption of HCO_3^- in the kidney so that there is an adequate supply of the buffer for maintaining whole body pH and also by intricately regulating the flux of HCO_3^- into cells to maintain a neutral pH. NBC3 has a more critical role of regulating pH_i rather than whole body pH. When NBC3 activity is disrupted there are detrimental effects to the tissue in which it is expressed. Often the acid overload leads to degeneration of the tissue, as seen in the degeneration of auditory and eye tissue in Usher syndrome [137, 139].

The association of CAII, the enzyme that generates HCO_3^-, enhances NBC3 activity. Upon mutation of the CAII binding site on NBC3, activity was reduced to 29 ± 22% of wild type activity [123]. The CAII/NBC3 interaction is electrostatic and has a Kd of 101 nM [123]. The CAII/NCB3 interaction is conserved in other bicarbonate transporters. Only one member of the bicarbonate transporter family, SLC26A3, fails to associate with CAII [118]. SLC26A3 lacks the CAII binding motif in the C-terminus that is present on all other bicarbonate transporters [118]. This is not surprising since SLC26A3 shows more sequence similarity to sulfate transporters than bicarbonate transporters [67, 85, 118].

The conservation of the CAB motif throughout the bicarbonate transporter family is indicative of the importance of this interaction. An X-ray crystal structure of CAII interacting with the C-terminus of a bicarbonate transporter would aid in identifying other modes of regulation. The interaction between CAII and NBC3 has been well studied and therefore acts as a good model system

for obtaining a 3D image of the complex. The quality of the crystals formed is dependent on the purity of the proteins to be crystallized. Our goal was to obtain a sufficient amount of purified NBC3Ct for co-crystallization with purified CAII. The challenge was to purify NBC3Ct without denaturing it.

3.2 Results

3.2.1 Purification of NBC3Ct

Maximal purification of NBC3Ct was necessary for co-crystallization of NBC3Ct and CAII. However, the ability of the purified NBC3Ct to maintain or return to native folding is also essential for an accurate crystal structure. This left us with the challenge of determining the best method for transport to Italy (liquid sample versus lyophilized sample) while maintaining the structural integrity. Several attempts were made at optimizing the system for purification and in the end the main difference was in the final purification step.

E. coli transformed with the GST.NBC3Ct plasmid underwent two solubilization steps. Sonication of the cells was the first step used to disrupt the cell wall, and the second step was digestion of the plasma membrane with Triton X-100, a non-ionic detergent. Once solubilized, the cell lysate was collected and incubated on glutathione sepharose resin. A clear increase in purity of the sample is noted throughout this process (Fig. 3.1 A). NBC3Ct was eluted from the resin by cleavage of the GST tag by protease. The yield of purified NBC3Ct was quantified by Bradford assay and calculated to be 1 mg of NBC3Ct/l of bacteria.

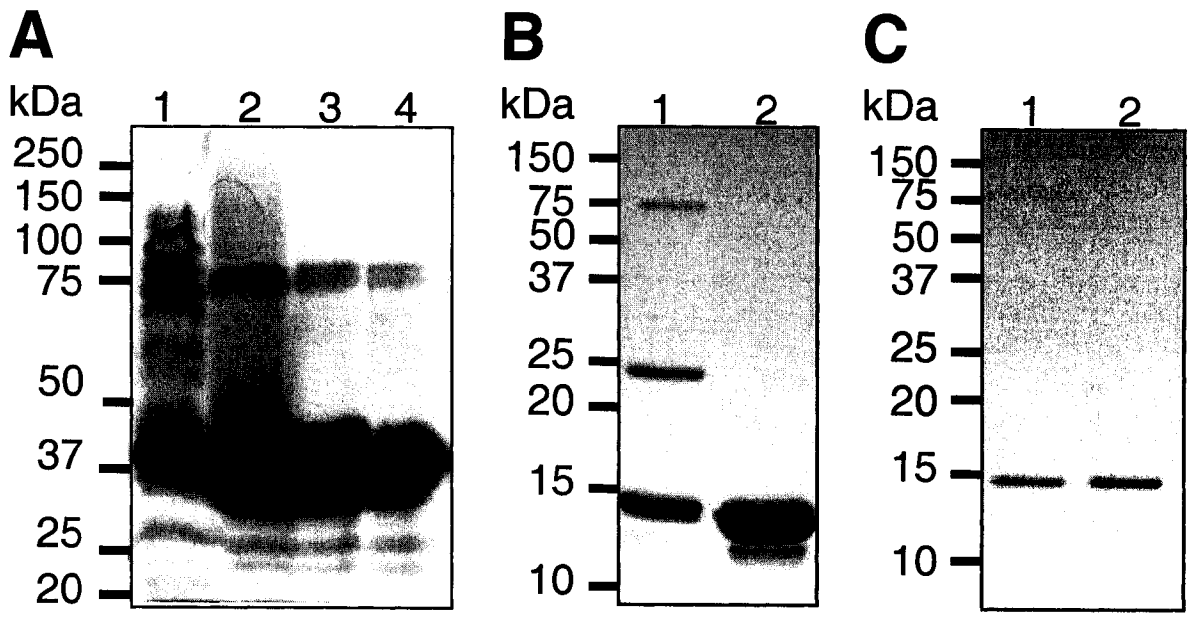

Figure 3.1: NBC3Ct purification.
Multiple steps of purification were necessary to achieve maximal purity. A, shows the increase in purity from cell lysate to purification with glutathione sepharose resin. Lane 1, cell lysate after sonication, lane 2, cell lysate after Triton X-100 treatment, lane 3, glutathione sepharose resin, lane 4, glutathione elution of GST.NBC3Ct. B, after PreScission protease cleavage of GST.NBC3Ct further resolution of contaminating products was achieved via ion exchange chromatography. Lane 1, NBC3Ct after treatment with PreScission protease, lane 2, NBC3Ct containing fraction off the ion exchange column. C, NBC3Ct fractions from the ion exchange column were pooled (lane 1) and then concentrated (lane 2).

The initial step of growing and isolating GST.NBC3Ct was efficient and therefore did not require further optimization. However, there were two contaminating proteins that remained in the sample after cleavage of the GST tag (Fig. 3.1 B). One protein resolved to the size of GST alone (26 kDa) and another that could be a protein from the commonly expressed Heat Shock Protein family, HSP70 (70 kDa). Some GST contamination could be due to two GST proteins self-associating and thereby preventing the glutathione sepharose resin from interacting with the dimeric GST. Incubating the cleavage product with more GSH-sepharose to remove the GST contaminant did not increase the purity of the product. HSPs are molecular chaperones that aid in folding immature proteins and protect cellular proteins under times of stress [177]. *E. coli* is subjected to cellular stress upon sonication of the cell wall and could thus trigger a stress response, which may result in HSP binding to GST or NBC3Ct at the time of solubilization.

To increase the purity of the yield, the cleavage products resolved on an Agilent Zorbax 300 SB-C8 reverse-phase HPLC column with an Agilent 1100 HPLC system (Fig. 3.2 A). This completely resolved the contaminating proteins from NBC3Ct and effectively purified the sample. The identity of the purified protein, NBC3Ct, was confirmed via mass spectrometry, using a Voyageur-DE Pro system from Applied Biosystems, as the determined molecular weight of the protein corresponds to the reported molecular weight (Fig. 3.2 B). Mass spectrometry also confirmed the second peak in the HPLC chromatogram was likely GST as the reported molecular weight was 25.7 kDa, which corresponds to the published molecular weight [178]. Since reverse-phase HPLC uses the organic solvents acetonitrile and TFA to resolve the proteins, which was

Figure 3.2: Identification and HPLC purification of NBC3Ct.
A, after cleavage of GST.NBC3Ct on the glutathione sepharose resin an Agilent Zorbax 300 SB-C8 HPLC column with an Agilent 1100 HPLC was used to further purify the NBC3Ct sample. The proteins were eluted in a 1% H_2O/acetonitrile gradient with 0.1%TFA. The peak at approximately 22 minutes was identified as NBC3Ct via mass spectrometry (panel B). B, mass spectrometry was performed on the purified sample from the HPLC with a Voyageur-DE Pro system from Applied Biosystems. The purified protein corresponds to the expected molecular weight of NBC3Ct (11.2 kDa).

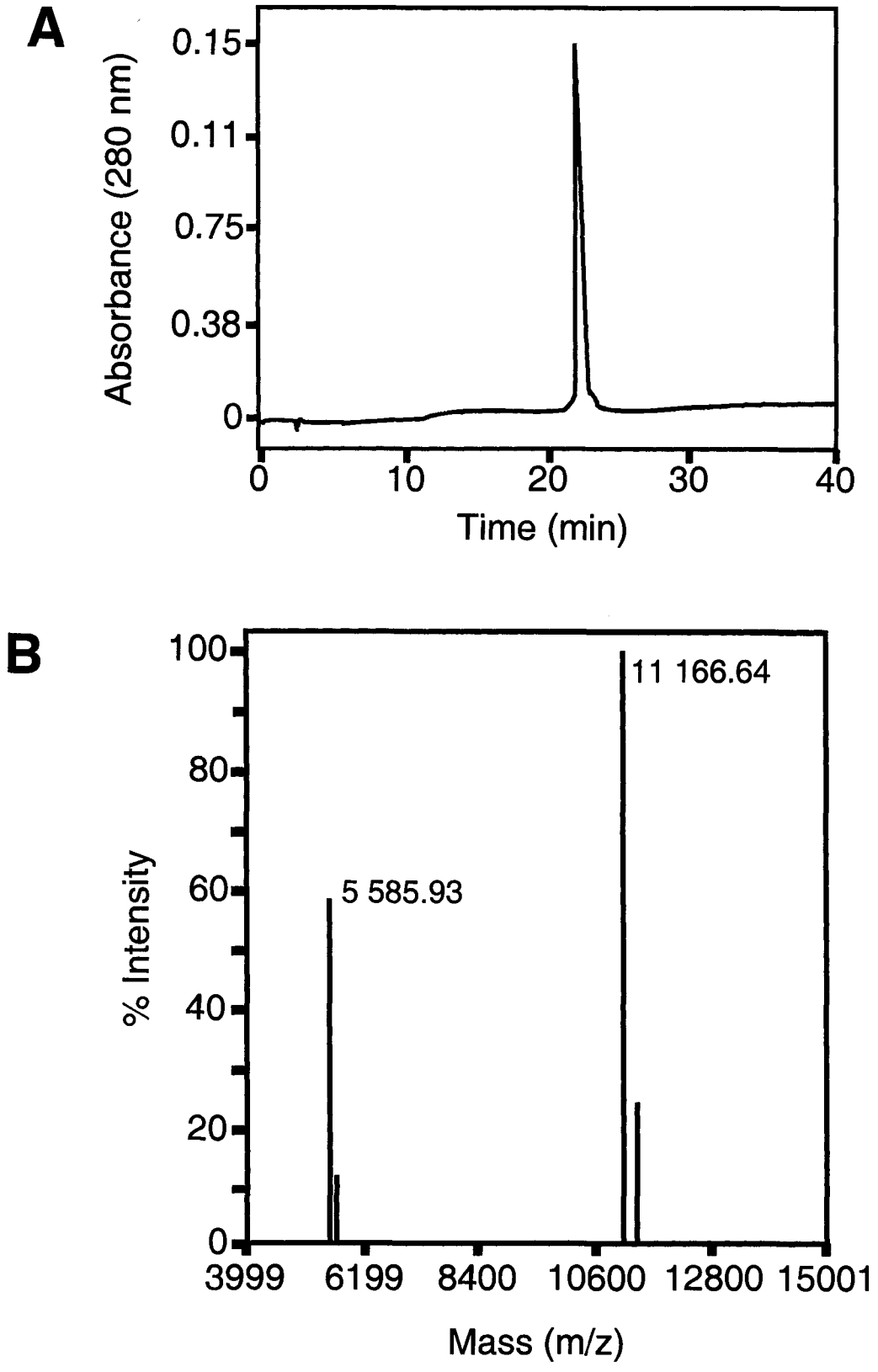

an inappropriate environment for the biological sample, and NBC3Ct was going to be shipped to Italy, the protein was lyophilized. Because of the harsh conditions that the protein endured, CD was performed on the protein to confirm that the rehydrated structure maintained the native conformation (Fig. 3.3). The CD spectra revealed no discernable differences from that of a previously published NBC3Ct spectra [124]. The sample was thus sent to our collaborators for co-crystallization trials with CAII.

Attempts at co-crystallization were unsuccessful and so a second attempt at NBC3Ct purification was made. Because of the harsh conditions that NBC3Ct encountered during reverse-phase HPLC and lyophilization, it was theorized that perhaps this impaired the ability of NBC3Ct and CAII to bind during crystallization. Therefore, anion-exchange chromatography, using a 10 ml mono-Q column from Pharmacia, was used to resolve NBC3Ct from the contaminants in a non-denaturing buffer. Proteins are resolved on anion-exchange columns based on their isoelectric points (pI). If the contaminants in the sample were in fact GST and HSP70, they would have sufficiently different pI's from that of NBC3Ct and would be eluted from the column with a different NaCl concentration. The anion-exchange column was used because the amino acid sequence of NBC3Ct suggests it is slightly electronegative and should be retained on the column longer than the contaminants. Surprisingly, NBC3Ct was not retained on the column and was found in the loading fractions (peak 1). Fortunately, the contaminating proteins were retained on the column (peak 2), so there was sufficient resolution between NBC3Ct and the contaminants in the collected fractions (Fig. 3.4) as no contaminating bands were detected on a Coomassie-stained SDS-PAGE gel (Fig. 3.1 C). Both contaminants were eluted at

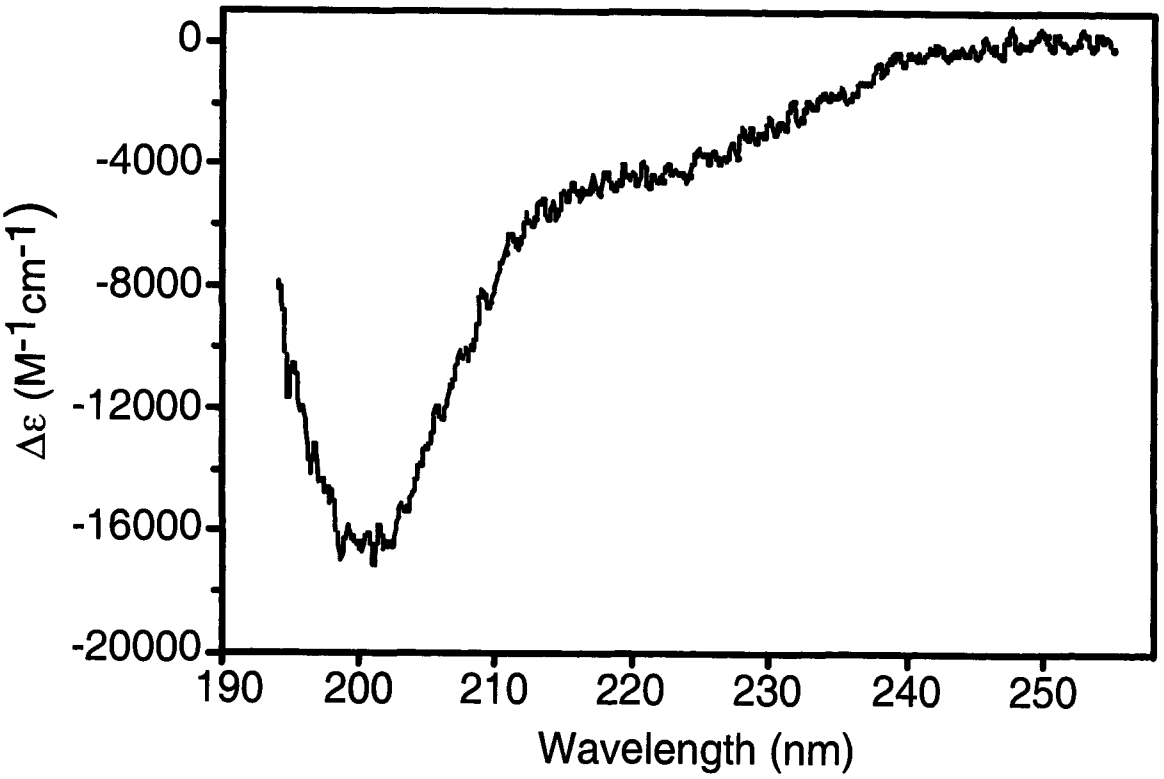

Figure 3.3: Circular dichroism spectra of NBC3Ct.
CD was performed on rehydrated NBC3Ct (40 μg) in order to assess structural integrity after reverse-phase HPLC. NBC3Ct was diluted in 100 mM KCl, 15 mM HEPES, pH 7.2 to a concentration of 0.2 mg/ml and stored at 4 °C. Experiments were performed with the following conditions: scan temperature of 25 °C, cell length 0.05 cm, scan range 194 nm to 255 nm, resolution 0.1 nm, sensitivity 20 mdeg, response 0.25 sec, speed, 10 nm/minute, and 8 accumulations per sample.

Figure 3.4: Anion exchange purification of NBC3Ct.
The sample collected from the glutathione sepharose resin after proteolysis with PreScission protease was loaded on a Mono-Q sepharose column from Pharmacia. GST and NBC3Ct were separated by their electrostatic interactions, using a NaCl gradient to elute GST from the column. NBC3Ct was not retained on the column and eluted as peak 1. GST/HSP70 was moderately retained on the resin and was eluted as the ionic concentration in the solution increased (peak 2).

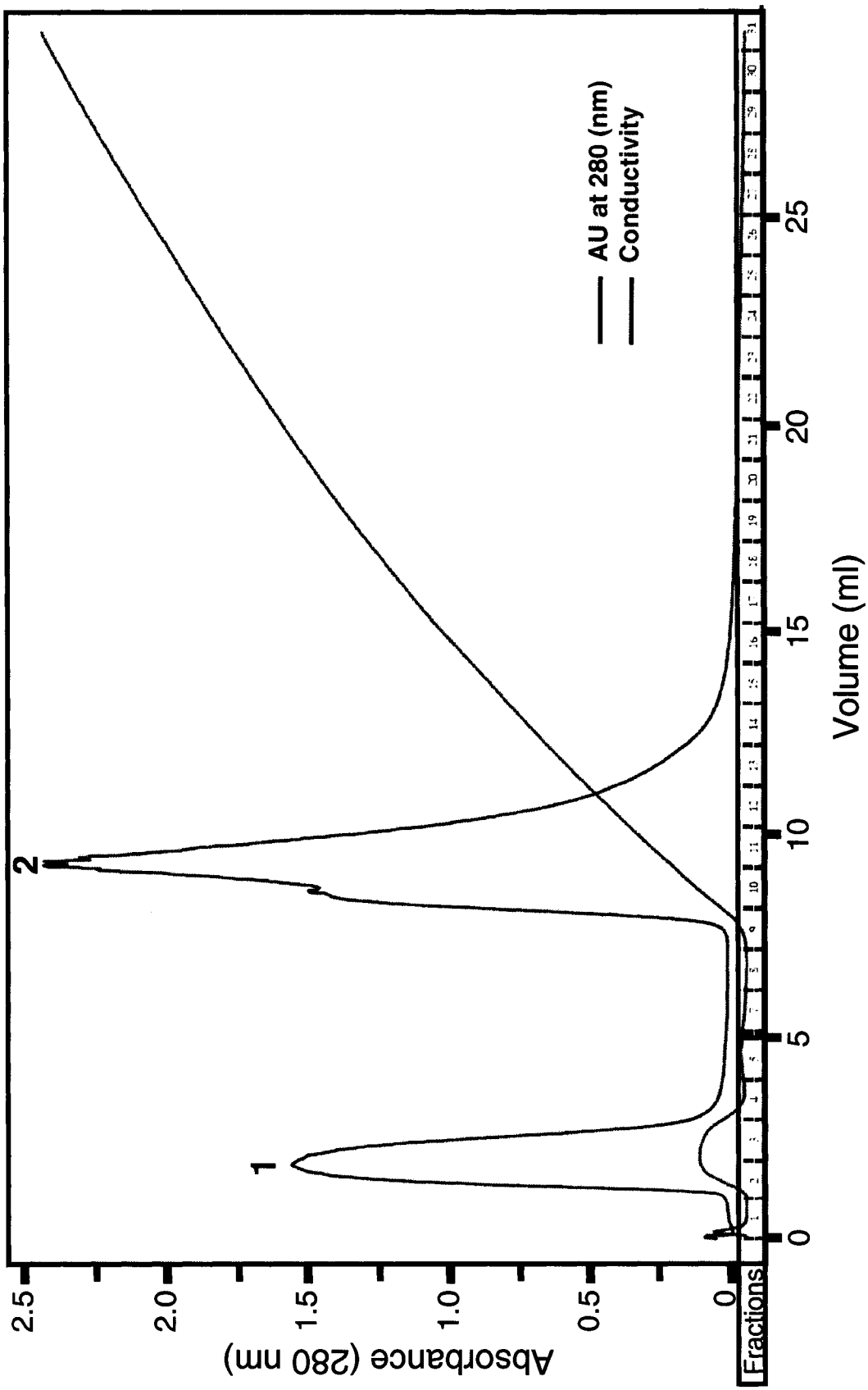

the same time, lending more support to the prediction that these contaminants were GST and HSP70. Because HSP70 is a chaperone protein, during solubilization it may have been associated with an immature GST or have bound GST in response to cellular stress. The benefit of the ion exchange column is that the protein remained in the same buffer (the cleavage buffer) and the only subsequent step needed was a concentrating column to obtain a concentration (200 μM) that was practical for crystallization trials.

3.3 Discussion

The interaction between CAII and bicarbonate transporters is important for achieving maximal flux of HCO_3^- through the transporter. Thus far the site of interaction for both CAII and NBC3Ct have been identified [123], and the crystal structure for CAII has been solved [179], but there is currently no crystal structure of the interaction between a bicarbonate transporter and CAII. In order to pursue this structure, using NBC3 as the bicarbonate transporter of interest, there needs to be an overproduction and purification of the C-terminus of NBC3. This was accomplished by obtaining a yield of 1 mg/l of culture and a two-step purification process that purified NBC3Ct completely. In the process, NBC3Ct was characterized by MS to identify the purified sample by molecular weight, by CD to ensure that structural integrity was maintained and by anion exchange chromatography that revealed there was no net negative charge on the protein.

Our collaborator, Dr. C. Supuran, requested a minimum protein concentration of 0.1 mM for crystallization trials. Obtaining approximately 1 mg after reverse-phase HPLC and then 199 μM in 2 ml cleavage buffer after the

anion exchange column accomplished this. The reason for two different approaches to the final step of NBC3Ct purification was because Dr. Supuran was unable to obtain co-crystals of NBC3Ct and CAII. Although we found that CD spectra of the NBC3Ct prep was comparable to the CD spectra published by another member of the Casey lab, Dr. Fred Loiselle [124], we suspected that there was some protein denaturation resulting from the use of acetonitrile and trifluoroacetic acid used in reverse-phase HPLC or lyophilization that was inhibiting the interaction between NBC3Ct and CAII.

Due to this concern we attempted another approach, which maintained physiological buffering conditions and avoided denaturing processes. The anion exchange column was selected because the protein is retained on the resin by an electrostatic interaction and is eluted by an increase in the ionic strength of the buffer. Fortunately, there was no need for a change in any of the buffering conditions since NBC3Ct was not retained on the column while the contaminating proteins were. This resulted in NBC3Ct flowing through column in the same buffer in which it was loaded.

Although NBC3Ct and CAII associate through a weak electrostatic interaction the affinity that NBC3Ct has for CAII should be sufficient for crystallization. For example, the Fab fragment of the ferrochelatase antibody associates with its substrate mesoporphyrin IX (MP) with a Kd of 2.0 μM [180]. This interaction is far less favourable than the interaction between NBC3Ct and CAII (Kd of 101 nM [123]), but still obtained co-crystals that X-ray diffracted to a resolution of 1.8 Å [180]. High affinity associations are considered to be in the low nM range [181]; therefore the association of NBC3Ct is within the limits of attainable co-crystals due to binding affinity.

A co-crystal structure of NBC3Ct and CAII would be an important asset to understanding their interaction. This interaction is highly conserved throughout members of the bicarbonate transport family [19] and is important for another family of pH regulating transporters, the Na^+/H^+ exchanger (NHE) family [123]. CAII also produces H^+ upon hydration of CO_2, which is the substrate for the NHEs. The interaction between CAII and bicarbonate transporters is important for maintaining the metabolon, thereby maintaining a pool of available substrate in close proximity to the transporter. Having a pool of substrate available for transport ensures that the transporter is working at a maximal rate. When a catalytically inactive CAII (V143Y) is co-expressed with NBC3 in HEK 293 cells the rate of NBC3 activity is decreased by 31 ± 3%, as compared to cells transfected with NBC3 alone [123]. This data is consistent with the observation that AE1 is impaired by 61 ± 4% in the presence of the inactive CAII mutant [108, 117]. This is a significant reduction in activity and thus demonstrates the importance of a functional transport metabolon.

Obtaining a co-crystal structure of CAII and NBC3Ct will allow for a better understanding of how the two proteins interact. Disruption of the activity of NBC3 can lead to problems with hearing [137, 182], vision [137] and likely affects kidney function in the renal outer medullary collecting duct as it plays in important role for maintaining pH homeostasis [55, 56]. Loss of internal pH homeostasis in sensory receptors leads to a degeneration of the receptors in the eye and inner ear leading to Usher syndrome [137]. Although Usher syndrome is linked to a genetic disorder affecting the scaffolding proteins that bind NBC3 [139], it is likely that decreased NBC3 activity via disruption of the metabolon could have similar results. In fact, a genetic mutation found in CAIV prevents

the enzyme from interacting with NBC1, which disrupts the external metabolon and leads to a decrease in HCO_3^- transport via NBC1. This disruption in the metabolon leads to blindness. When CAIV does not associate with NBC1 the transport of HCO_3^- decreases. Cytosolic HCO_3^- concentration is now no longer sufficient to quench the acid load produced by active tissue [141]. Therefore, it is important to further understand the mechanism by which bicarbonate transport metabolons are regulated in order to prevent or treat diseases.

The co-crystal structure of NBC3Ct and CAII will be able to provide clues into the regulation of that metabolon and could also provide a model for other bicarbonate transport metabolons that are formed in a similar manner. Now that overproduction and purification of NBC3Ct has been achieved it is the co-crystallization that poses the next hurdle in our search for a structure.

Chapter 4

Regulation of the CAII/BT interaction[1]

[1]**Portions of this chapter are in the process of preparation for publication:**
McMurtrie, H.L., and Casey, J.R. Glutamate Regulates Bicarbonate Transport Metabolon Function

4.1 Introduction

A recent study demonstrated glutamate regulation of HCO_3^- transport in sweat gland epithelial cells [160]. This effect was noticed upon a decrease in HCO_3^- conductance across CFTR while there was an increase in Cl^- conductance [160]. Since glutamate is affecting HCO_3^- transport and glutamate is a negatively charged amino acid that is highly regulated throughout the body, we wanted to investigate the role of glutamate on the bicarbonate transport metabolon.

The bicarbonate transport metabolon is mediated by an electrostatic interaction between CAII and bicarbonate transporters. The interaction occurs between an acidic motif on the C-terminus of the bicarbonate transporter and a basic region on the N-terminus of CAII. This metabolon is important for maintaining maximal transport across the bicarbonate transporter as the substrate for transport, HCO_3^-, is channelled from CAII, which catalyzes the reversible hydration of CO_2 into HCO_3^-, to the opening of the bicarbonate transporter. Disruption of the metabolon leads to a decrease in transport.

Due to the negative charge on glutamate, we hypothesized that glutamate could interrupt the electrostatic interaction between CAII and a bicarbonate transporter. AE1 was used as a model bicarbonate transporter because there is a robust and well-documented interaction between CAII and AE1. While the AE1/CAII interaction is important, it is the Cl^-/HCO_3^- exchanger, SLC26A6, however, that is of most interest because of its relationship with CFTR. SLC26A6 associates with CFTR through its STAS domain [80]. SLC26A6 and CFTR are located in many of the same tissues, tissues that are affected in CF.

4.2 Results

4.2.1 CAII/AE1 binding in the presence of glutamate

Glutamate has important signalling properties in the human body and is thus in constant flux throughout the body. This important biomolecule may now also be linked to the regulation of HCO_3^- flux across a cell membrane as demonstrated in the sweat gland [160]. To further understand the regulation of HCO_3^- via glutamate flux the affinity of CAII for AE1 or SLC26A6 was measured in the presence of glutamate. A microtitre dish binding assay (Fig. 4.1) was used to determine the binding affinity of the bicarbonate transporters for CAII. The assay involved the incubation of purified GST-fusion proteins of the C-terminus of AE1 and SLC26A6 (Fig. 4.2, lanes 1 & 2, respectively) with purified CAII (Fig. 4.2, lane 4) that had been coupled to the bottom of a microtitre dish. The average affinity of CAII for AE1 is 120 ± 11 nM (n = 17) as determined by the microtitre CAII-binding assay (Fig. 4.3). This affinity was dramatically decreased with the increase in glutamate concentration resulting in an increase in Kd (Fig. 4.4A). In the presence of gluconate, however, there was no significant change in binding affinity (Fig. 4.4B). Increasing the concentration of glutamate created a saturable curve of the binding affinity of CAII for AE1, represented by the Kd (Fig. 4.5A). Glutamate has a half-maximal effect on the binding of CAII and AE1 at 7 ± 3 mM glutamate, which is within the physiological range of cytosolic glutamate levels [160]. Saturation occurs at around 10 mM glutamate and thus the difference between the binding affinity at 0 mM glutamate versus that at 10 mM glutamate provides a way to compare the effect of anions on binding affinity. Glutamate decreased CAII/AE1 binding affinity by 110 ± 17% comparing 0 and 10 mM

glutamate, whereas gluconate, aspartate and leucine have statistically insignificant ($p > 0.05$ from paired t-test, $n = 17$) differences of $8 \pm 10\%$, $17 \pm 5\%$ and $19 \pm 5\%$, respectively (Fig. 4.5B).

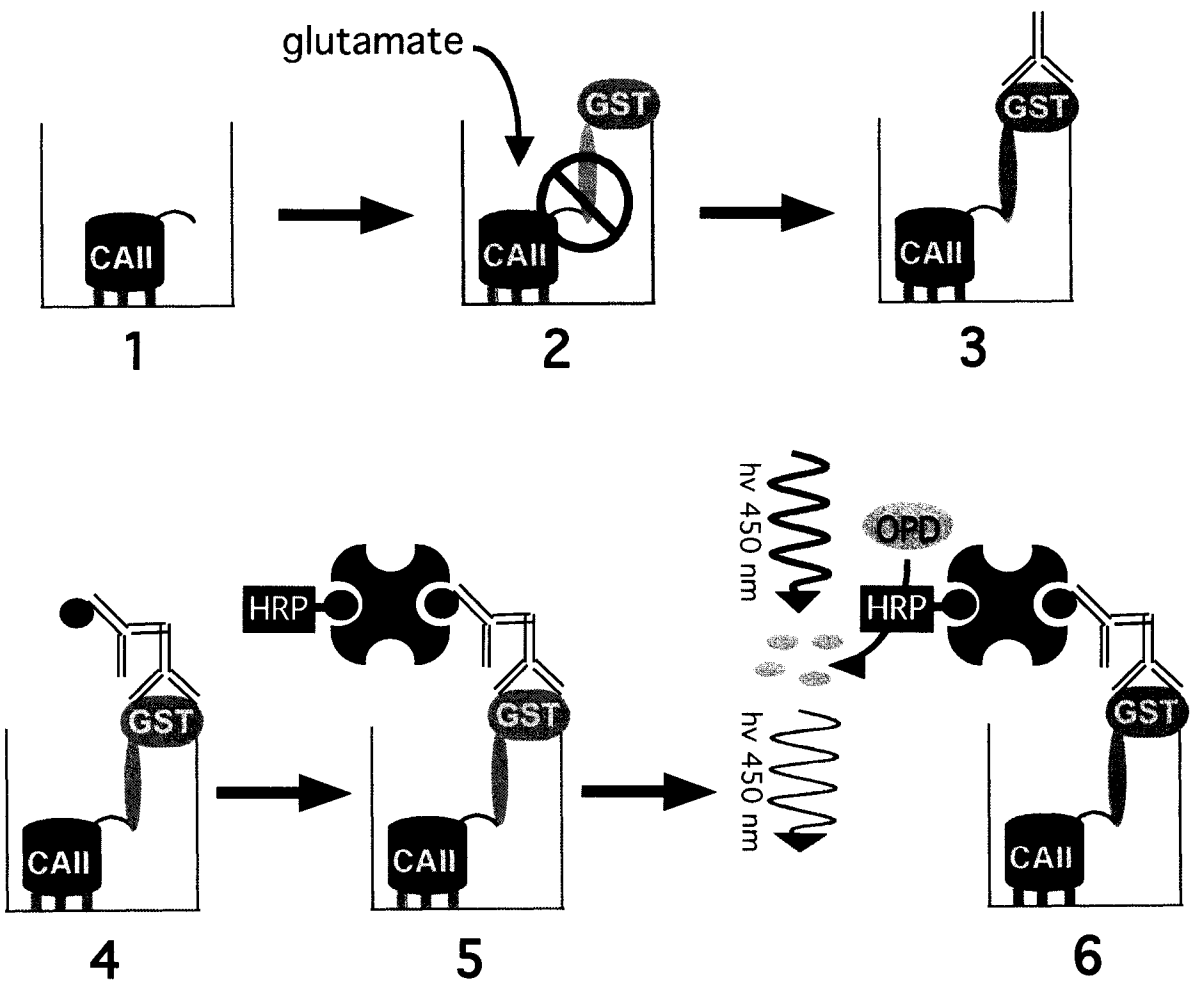

Figure 4.1: Microtitre dish binding assay.
The microtitre dish binding assay utilizes the principles of an enzyme linked immunosorbent assay (ELISA) [49]. The first protein is coupled to the bottom of the well by incubating CAII with carbodiimide for 30 min at room temperature (step 1). The GST fusion protein of either AE1Ct or SLC26A6Ct is added to the well and incubated with CAII overnight at room temperature (step 2). The GST fusion constructs were incubated with varying amounts of glutamate to detect the effect of glutamate on the interaction between CAII and bicarbonate transporters. After washing the plates, a GST antibody was used to probe for the presence of the fusion protein (step 3). A biotinylated secondary antibody detects the GST antibody (step 4) and a horseradish peroxidase (HRP) substrate conjugated to streptavidin was used to detect the biotinylated secondary antibody (step 5). The final step involved the cleavage of OPD substrate by HRP, which results in a change in absorbance that can be detected by a microtitre dish reader at a wavelength of 450 nm (step 6).

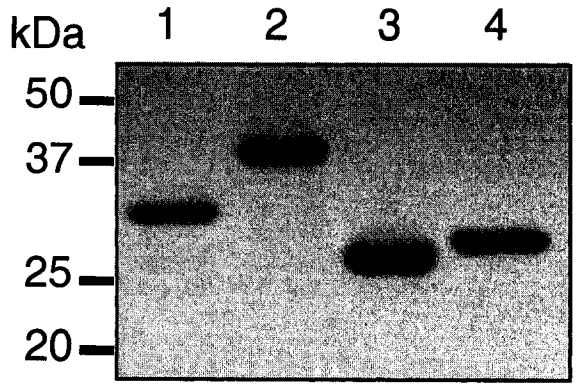

Figure 4.2: Purified GST fusion proteins and purified CAII for binding assay. Proteins were purified on glutathione sepharose resin (1-3) or on pAMBS resin (4) and then 5 μg were loaded on a 12.5 % SDS-PAGE gel and stained with Coomassie dye. Lanes 1 – 3 are GST-fusion proteins: 1) GST.AE1Ct, 2) GST.SLC26A6Ct, 3) GST alone. Lane 4 is purified CAII.

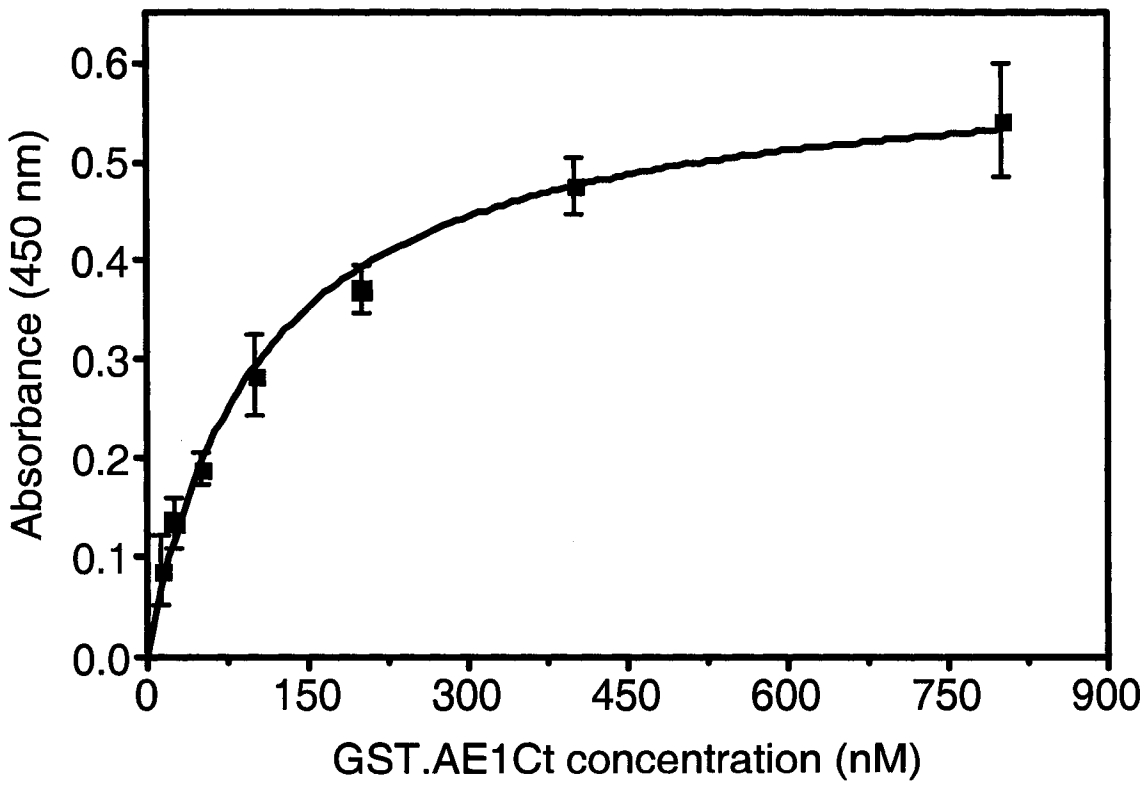

Figure 4.3: Binding curve of GST.AE1Ct binding to CAII.
Purified CAII (200 ng) was coupled to the bottom of each well. Varying amounts of purified GST.AE1Ct were added to the wells and incubated for 20 h at room temperature. The Kd determined from the binding curve is 120 ± 11 nM. Error bars represent the standard error of the mean, n = 17.

Figure 4.4: Representative binding curves demonstrating the affinity of CAII for AE1 in the presence of ions.
Buffers containing 0.5 mM, 1 mM, 5 mM, and 10 mM of glutamate (A) or gluconate (B) were used during the incubation of GST.AE1Ct with CAII coupled to the plate. A constant concentration of salt was maintained by varying the concentration of NaCl. The Kd of the curve is reported for each ionic concentration. Error bars represent the standard error of the trial, n = 3.

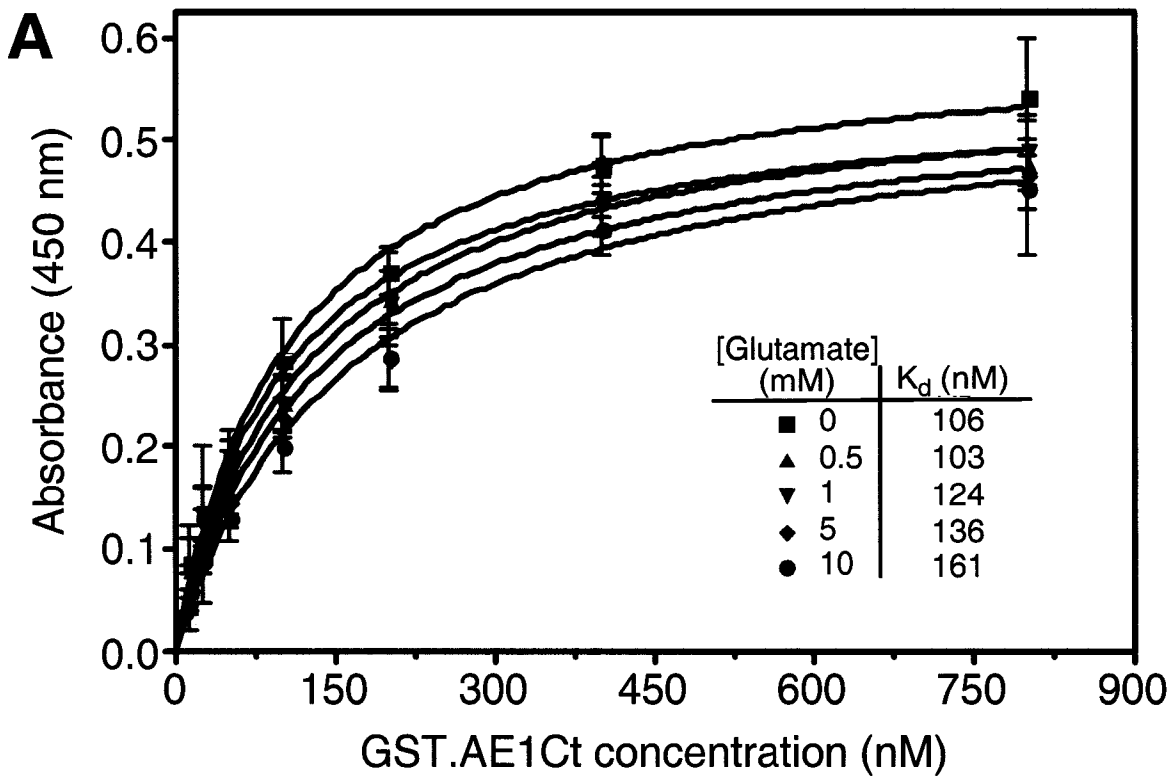

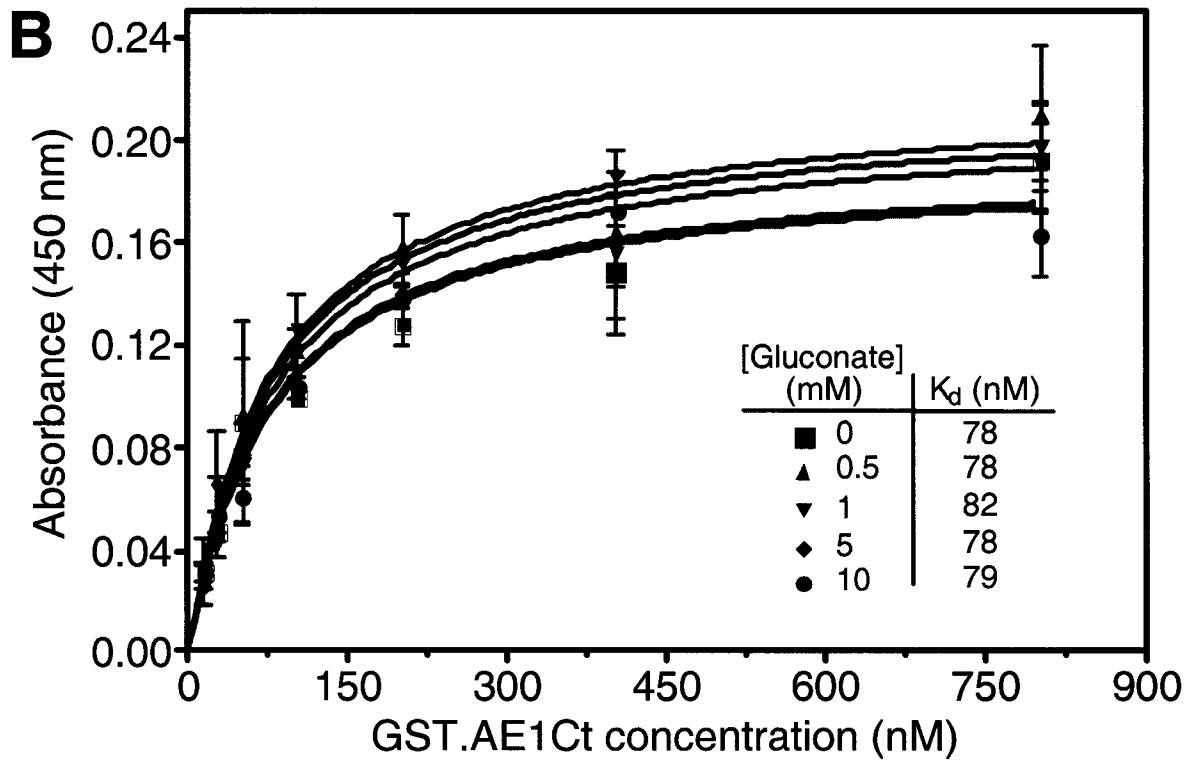

Figure 4.5: Effect of anions on CAII affinity for AE1.
A, The AE1/CAII Kd, obtained from the binding curves at each ion concentration, is plotted versus the concentration of glutamate present. B, The percent change in affinity is the difference of Kd at 0 mM and 10 mM divided by the Kd at 0 mM. Statistical significance for an n value of 17 was determined by a paired t-test in which $p < 0.05$ is significant. The error bars represent the standard error.

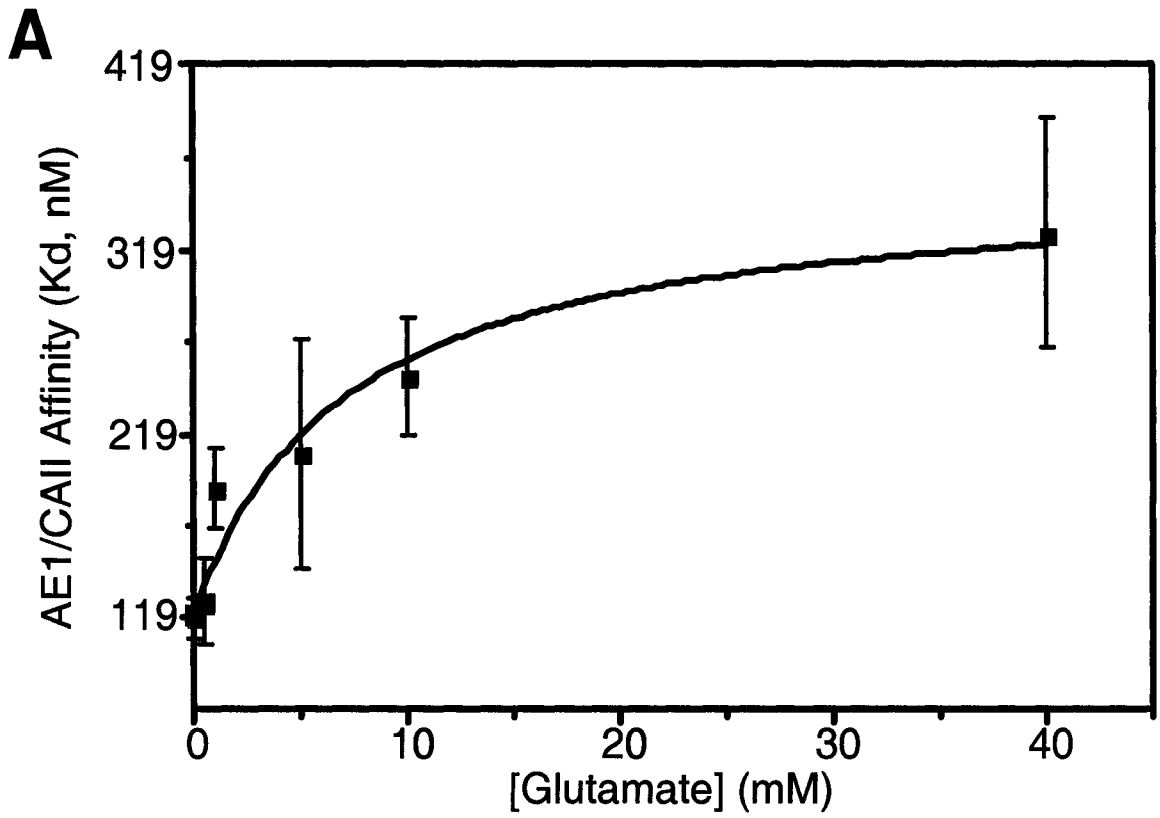

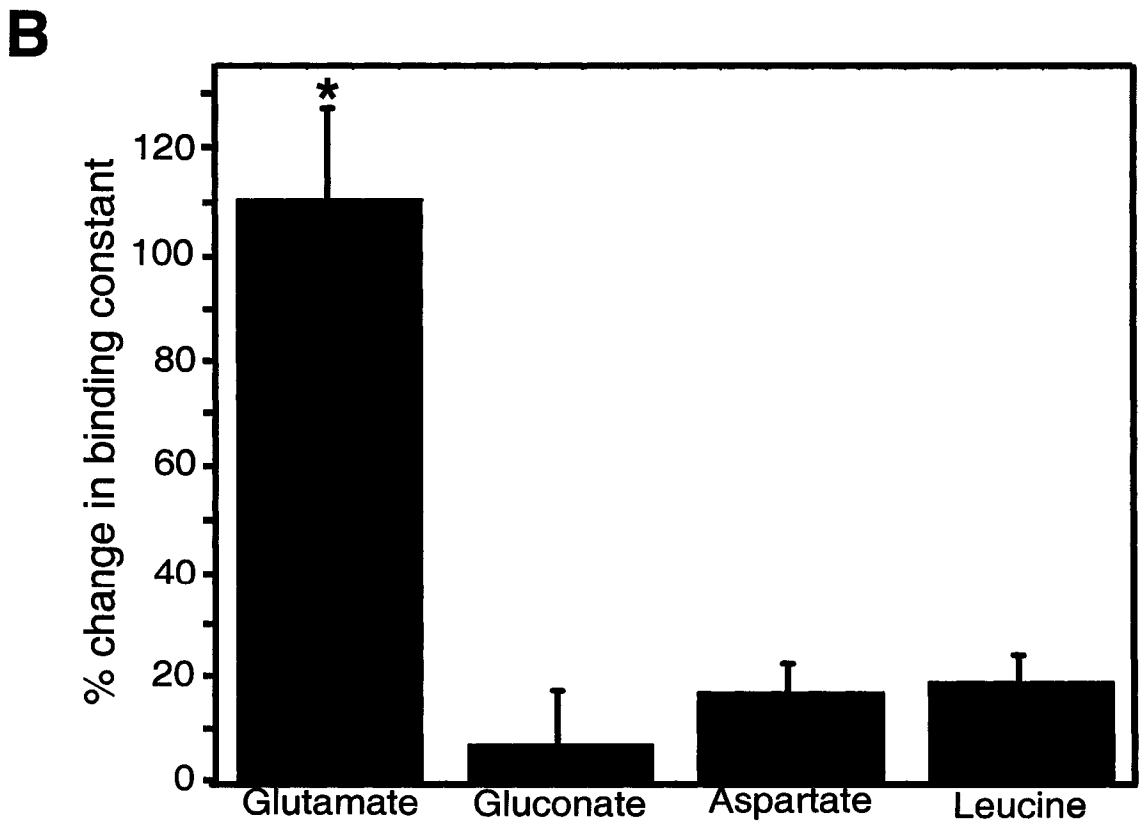

4.2.2 CAII/SLC26A6 binding in the presence of glutamate

Reddy and Quinton showed that the HCO_3^- flux through CFTR was affected by glutamate [160]. Given that CFTR associates with the STAS domain of SLC26A6 [80], we reasoned that glutamate could have an indirect effect on CFTR by disrupting the SLC26A6/CAII interaction, leading to the decrease in total HCO_3^- movement. The CFTR HCO_3^- conductance (CFTR-g_{HCO3-}) may in turn be representative of the state of HCO_3^- movement across the plasma membrane because SLC26A6 and CFTR are linked. We thus examined the effect of glutamate on the SLC26A6/CAII interaction.

A microtitre dish binding assay was used to determine the affinity of CAII for SLC26A6 (Fig. 4.1). Purified CAII was coupled to the bottom of each well to which purified GST.SLC26A6Ct was added (Fig. 4.2). The affinity of CAII for SLC26A6 in this assay was slightly stronger then that for AE1 with a determined Kd of 53 ± 7 nM, n = of 11 (Fig. 4.6). Similarly to AE1, glutamate had a negative affect on the affinity of CAII for SLC26A6. As the concentration of glutamate increased in the experimental system the Kd of CAII for SLC26A6 increased (Fig. 4.7A). The increase in Kd occurred to a saturable level at approximately 10 mM glutamate. This hyperbolic curve allowed for the determination of the half-maximal effect of glutamate on the binding. The half-maximal binding of glutamate is 4 ± 2 mM, lower than that for AE1 and CAII, but still in the physiological range of glutamate concentrations. When comparing the affinity of CAII for SLC26A6Ct at 10 mM glutamate to the affinity at 0 mM glutamate there is an 85 ± 2% decrease in affinity, n value of 11 (Fig. 4.7B). The corresponding change in the presence of gluconate was not statistically different ($p > 0.05$, paired t-test).

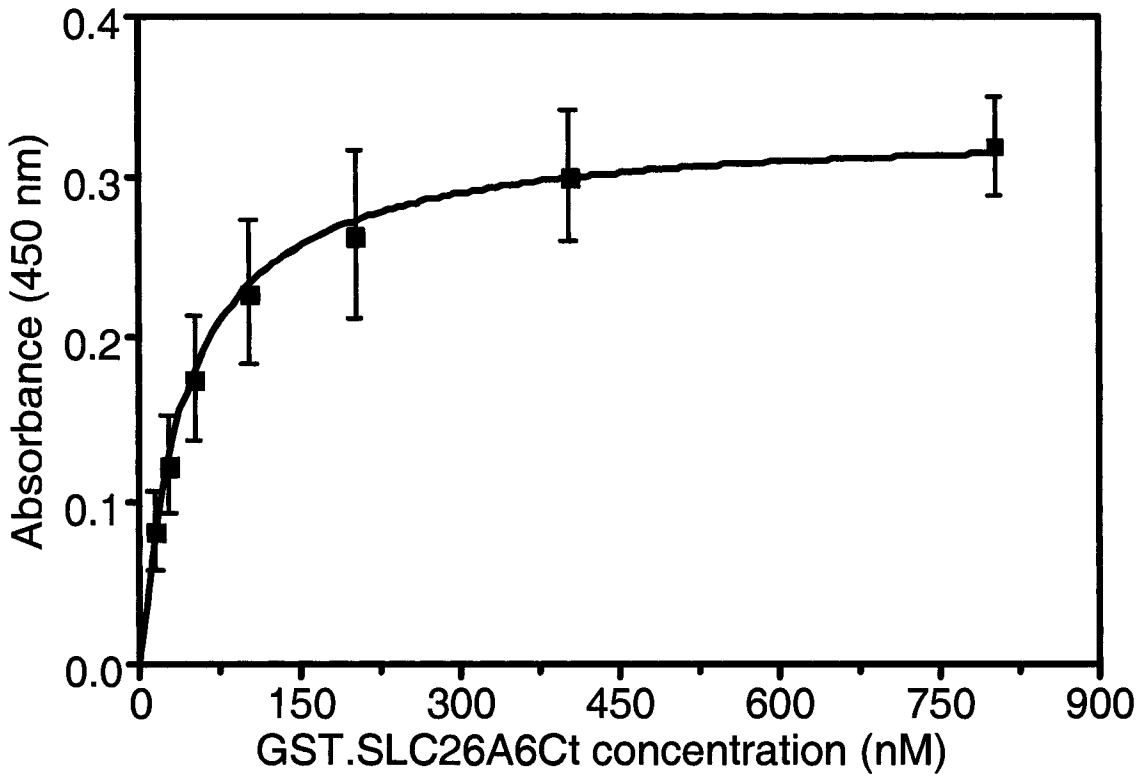

Figure 4.6: Binding curve of GST.SLC26A6Ct binding to CAII.
Purified CAII (200 ng) was coupled to the bottom of each well. Varying amounts of purified GST.SLC26A6Ct were added to the wells and incubated for 20 hours at room temperature. The Kd determined from the binding curve is 53 ± 7 nM. Error bars represent the standard error of the mean, n = 11.

Figure 4.7: Effect of anions on SLC26A6/CAII affinity.
A, The SLC26A6/CAII Kd, obtained from the binding curves at each ion concentration, is plotted versus the concentration of glutamate present. B, The percent change in affinity is the difference of Kd at 0 mM and 10 mM divided by the Kd at 0 mM. Statistical significance for an $n = 11$ was determined by a paired t-test in which $p < 0.05$ is significant. The error bars represent the standard error. Gluconate was the only control used because the regulation by glutamate on the SLC26A6/CAII interaction followed the same trend as the AE1/CAII interaction.

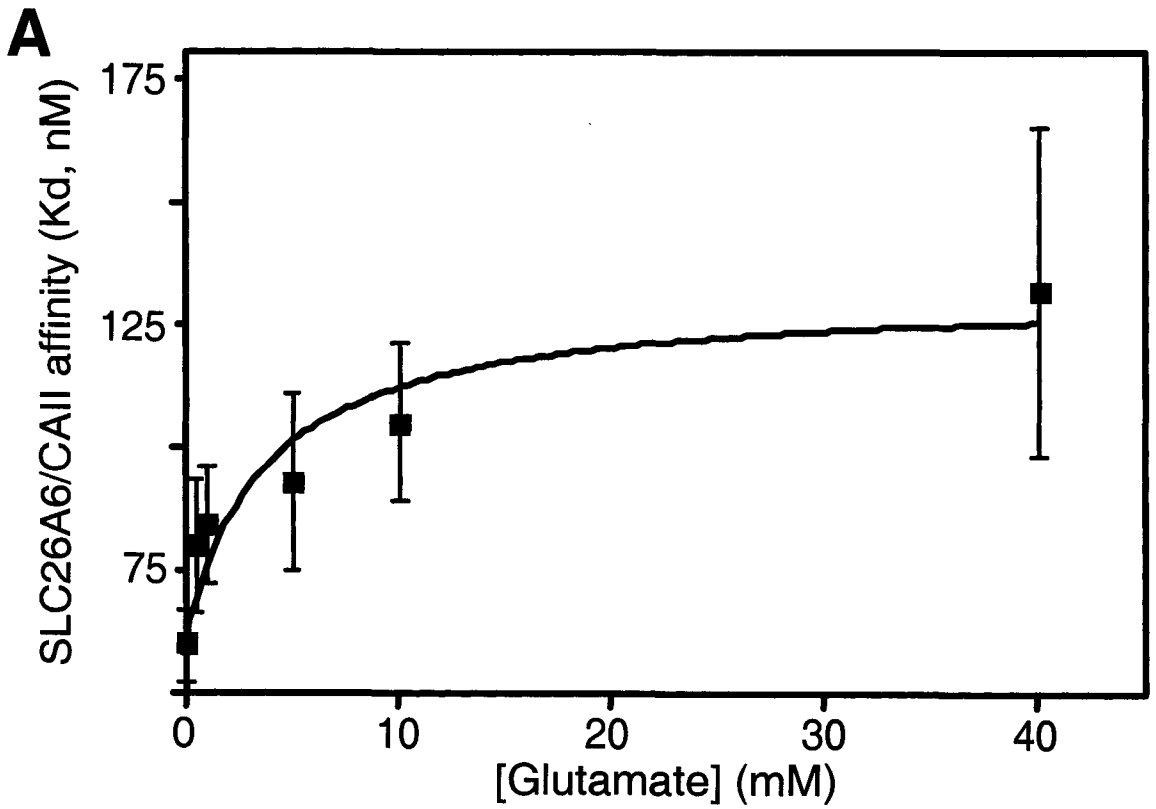

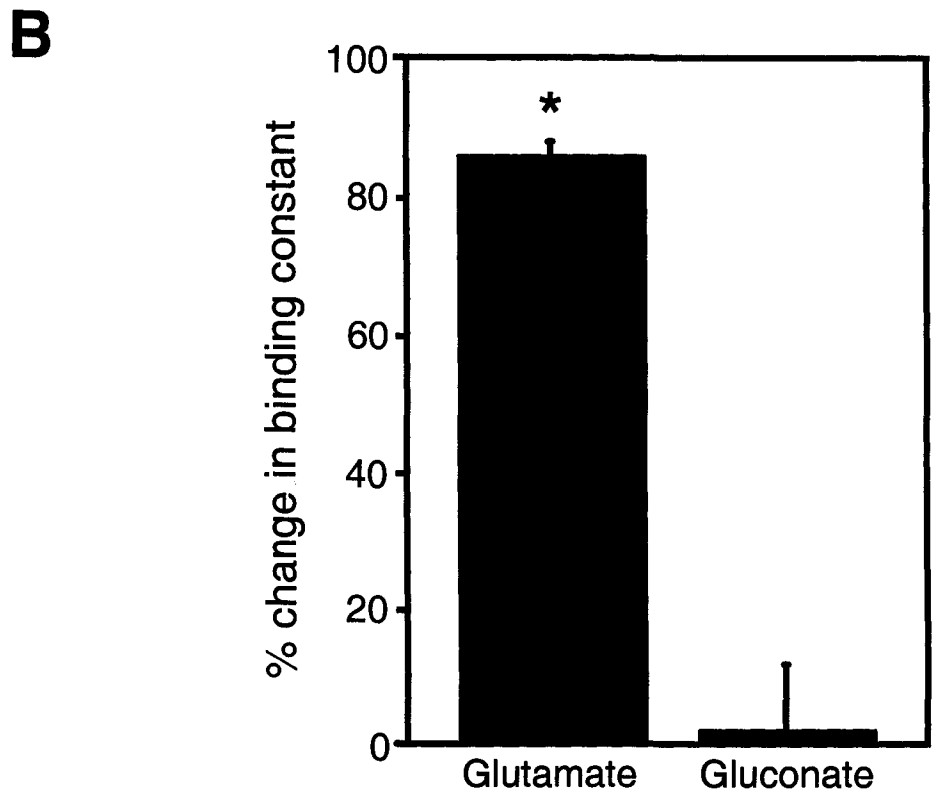

4.2.3 CAII activity

There are two criteria that CAII must meet for maximal transport of HCO_3^- through the metabolon to occur. First, CAII is required to be in close proximity to the transporter, and thus physically interact. Secondly, CAII needs to be functional. The evidence presented suggests that glutamate can disrupt the physical interaction between the bicarbonate transporter and CAII, but glutamate could also affect the activity of CAII. To address the second issue, CAII activity assays were performed in the presence of the anions previously mentioned (glutamate, gluconate, aspartate, and leucine). The activity of 1 μg of CAII was monitored over a pH range of 7 to 6.5 in the presence of 0 mM, 0.5 mM, 1 mM, 5 mM, 10 mM, and 40 mM glutamate (Fig. 4.8 A). Even at 40 mM, glutamate did not significantly affect the activity of CAII, n = 8 (paired t-test). Similarly, aspartate did not have a significant effect on the activity of CAII up to and including a concentration of 40 mM, n = 8 (Fig. 4.8 B). Leucine also did not affect the activity of CAII. The effect, however, was only tested until 10 mM leucine as it is insoluble at 40 mM, n = 8 (Fig. 4.9 A). Interestingly, gluconate did significantly affect CAII catalytic activity at 1 mM with the activity dropping to 72 ± 6% of the control (Fig. 4.9 B). Maximal inhibition of CAII by gluconate was reached at 5 mM gluconate when CAII activity was reduced by 34 ± 12%. Oddly, the activity of CAII recovered and reached 89 ± 16% of normal activity at 40 mM gluconate. No further tests were performed to address this anomaly because gluconate is not membrane permeable and likely does not have a real effect *in vivo*.

To validate the activity assay, CAII catalysis was tested in the presence of a known inhibitor, acetazolamide (ACTZ) (Fig. 4.10). Following the same

protocol, the activity of 1 μg of CAII was significantly ($p < 0.05$) inhibited, as expected, with as little as 5 nM ACTZ, reducing the activity by 43 ± 5%. Saturation of the inhibitory affect was reached near 25 nM when CAII activity was reduced to 30 ± 7% of the control, which is consistent with the potency of ACTZ (IC_{50} = 25 nM) determined by a 96 well plate hCAII activity assay [183]. Therefore glutamate can only be attributed to the disruption of the metabolon, the physical interaction between CAII and AE1 or SLC26A6, and not to any direct inhibition of CAII.

Figure 4.8: Catalytic activity of CAII in the presence of glutamate and aspartate. A, the activity of CAII was tested at different concentrations of glutamate (0, 0.5, 1, 5, 10, 40 mM). With an n of 8 for each trial there was no statistical difference ($p > 0.05$) between the activity of CAII at 0 mM and any of the glutamate concentrations as determined by a paired t-test. B, the activity of CAII was tested in different concentrations of aspartate (0, 0.5, 1, 5, 10, 40 mM). With an n of 8 for each trial there was no statistical difference ($p > 0.05$) between the activity of CAII at 0 mM and any of the aspartate concentrations as determined by a paired t-test.

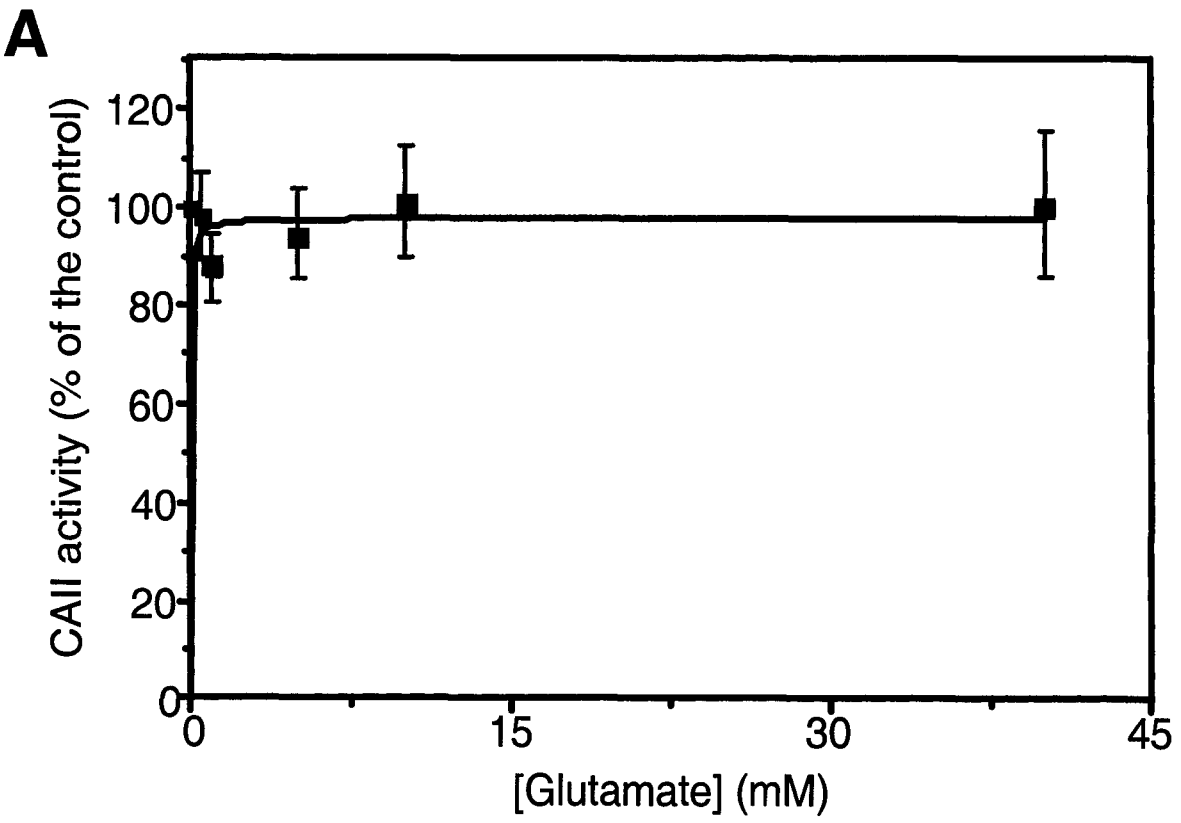

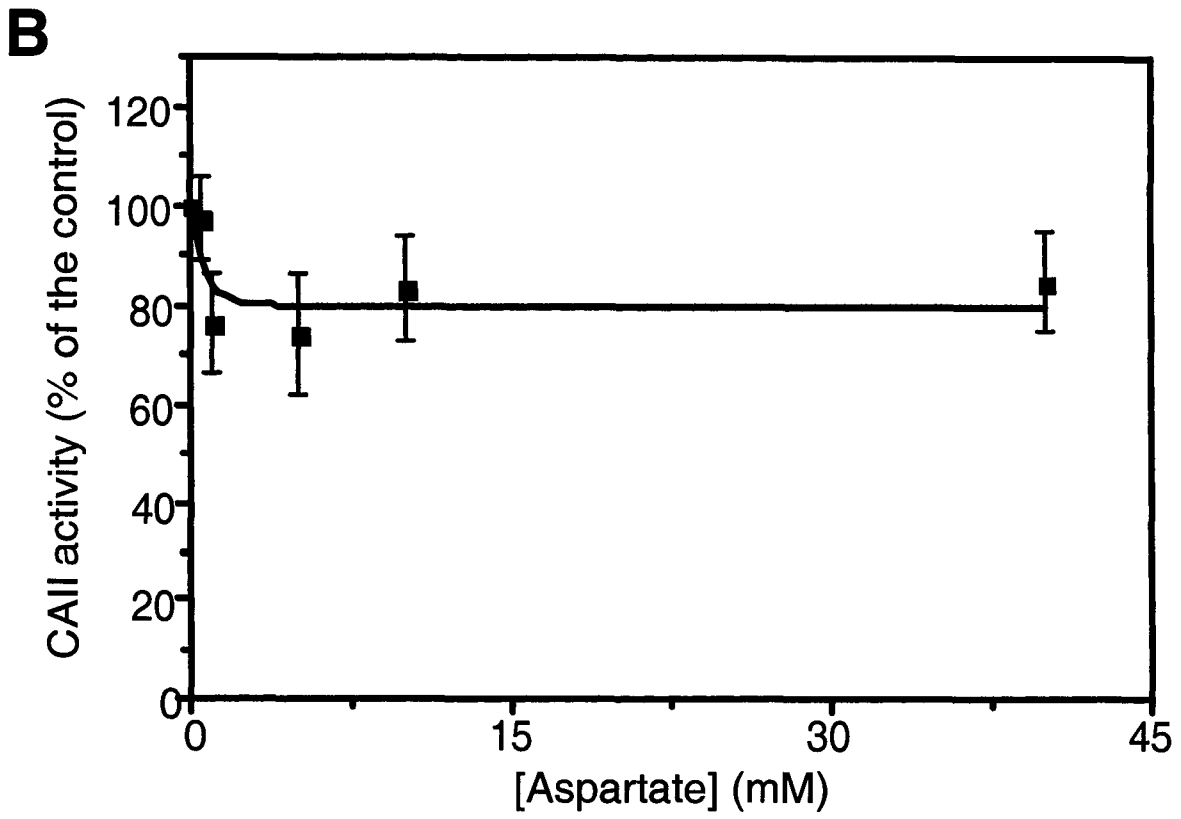

Figure 4.9: Catalytic activity of CAII in the presence of leucine and gluconate. A, the activity of CAII was tested in different concentrations of leucine (0, 0.5, 1, 5, 10 mM). With an n of 8 for each concentration there was no statistical difference ($p > 0.05$) between the activity of CAII at 0 mM and any of the leucine concentrations as determined by a paired t-test. B, the activity of CAII was tested in different concentrations of gluconate (0, 0.5, 1, 5, 10, and 40 mM). With an n of 8 for each concentration there was a significant reduction of CAII activity ($p < 0.05$) as determined by a paired t-test, as indicated by *. CAII activity was reduced to 72 ± 6% of normal CAII activity. Maximal inhibition was reached at 5 mM gluconate when activity was reduced to 66 ± 12% of the norm. CAII activity recovered with 40 mM gluconate, reaching 89 ± 16% of baseline activity.

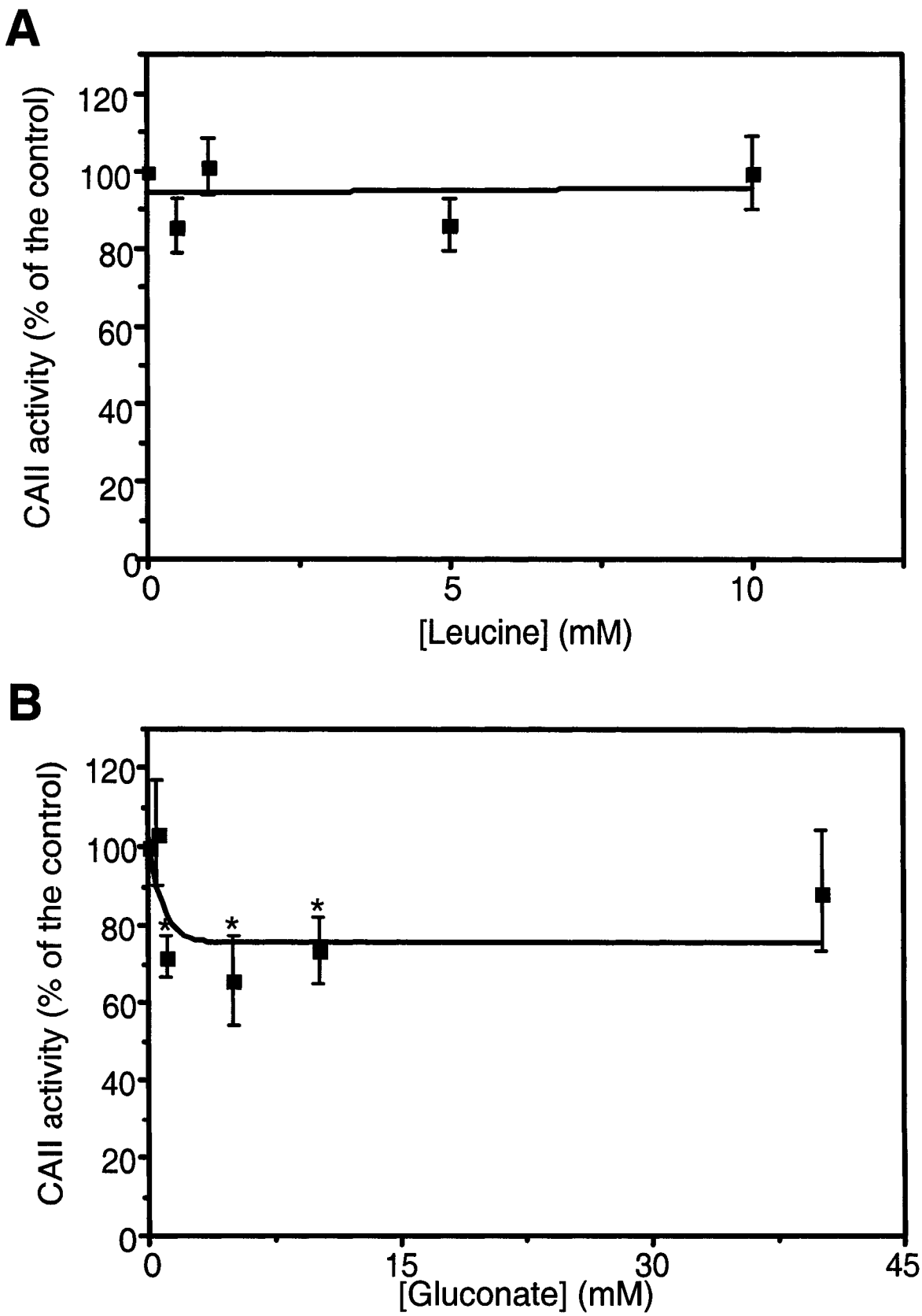

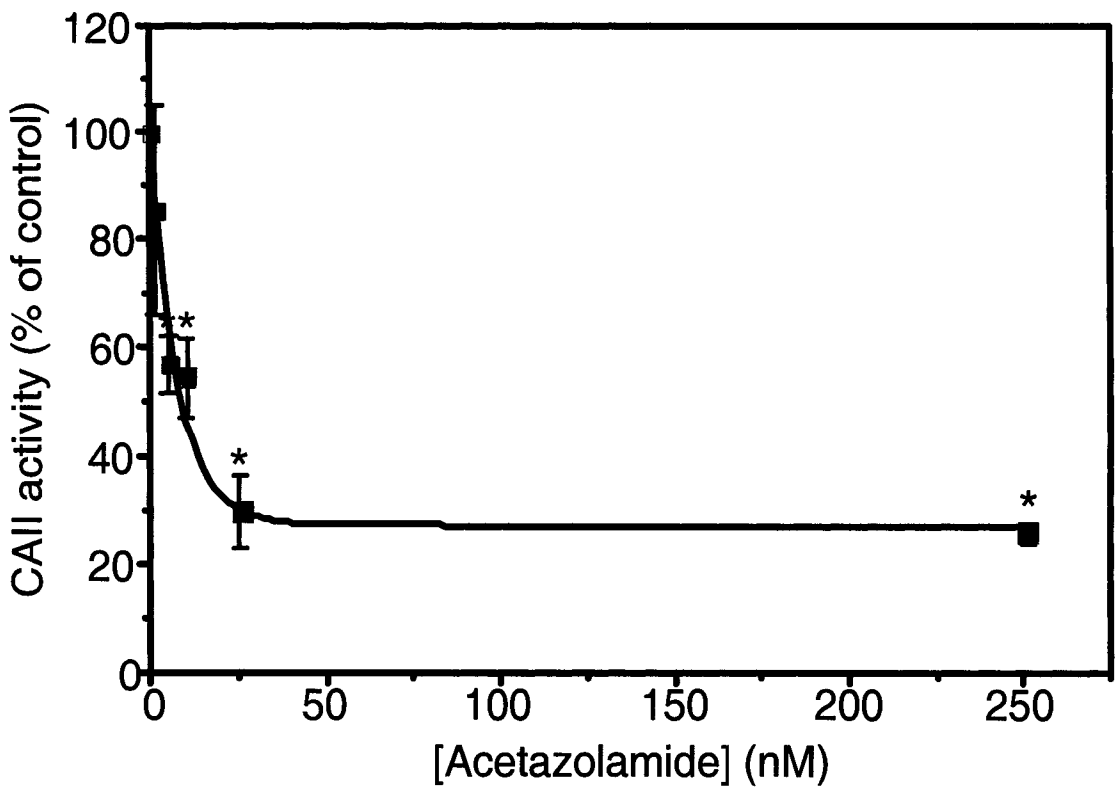

Figure 4.10: Activity of CAII in the presence of acetazolamide.
ACTZ was added to the sample buffer containing 1 μg of CAII at increasing concentrations (0, 1, 5, 10, 25, and 250 nM) with an n of 3 for each concentration. CAII activity was significantly ($p < 0.05$) inhibited with 5 nM ACTZ as determined by a paired t-test, as indicated by *, inhibiting CAII to 57 ± 5% of normal activity. Inhibition of catalytic activity reached saturation at about 25 nM, when CAII when CAII catalytic activity reached 30 ± 7% of the control.

4.3 Discussion

4.3.1 Effect of glutamate on CAII and BT binding

Glutamate, a small signalling molecule, has a profound effect on the interaction between CAII and bicarbonate transporters. It regulates the bicarbonate transport metabolon by disrupting the physical interaction between CAII and bicarbonate transporters, but does not regulate CAII catalytic activity. Glutamate, but no other ion tested, disrupted the interaction between CAII and AE1 or CAII and SLC26A6. Glutamate regulation is so specific that although aspartate and glutamate differ only in one additional hydrocarbon in the sidechain there is no discernible effect of aspartate on the binding of CAII and bicarbonate transporters. This may have to do with evolutionary regulation. Glutamate is in constant flux around the body, and acts as a signalling molecule in other processes, such as neuronal stimulation. Perhaps this molecule was also harnessed as a way of regulating the movement of HCO_3^- across the cellular plasma membrane.

Glutamate significantly reduced the affinity of CAII for AE1 by 110 ± 17%, which corresponded to a 132 ± 31 nM change in affinity. Similarly, the CAII/SLC26A6 interaction was reduced by 85 ± 2%. This shows conservation in glutamate regulation within two bicarbonate transport metabolons, suggesting this is a relevant finding. Additionally, the half-maximal effect of glutamate on the metabolon is approximately 5 mM, which is both in the physiological range and is consistent with the results by Reddy and Quinton who found that the half-maximal effect of glutamate on CFTR occurred at 3 mM [160]. Although glutamate significantly disrupted the CAII/bicarbonate transporter interaction, it

did not interfere with the activity of CAII. The lack of inhibition was verified by the ability to detect inhibition of CAII in the presence of ACTZ, a CAII inhibitor.

The important interaction between CAII and bicarbonate transporters is an electrostatic interaction since it is sensitive to pH, ionic concentration and temperature [116]. The presence of CAII at the C-terminus of a bicarbonate transporter increases the local concentration of HCO_3^- close to the pore of the transporter, providing the substrate for transport. If this interaction is disrupted there is a significant decrease in activity of the bicarbonate transporter [81, 94, 108, 118, 123]. The electrostatic interaction occurs between an acidic motif located on the C-terminus of the bicarbonate transporter and a basic region on the N-terminus of CAII [48, 107]. The electrostatic interaction is susceptible to high ionic strength and alkaline pH [49]. Therefore, it is not surprising that another factor, such as an acidic molecule like glutamate, would disrupt the interaction. Glutamate likely competes with the acidic CAB site on the bicarbonate transporters for association with the basic bicarbonate transporter binding site on CAII. Essentially, glutamate knocks CAII off the C-terminal tail of the bicarbonate transporter or prevents CAII from associating with it. It is not unreasonable that glutamate may be a regulator in epithelial cells since many glutamate receptors localize to the epithelial plasma membrane [160, 161].

4.3.2 Physiological relevance for regulation by glutamate

Glutamate must be able to enter, or exit, all types of cells because it is an important molecule for energy metabolism [168] in addition to being an important signalling molecule. Considering the important role that glutamate transporters play, there is relatively little known about their molecular structure

and kinetic properties [184]. Four glutamate transporters have been identified in tissue outside of the central nervous system [168]. These transporters, GLAST1 (EAAT1), GLT-1 (EAAT2), EAAC1 (excitatory amino acid carrier, EAAT3) and EAAT4 all belong to the excitatory amino acid transporter family (EAAT) [166]. EAATs are concentrative Na^+-dependent glutamate transporters and are located in the basolateral membrane of many polarized cells, including pancreatic cells [168]. Of those four, EAAC1 has been located in tissue where bicarbonate transporters are also present such as heart [185], intestine [168, 186, 187], lung [166], pancreas, kidney and liver [168], lending support to glutamate acting as a bicarbonate transport regulator.

Glutamate transport utilizes the Na^+ gradient to maximize the speed of glutamate transport. Three Na^+ and one H^+ are coupled to one glutamate molecule with counter transport of one K^+ molecule [188, 189]. Glutamate transporters are predicted to have three or five independently working subunits each with 8 transmembrane spanning domains [184]. Fluorescence resonance energy transfer (FRET) analysis demonstrated small conformational changes around the glutamate-binding site, which could contribute to the fast kinetics of the glutamate transporters [184]. The mechanism for glutamate transport regulation within epithelial cells is still under investigation.

Because of the Na^+-dependence of glutamate transporters, glutamate transport is affected during ischemia. During an ischemic attack there is a lack of glucose and oxygen delivered to the cell. The loss of essential nutrients leads to a collapse of the Na^+ gradient across the plasma membrane [190]. Glutamate can no longer be cleared from the synaptic cleft because of its dependence on the Na^+ gradient [190]. The presence of glutamate in the synapse overstimulates

glutamate receptors, which causes an influx and an accumulation of Ca^{2+} and Na^{+}. The presence of excess Na^{+} will reverse the Na^{+}/Ca^{2+} exchanger, accumulating even more Ca^{2+} leading to rapid swelling and subsequent neuronal death within a few hours [191]. A similar response is possible in epithelial cells. Glutamate may be prevented from entering the cell and could thus no longer interfere with the CAII/bicarbonate transport interaction. This would allow the NBCs to continue working at optimal levels, pumping in more HCO_3^- and Na^{+}, contributing to the lethal accumulation of Na^{+}. Had glutamate been able to enter the cell, then it may have been able to disrupt the interaction between CAII and NBC1.

We have demonstrated that glutamate interferes with the CAII/bicarbonate transporter interaction, however the CAB motifs on the C-terminus of AE1 and SLC26A6 contain aspartic acid residues rather than glutamate residues. This implies that the competition for the basic region on CAII is between two different amino acids. Does glutamate interact with basic regions more tightly than aspartate? Perhaps if the CAB site were mutated to contain glutamate residues the disruption of the interaction would be less severe. More likely the strength of the effect by glutamate has to do with evolutionary regulation. Glutamate is in constant flux around the body, and acts as a signalling molecule to other membrane bound proteins, such as glutamate receptors in neuronal cells. Perhaps this molecule was also harnessed as a way of regulating HCO_3^- transport across the cellular plasma membrane.

4.3.3 Relationship between CFTR and bicarbonate transporters

The attention for this research first started from the discovery that glutamate affected CFTR. In sweat gland epithelial cells the activity of CFTR-g_{Cl-} was activated, but the CFTR-g_{HCO3-} was not [160]. This may indicate an intricate relationship between CFTR and bicarbonate transporters. When CFTR is activated by glutamate, there is only Cl^- available for transport because the supply of available HCO_3^- is diminished. Perhaps glutamate regulates Cl^- movement in CFTR, by decreasing HCO_3^- flux. As previously mentioned, it is interesting that both the Km of CFTR activation and the half-maximal effect of glutamate on the CAII/bicarbonate transporter interaction is in the same approximate range. The Km for CFTR is approximately 3 mM [160] while the half-maximal effect on the CAII/AE1 interaction is 7 mM and 4 mM for the CAII/SLC26A6 interaction, both of which are in the physiological range of ~10 mM cytosolic glutamate [192, 193]. Furthermore, as in the sweat glands, gluconate, aspartate, and leucine did not have an effect on the interaction between CAII and the bicarbonate transporters. This leads to the theory that CFTR and bicarbonate transporters work together to regulate HCO_3^-, perhaps in a feedback mechanism. There is evidence that CFTR physically interacts with two bicarbonate transporters, SLC26A6 and NBC3 [80, 159]. The bicarbonate transporters interact with CFTR at a site that is separate from the CAII binding site, which in theory leaves room for CAII to also be brought into the complex. This theory is supported by the co-localization of CAII and CFTR in the microvilli of rat bile duct brush cells when AE2 is also present [194].

If this theory is valid and CFTR, SLC26A6 and CAII form a complex, the next step is to look for the complex *in vivo*. It will also be interesting to see if CFTR in fact regulates SLC26A6 activity or if it is actually the activity of

SLC26A6 that regulates CFTR-g_{HCO3-} (Fig. 4.11). Given what we have learned from these experiments, it is likely the association of CAII to the complex that regulates HCO_3^- activity.

4.3.4 Conclusion

Use of the microtitre dish binding assay identified another mechanism for HCO_3^- transport regulation. Glutamate significantly disrupted the interaction between CAII and two separate bicarbonate transporters, AE1 and SLC26A6. Since a disruption in the metabolon is known to decrease HCO_3^- transport, this evidence implies an important role of glutamate in the regulation of the HCO_3^- transport metabolon.

Figure 4.11: Model for glutamate regulation of bicarbonate transport.
A, Full transport activity of SLC26A6 occurs when CAII and SLC26A6 interact (left panel). In the presence of glutamate CAII is displaced from the C-terminus of SLC26A6, thereby decreasing HCO_3^- transport (right panel). B, In epithelial cells co-expressing CFTR and SLC26A6, interaction between these ion moving pathways may occur. Glutamate displaces CAII from the C-terminus of SLCA26A6. If CAII also provides the HCO_3^- that flows through CFTR, then the displacement of CAII will diminish the pool of available HCO_3^- for CFTR. Therefore a decrease in HCO_3^- flux through CFTR could allow more space for Cl^- to move through CFTR. The CFTR/SLC26A6 occurs through the CFTR R domain and the SLC26A6 STAS domain [80].

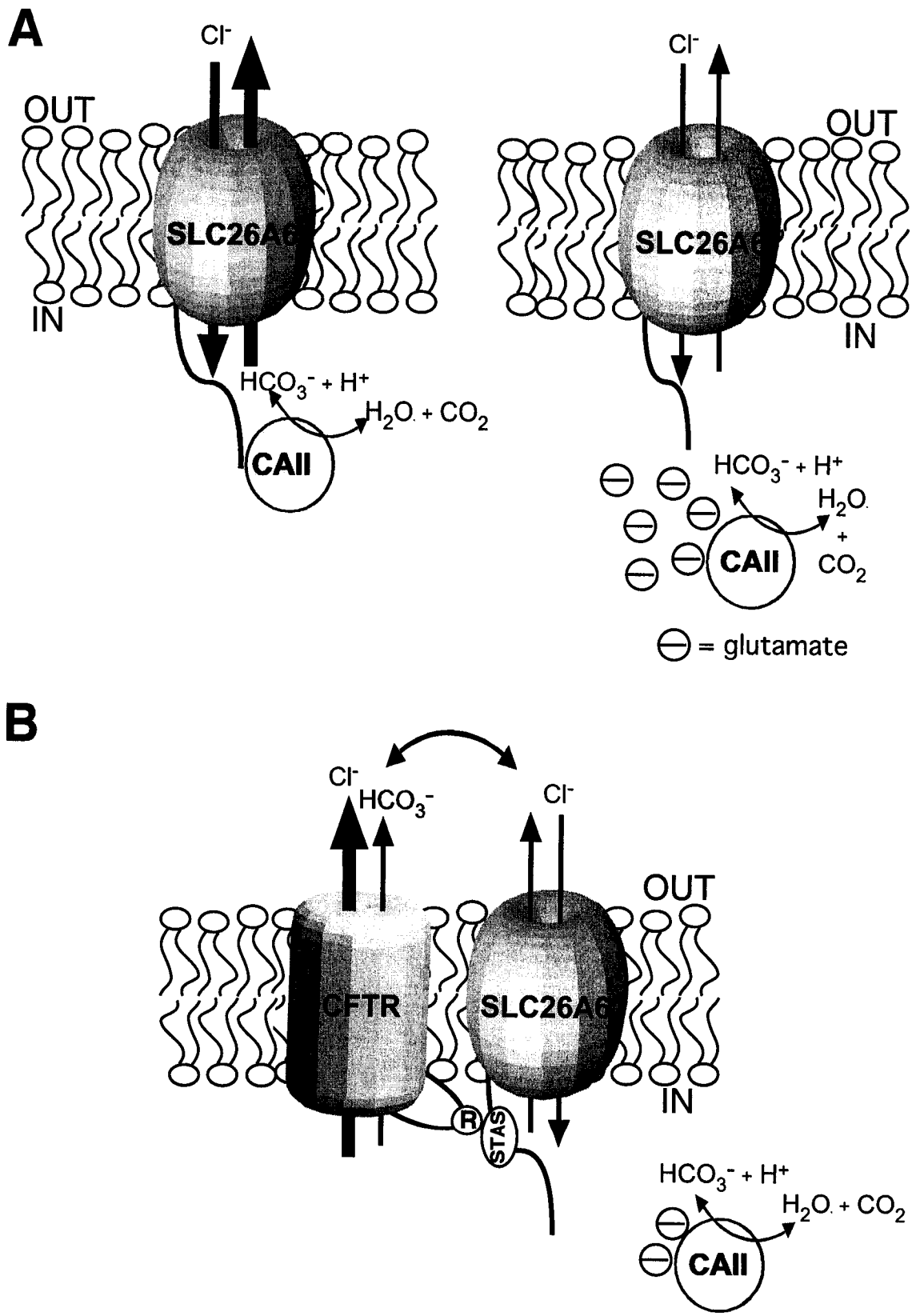

Chapter 5

Summary and Future Directions

5.1 Summary

The bicarbonate transport metabolon is a physical interaction between a bicarbonate transporter and a CA enzyme. This interaction can occur on the intracellular or extracellular surface of the plasma membrane generating a microenvironment of high substrate concentration on one side and an area of low substrate concentration on the other. Manipulation of the microenvironmental substrate concentrations aids in maximizing the activity of the transporter by creating a concentration gradient across the cell membrane. The importance of this interaction is highlighted by the dramatic decrease in activity when the CA enzyme is inhibited [18, 94, 108, 121, 123]. There are times when optimal activity of the bicarbonate transporter is undesirable. For instance, during a myocardial infarction the overcompensation by pH regulating proteins, including bicarbonate transporters, during the initial acidification of the cell is more detrimental to the myocardiocytes than the acidification itself [144, 145, 195, 196]. It would therefore be beneficial to determine ways to regulate the association of CA and bicarbonate transporter.

A structure of CAII in contact with the binding site of a bicarbonate transporter would provide a good reference for identifying sites of regulation and interaction. We have moved one step closer to obtaining the structure of CAII in contact with the C-terminus of NBC3. I was able to purify large quantities of NBC3Ct and determined that it maintained structural integrity throughout the process.

Although my purified CAII was not used for co-crystallization with NBC3Ct, I was successful in this attempt and have subsequently used it to study the interaction of two other bicarbonate transporters, AE1 and SLC26A6, with

CAII. I successfully optimized a protocol to look at the affinity of CAII for these bicarbonate transporters in the presence of a highly regulated biomolecule. The biomolecule glutamate plays an important role in regulating ion channels in neurons and other epithelial cells [160] and was therefore hypothesized to have an affect on the bicarbonate transporters. Glutamate does interfere with the binding of CAII and bicarbonate transporters. A notable decrease in affinity of between 85% and 120% was measured for both CAII/AE1 and CAII/SLC26A6. Most importantly glutamate had a half-maximal affect on the binding at physiological levels of glutamate. These levels of glutamate also agree with the levels of glutamate that affected the conductance of HCO_3^- through CFTR [160].

A model for how glutamate may regulate HCO_3^- flux across epithelial plasma membrane can thus be drawn from findings in the literature and what is reported in this thesis (Fig. 4.11). CFTR associates with at least two bicarbonate transporters, SLC26A6 [80] and NBC3 [159], both of which associate with CAII [81, 123]. The bicarbonate transporter can thus bring CAII into complex with CFTR. Since CFTR also conducts HCO_3^-, CAII can provide the substrate to the opening of the channel, changing the concentration of HCO_3^- in the microenvironment surrounding the channel (Fig. 4.11). Alternatively, it may not be CAII that provides the HCO_3^- for conductance through CFTR but rather the bicarbonate transporter. As SLC26A6 or NBC3 transports HCO_3^- across the plasma membrane it changes the HCO_3^- concentration surrounding the opening of CFTR. This change in substrate concentration can then increase the conductance of HCO_3^- resulting in a decrease in Cl^- conductance due to competition for the opening of the channel (left panel Fig. 4.11). This would explain why there is a decrease in CFTR-g_{HCO3-} upon addition of glutamate to the

system (right panel Fig 4.11). This is physiologically plausible since glutamate transporters are expressed in the same tissues as bicarbonate transporters and CFTR and the transporters could control the local concentration of glutamate thereby regulating HCO_3^- and subsequently Cl^- conductance.

5.2 Future Directions

The bicarbonate transport metabolon is an important interaction for maintaining maximal flux of HCO_3^- across the membrane. The effect is found across most bicarbonate transporter proteins identified to contain a CAII binding site, indicating that it is a highly specific and well-conserved interaction. Because of this specificity it is likely there are multiple ways to regulate the interaction. Some types of regulation have already been identified, and this work has identified another biomolecule involved in the regulation. The search for new regulating factors, however, is not over. An X-ray crystal structure of the NBC3Ct and CAII will be extremely important for identifying other potential sites of regulation. The largest roadblock to obtaining the structure appears to be obtaining a form of the purified NBC3Ct that is conducive to binding with CAII. This may require further exploration into the buffers used throughout the purification process.

Glutamate interrupts the binding of CAII with bicarbonate transporters. This is a significant effect *in vitro;* however it is still necessary to demonstrate this effect *in vivo*. Multiple steps need to be taken to support the predicted model of regulation. It is necessary to first identify the association of CAII with the CFTR/SLC26A6 or CFTR/NBC3 complex. Association of the three proteins would support a reciprocal affect of glutamate on CFTR by disruption of the

CAII/bicarbonate transporter metabolon. This would suggest that they are in the same environment and a decrease in available HCO_3^- for the bicarbonate transporters could result in a decrease in the available pool of substrate for CFTR to transport. Work on demonstrating this large complex has begun. I have attempted to co-immunoprecipitate CFTR in complex with SLC26A6 and CAII. Unfortunately, time constraints and difficulties with expressing CFTR in HEK293 cells have prevented me from obtaining these results prior to submission of my thesis.

We have also considered other approaches to determining the formation of the complex. Complexes can be identified through blue-native gels. Blue-native (BN) gels are non-denaturing poly-acrylamide gels. Solubilized cell lysates in non-denaturing sample buffer are run on the BN-gel and the intact protein complexes can be resolved based on their charge to mass ratio. Once the complexes are resolved on the gel, two different methods can be used to identify the members of the complex. Firstly, the BN-gel can be transferred to PVDF membrane and antibodies can detect members of the complex in the same manner as SDS-PAGE immunoblots. Proteins are determined to be in a complex if there are overlapping bands for CAII, CFTR and SLC26A6 or NBC3 on the immunoblot. The problem with this approach is that interacting proteins may hide the antibody epitopes or the epitopes are not exposed at the surface when the proteins are in their native conformations. The second approach avoids this problem by further resolving the protein complexes in a second denaturing gel. The lanes in the BN-gel are excised and placed horizontally on the top of a second denaturing gel and run in a denaturing anode buffer. The members of the complex are resolved according to their molecular weight and then

transferred to an immunoblot for antibody detection. Members of a complex will be located in the same lane on the second gel. The problem with this approach is that the excised lane from one gel does not fully adhere to the second gel and can therefore cause smearing of proteins in the second gel. This makes it difficult to identify when members of the complex are in the same lane as there is not a straight lane to follow.

Once a physical interaction between CAII, CFTR and bicarbonate transporters has been identified it is necessary to demonstrate that glutamate has an effect on the transport of HCO_3^- via SLC26A6 or NBC3. Transport activity assays can be used to show if there is a change in bicarbonate transport activity in the presence of glutamate. From this the Km of bicarbonate transporters in the presence of glutamate can be determined and possibly linked to physiological levels of glutamate.

To apply this research clinically it would be interesting to determine which bicarbonate transporters are located in and interact with CFTR in CF tissue. CF largely affects the lung, pancreas and sweat gland tissue. Several bicarbonate transporters have been detected in these tissues [22, 29, 31, 32, 69, 73, 197-199] but only one transporter, DRA, has been linked directly to CFTR *in vivo* [199]. Furthermore, the main bicarbonate transporter in the sweat gland has not yet been identified. There is speculative evidence to link SLC26A6 to the sweat gland [73, 197] but this has not yet been confirmed. If bicarbonate transporters and CFTR are determined to interact in tissue then the regulation by glutamate can be studied in mammalian tissue and perhaps a better understanding of bicarbonate transport regulation *in vivo* can be reached.

Bibliography

1. Pucéat, M., *pH_i regulatory ion transporters: an update on structure, regulation and cell function.* Cell Mol Life Sci, 1999. **55**(10): 1216-1229.

2. Richards, S.M., Jaconi, M.E., Vassort, G., and Puceat, M., *A spliced variant of AE1 gene encodes a truncated form of Band 3 in heart: the predominant anion exchanger in ventricular myocytes.* J Cell Sci, 1999. **112**(Pt 10): 1519-1528.

3. Ives, H.E. and Rector, F.C., Jr., *Proton transport and cell function.* J Clin Invest, 1984. **73**(2): 285-290.

4. Sardet, C., Counillon, L., Franchi, A., and Pouysségur, J., *Growth factors induce phosphorylation of the Na^+/H^+ antiporter, a glycoprotein of 110 kD.* Science, 1990. **247**: 723-726.

5. Sardet, C., Franchi, A., and Pouyssegur, J., *Molecular cloning, primary structure, and expression of the human growth factor-activatable Na^+/H^+ antiporter.* Cell, 1989. **56**(2): 271-280.

6. Loh, S.H., Chen, W.H., Chiang, C.H., Tsai, C.S., Lee, G.C., Jin, J.S., Cheng, T.H., and Chen, J.J., *Intracellular pH regulatory mechanism in human atrial myocardium: functional evidence for Na^+/H^+ exchanger and Na^+/HCO_3^- symporter.* J Biomed Sci, 2002. **9**(3): 198-205.

7. Rakonczay, Z., Jr., Fearn, A., Hegyi, P., Boros, I., Gray, M.A., and Argent, B.E., *Characterization of H^+ and HCO_3^- transporters in CFPAC-1 human pancreatic duct cells.* World J Gastroenterol, 2006. **12**(6): 885-895.

8. Paillard, M., *H^+ and HCO_3^- transporters in the medullary thick ascending limb of the kidney: molecular mechanisms, function and regulation.* Kidney Int Suppl, 1998. **65**: S36-41.

9. Kopito, R.R., *Molecular biology of the anion exchanger gene family.* Int. Rev. Cytol., 1990. **123**: 177-199.

10. Sekler, I., Lo, R.S., and Kopito, R.R., *A conserved glutamate is responsible for ion selectivity and pH dependence of the mammalian anion exchangers AE1 and AE2.* J. Biol. Chem., 1995. **270**: 28751-28758.

11. Reddy, M.M. and Quinton, P.M., *Selective activation of cystic fibrosis transmembrane conductance regulator Cl^- and HCO_3^- conductances.* J. Pancreas, 2001. **2**(4 Suppl): 212-218.

12. Clarke, L.L., Stien, X., and Walker, N.M., *Intestinal bicarbonate secretion in cystic fibrosis mice.* Jop, 2001. **2**(4 Suppl): 263-267.

13. Wright, A.M., Gong, X., Verdon, B., Linsdell, P., Mehta, A., Riordan, J.R., Argent, B.E., and Gray, M.A., *Novel regulation of cystic fibrosis transmembrane conductance regulator (CFTR) channel gating by external chloride.* J Biol Chem, 2004. **279**(40): 41658-41663.

14. Wang, X., Lytle, C., and Quinton, P.M., *Predominant constitutive CFTR conductance in small airways.* Respir Res, 2005. **6**(1): 7.

15. Ko, S.B., Shcheynikov, N., Choi, J.Y., Luo, X., Ishibashi, K., Thomas, P.J., Kim, J.Y., Kim, K.H., Lee, M.G., Naruse, S., and Muallem, S., *A molecular mechanism for aberrant CFTR-dependent HCO_3^- transport in cystic fibrosis.* EMBO J, 2002. **21**(21): 5662-5672.

16. Hug, M.J., Tamada, T., and Bridges, R.J., *CFTR and Bicarbonate Secretion to Epithelial Cells.* News Physiol Sci, 2003. **18**: 38-42.

17. Choi, J.Y., Muallem, D., Kiselyov, K., Lee, M.G., Thomas, P.J., and Muallem, S., *Aberrant CFTR-dependent HCO_3^- transport in mutations associated with cystic fibrosis.* Nature, 2001. **410**(6824): 94-97.

18. Sterling, D. and Casey, J.R., *Bicarbonate Transport Proteins.* Biochem. Cell Biol., 2002. **80**: 483-497.

19. McMurtrie, H.L., Cleary, H.J., Alvarez, B.V., Loiselle, F.B., Sterling, D., Morgan, P.E., Johnson, D.E., and Casey, J.R., *The bicarbonate transport metabolon.* J Enzyme Inhib Med Chem, 2004. **19**(3): 231-236.

20. http://clustalw.genome.jp, *Multiple Sequence Alignment.* 2003, CLUSTALW.

21. Kopito, R.R. and Lodish, H.F., *Primary structure and transmembrane orientation of the murine anion exchange protein.* Nature, 1985. **316**: 234-238.

22. Alper, S.L., Kopito, R.R., Libresco, S.M., and Lodish, H.F., *Cloning and characterization of a murine Band 3-related cDNA from kidney and a lymphoid cell line.* J. Biol. Chem., 1988. **263**: 17092-17099.

23. Kudrycki, K.E., Newman, P.R., and Shull, G.E., *cDNA cloning and tissue distribution of mRNAs for two proteins that are related to the Band 3 Cl^-/HCO_3^- exchanger.* J. Biol. Chem., 1990. **265**: 462-471.

24. Burnham, C.E., Amlal, H., Wang, Z., Shull, G.E., and Soleimani, M., *Cloning and functional expression of a human kidney $Na^+:HCO_3^-$ cotransporter.* J. Biol. Chem., 1997. **272**(31): 19111-19114.

25. Romero, M.F., Hediger, M.A., Boulpaep, E.L., and Boron, W.F., *Expression cloning and characterization of a renal electrogenic Na^+/HCO_3^- cotransporter.* Nature, 1997. **387**(6631): 409-413.

26. Pushkin, A., Abuladze, N., Newman, D., Lee, I., Xu, G., and Kurtz, I., *Two C-terminal variants of NBC4, a new member of the sodium bicarbonate cotransporter family: cloning, characterization, and localization.* IUBMB Life, 2000. **50**(1): 13-19.

27. Tsuganezawa, H., Kobayashi, K., Iyori, M., Araki, T., Koizumi, A., Watanabe, S.I., Kaneko, A., Fukao, T., Monkawa, T., Yoshida, T., Kim,

D.K., Kanai, Y., Endou, H., Hayashi, M., and Saruta, T., *A new member of the HCO_3^- transporter superfamily is an apical anion exchanger of beta-intercalated cells in the kidney.* J Biol Chem, 2001. **276**: 8180-8189.

28. Romero, M.F., Henry, D., Nelson, S., Harte, P.J., Dillon, A.K., and Sciortino, C.M., *Cloning and characterization of a Na^+ driven anion exchanger (NDAE1): a new bicarbonate transporter.* J. Biol. Chem., 2000. **275**(32): 24552-24559.

29. Schweinfest, C.W., Henderson, K.W., Suster, S., Kondoh, N., and Papas, T.S., *Identification of a colon mucosa gene that is down-regulated in colon adenomas and adenocarcinomas.* Proc Natl Acad Sci U S A, 1993. **90**(9): 4166-4170.

30. Scott, D.A., Wang, R., Kreman, T.M., Sheffield, V.C., and Karnishki, L.P., *The Pendred syndrome gene encodes a chloride-iodide transport protein.* Nat Genet, 1999. **21**(4): 440-443.

31. Waldegger, S., Moschen, I., Ramirez, A., Smith, R.J., Ayadi, H., Lang, F., and Kubisch, C., *Cloning and characterization of SLC26A6, a novel member of the solute carrier 26 gene family.* Genomics, 2001. **72**(1): 43-50.

32. Lohi, H., Kujala, M., Makela, S., Lehtonen, E., Kestila, M., Saarialho-Kere, U., Markovich, D., and Kere, J., *Functional characterization of three novel tissue-specific anion exchangers: SLC26A7, A8 and A9.* J Biol Chem, 2002. **7**: 14246-14254.

33. Vincourt, J.B., Jullien, D., Kossida, S., Amalric, F., and Girard, J.P., *Molecular Cloning of SLC26A7, a Novel Member of the SLC26 Sulfate/Anion Transporter Family, from High Endothelial Venules and Kidney.* Genomics, 2002. **79**(2): 249-256.

34. Alper, S.L., *The Band 3-related anion exchanger family.* Annu. Rev. Physiol., 1991. **53**: 549-564.

35. Brosius-III, F.C., Alper, S.L., Garcia, A.M., and Lodish, H.F., *The major kidney Band 3 gene transcript predicts an amino-terminal truncated Band 3 polypeptide.* J. Biol. Chem., 1989. **264**: 7784-7787.

36. Wall, S.M., *Recent advances in our understanding of intercalated cells.* Curr Opin Nephrol Hypertens, 2005. **14**(5): 480-484.

37. Kopito, R.R., Lee, B.S., Simmons, D.M., Lindsey, A.E., Morgans, C.W., and Schneider, K., *Regulation of intracellular pH by a neuronal homolog of the erythrocyte anion exchanger.* Cell, 1989. **59**: 927-937.

38. Linn, S.C., Kudrycki, K.E., and Shull, G.E., *The predicted translation product of a cardiac AE3 mRNA contains an N-terminus distinct from that of the brain AE3 Cl^-/HCO_3^- exchanger.* J. Biol. Chem, 1992. **267**(11): 7927-7935.

39. Kobayashi, S., Morgans, C.W., Casey, J.R., and Kopito, R.R., *AE3 Anion exchanger isoforms in the vertebrate retina: developmental regulation and differential expression in neurons and glia.* J. Neurosci., 1994. **14**: 6266-6279.

40. Zhu, Q., Lee, D.W.K., and Casey, J.R., *Novel Topology in C-terminal Region of the Human Plasma membrane anion exchanger, AE1.* J. Biol. Chem., 2003. **278**: 3112-3120.

41. Low, P.S., *Structure and function of the cytoplasmic domain of Band 3: center of erythrocyte membrane-peripheral protein interactions.* Biochim. Biophys. Acta, 1986. **864**: 145-167.

42. Popov, M., Tam, L.Y., Li, J., and Reithmeier, R.A.F., *Mapping the ends of transmembrane segments in a polytopic membrane protein. Scanning N-*

glycosylation mutagenesis of extracytosolic loops in the anion exchanger, band 3. J. Biol. Chem., 1997. **272**(29): 18325-18332.

43. Grinstein, S., Ship, S., and Rothstein, A., *Anion transport in relation to proteolytic dissection of Band 3 protein.* Biochim. Biophys. Acta, 1979. **507**: 294-304.

44. Tang, X.B., Fujinaga, J., Kopito, R., and Casey, J.R., *Topology of the region surrounding Glu681 of human AE1 protein, the erythrocyte anion exchanger.* J. Biol. Chem., 1998. **273**(35): 22545-22553.

45. Fujinaga, J., Tang, X.-B., and Casey, J.R., *Topology of the membrane domain of human anion exchange protein, AE1. J. Biol. Chem.*, 1999. **274**: 6626-6633.

46. Hamasaki, N., Okubo, K., Kuma, H., Kang, D., and Yae, Y., *Proteolytic cleavage sites of band 3 protein in alkali-treated membranes: fidelity of hydropathy prediction for band 3 protein [In Process Citation].* J Biochem (Tokyo), 1997. **122**(3): 577-585.

47. Popov, M., Li, J., and Reithmeier, R.A., *Transmembrane folding of the human erythrocyte anion exchanger (AE1, Band 3) determined by scanning and insertional N-glycosylation mutagenesis.* Biochem. J., 1999. **339**(Pt 2): 269-279.

48. Vince, J.W. and Reithmeier, R.A., *Identification of the Carbonic Anhydrase II Binding Site in the Cl^-/HCO_3^- Anion Exchanger AE1.* Biochemistry, 2000. **39**(18): 5527-5533.

49. Vince, J.W. and Reithmeier, R.A.F., *Carbonic anhydrase II binds to the carboxyl-terminus of human band 3, the erythrocyte Cl^-/HCO_3^- exchanger.* J. Biol. Chem, 1998. **273**(43): 28430-28437.

50. Romero, M.F., *Molecular pathophysiology of SLC4 bicarbonate transporters.* Curr Opin Nephrol Hypertens, 2005. **14**(5): 495-501.

51. Aalkjaer, C., Frische, S., Leipziger, J., Nielsen, S., and Praetorius, J., *Sodium coupled bicarbonate transporters in the kidney, an update.* Acta Physiol Scand, 2004. **181**(4): 505-512.

52. Romero, M.F., *The electrogenic Na^+/HCO_3^- cotransporter, NBC.* Jop, 2001. **2**(4 Suppl): 182-191.

53. Choi, I., Romero, M.F., Khandoudi, N., Bril, A., and Boron, W.F., *Cloning and characterization of a human electrogenic Na^+-HCO_3^- cotransporter isoform (hhNBC).* Am. J. Physiol., 1999. **276**(3 Pt 1): C576-584.

54. Abuladze, N., Lee, I., Newman, D., Hwang, J., Boorer, K., Pushkin, A., and Kurtz, I., *Molecular cloning, chromosomal localization, tissue distribution, and functional expression of the human pancreatic sodium bicarbonate cotransporter.* J. Biol. Chem., 1998. **273**(28): 17689-17695.

55. Pushkin, A., Yip, K.P., Clark, I., Abuladze, N., Kwon, T.H., Tsuruoka, S., Schwartz, G.J., Nielsen, S., and Kurtz, I., *NBC3 expression in rabbit collecting duct: colocalization with vacuolar H^+-ATPase.* Am. J. Physiol., 1999. **277**(6 Pt 2): F974-981.

56. Kwon, T.H., Pushkin, A., Abuladze, N., Nielsen, S., and Kurtz, I., *Immunoelectron microscopic localization of NBC3 sodium-bicarbonate cotransporter in rat kidney.* Am. J. Physiol. Renal Physiol., 2000. **278**(2): F327-336.

57. Vorum, H., Kwon, T.H., Fulton, C., Simonsen, B., Choi, I., Boron, W., Maunsbach, A.B., Nielsen, S., and Aalkjaer, C., *Immunolocalization of electroneutral Na^+-HCO_3^- cotransporter in rat kidney.* Am J Physiol Renal Physiol, 2000. **279**(5): F901-909.

58. Praetorius, J., Kim, Y.H., Bouzinova, E.V., Frische, S., Rojek, A., Aalkjaer, C., and Nielsen, S., *NBCn1 is a basolateral Na^+-HCO_3^- cotransporter in rat kidney inner medullary collecting ducts.* Am J Physiol Renal Physiol, 2004. **286**(5): F903-912.

59. Kwon, T.H., Fulton, C., Wang, W., Kurtz, I., Frokiaer, J., Aalkjaer, C., and Nielsen, S., *Chronic metabolic acidosis upregulates rat kidney Na^+-HCO_3^- cotransporters NBCn1 and NBC3 but not NBC1.* Am J Physiol Renal Physiol, 2002. **282**(2): F341-351.

60. Jakobsen, J.K., Odgaard, E., Wang, W., Elkjaer, M.L., Nielsen, S., Aalkjaer, C., and Leipziger, J., *Functional up-regulation of basolateral Na^+-dependent HCO_3^- transporter NBCn1 in medullary thick ascending limb of K^+-depleted rats.* Pflugers Arch, 2004. **448**(6): 571-578.

61. Odgaard, E., Jakobsen, J.K., Frische, S., Praetorius, J., Nielsen, S., Aalkjaer, C., and Leipziger, J., *Basolateral Na^+-dependent HCO_3^- transporter NBCn1-mediated HCO_3^- influx in rat medullary thick ascending limb.* J Physiol, 2004. **555**(Pt 1): 205-218.

62. Pushkin, A., Abuladze, N., Lee, I., Newman, D., Hwang, J., and Kurtz, I., *Cloning, tissue distribution, genomic organization, and functional characterization of NBC3, a new member of the sodium bicarbonate cotransporter family.* J. Biol. Chem., 1999. **274**(23): 16569-16575.

63. Ishibashi, K., Sasaki, S., and Marumo, F., *Molecular cloning of a new sodium bicarbonate cotransporter cDNA from human retina.* Biochem. Biophys. Res. Commun., 1998. **246**(2): 535-538.

64. Kristensen, J.M., Kristensen, M., and Juel, C., *Expression of Na^+/HCO_3^- co-transporter proteins (NBCs) in rat and human skeletal muscle.* Acta Physiol Scand, 2004. **182**(1): 69-76.

65. Everett, L.A. and Green, E.D., *A family of mammalian anion transporters and their involvement in human genetic diseases.* Hum. Mol. Genetics, 1999. **8**: 1883-1891.

66. Soleimani, M., Greeley, T., Petrovic, S., Wang, Z., Amlal, H., Kopp, P., and Burnham, C.E., *Pendrin: an apical $Cl^-/OH^-/HCO_3^-$ exchanger in the kidney cortex.* Am J Physiol Renal Physiol, 2001. **280**(2): F356-364.

67. Hastbacka, J., de la Chapelle, A., Mahtani, M.M., Clines, G., Reeve-Daly, M.P., Daly, M., Hamilton, B.A., Kusumi, K., Trivedi, B., and Weaver, A., *The diastrophic dysplasia gene encodes a novel sulfate transporter: positional cloning by fine-structure linkage disequilibrium mapping.* Cell, 1994. **78**(6): 1073-1087.

68. Markovich, D., Bissig, M., Sorribas, V., Hagenbuch, B., Meier, P.J., and Murer, H., *Expression of rat renal sulfate transport systems in Xenopus laevis oocytes. Functional characterization and molecular identification.* J Biol Chem, 1994. **269**(4): 3022-3026.

69. Melvin, J.E., Park, K., Richardson, L., Schultheis, P.J., and Shull, G.E., *Mouse down-regulated in adenoma (DRA) is an intestinal Cl^-/HCO_3^- exchanger and is up-regulated in colon of mice lacking the NHE3 Na^+/H^+ exchanger.* J. Biol. Chem., 1999. **274**(32): 22855-22861.

70. Xie, Q., Welch, R., Mercado, A., Romero, M.F., and Mount, D.B., *Molecular characterization of the murine Slc26a6 anion exchanger: functional comparison with Slc26a1.* Am J Physiol Renal Physiol, 2002. **283**(4): F826-838.

71. Mount, D.B. and Romero, M.F., *The SLC26 gene family of multifunctional anion exchangers.* Pflugers Arch, 2004. **447**(5): 710-721.

72. Toure, A., Morin, L., Pineau, C., Becq, F., Dorseuil, O., and Gacon, G., *Tat1, a novel sulfate transporter specifically expressed in human male germ cells and potentially linked to rhoGTPase signaling.* J Biol Chem, 2001. **276**(23): 20309-20315.

73. Wang, Z., Petrovic, S., Mann, E., and Soleimani, M., *Identification of an apical Cl^-/HCO_3^- exchanger in the small intestine.* Am J Physiol Gastrointest Liver Physiol, 2002. **282**(3): G573-579.

74. Alvarez, B.V., Kieller, D.M., Quon, A.L., Markovich, D., and Casey, J.R., *Slc26a6: A cardiac chloride/hydroxyl exchanger and predominant chloride/bicarbonate exchanger of the heart.* J. Physiol., 2004. **561**: 721-734.

75. Lohi, H., Kujala, M., Kerkela, E., Saarialho-Kere, U., Kestila, M., and Kere, J., *Mapping of five new putative anion transporter genes in human and characterization of SLC26A6, a candidate gene for pancreatic anion exchanger.* Genomics, 2000. **70**(1): 102-112.

76. Petrovic, S., Wang, Z., Ma, L., Seidler, U., Forte, J.G., Shull, G.E., and Soleimani, M., *Colocalization of the apical Cl^-/HCO_3^- exchanger PAT1 and gastric H^+-K^+-ATPase in stomach parietal cells.* Am J Physiol Gastrointest Liver Physiol, 2002. **283**(5): G1207-1216.

77. Kujala, M., Tienari, J., Lohi, H., Elomaa, O., Sariola, H., Lehtonen, E., and Kere, J., *SLC26A6 and SLC26A7 anion exchangers have a distinct distribution in human kidney.* Nephron Exp Nephrol, 2005. **101**(2): e50-58.

78. Knauf, F., Yang, C.L., Thomson, R.B., Mentone, S.A., Giebisch, G., and Aronson, P.S., *Identification of a chloride-formate exchanger expressed on the*

brush border membrane of renal proximal tubule cells. Proc Natl Acad Sci U S A, 2001. **98**(16): 9425-9430.

79. Petrovic, S., Ju, X., Barone, S., Seidler, U., Alper, S.L., Lohi, H., Kere, J., and Soleimani, M., *Identification of a basolateral Cl^-/HCO_3^- exchanger specific to gastric parietal cells.* Am J Physiol Gastrointest Liver Physiol, 2003. **284**(6): G1093-1103.

80. Ko, S.B., Zeng, W., Dorwart, M.R., Luo, X., Kim, K.H., Millen, L., Goto, H., Naruse, S., Soyombo, A., Thomas, P.J., and Muallem, S., *Gating of CFTR by the STAS domain of SLC26 transporters.* Nat Cell Biol, 2004. **28**: 28.

81. Alvarez, B.V., Vilas, G.L., and Casey, J.R., *Metabolon disruption: a mechanism that regulates bicarbonate transport.* EMBO J, 2005. **24**: 2499-2511.

82. Aravind, L. and Koonin, E.V., *The STAS domain - a link between anion transporters and antisigma-factor antagonists.* Curr Biol, 2000. **10**(2): R53-55.

83. Lee, M.G., Choi, J.Y., Luo, X., Strickland, E., Thomas, P.J., and Muallem, S., *Cystic fibrosis transmembrane conductance regulator regulates luminal Cl^-/HCO_3^- exchange in mouse submandibular and pancreatic ducts.* J Biol Chem, 1999. **274**(21): 14670-14677.

84. Lohi, H., Lamprecht, G., Markovich, D., Heil, A., Kujala, M., Seidler, U., and Kere, J., *Isoforms of SLC26A6 mediate anion transport and have functional PDZ interaction domains.* Am J Physiol Cell Physiol, 2003. **284**(3): C769-779.

85. Greeley, T., Shumaker, H., Wang, Z., Schweinfest, C.W., and Soleimani, M., *Downregulated in adenoma and putative anion transporter are regulated by CFTR in cultured pancreatic duct cells.* Am J Physiol Gastrointest Liver Physiol, 2001. **281**(5): G1301-1308.

86. Cheng, H.S., Wong, W.S., Chan, K.T., Wang, X.F., Wang, Z.D., and Chan, H.C., *Modulation of Ca^{2+}-dependent anion secretion by protein kinase C in normal and cystic fibrosis pancreatic duct cells.* Biochim Biophys Acta, 1999. **1418**(1): 31-38.

87. Brown, D., Zhu, X.L., and Sly, W.S., *Localization of membrane-associated carbonic anhydrase type IV in kidney epithelial cells.* Proc Natl Acad Sci U S A, 1990. **87**(19): 7457-7461.

88. Mori, K., Ogawa, Y., Ebihara, K., Tamura, N., Tashiro, K., Kuwahara, T., Mukoyama, M., Sugawara, A., Ozaki, S., Tanaka, I., and Nakao, K., *Isolation and characterization of CA XIV, a novel membrane-bound carbonic anhydrase from mouse kidney.* J Biol Chem, 1999. **274**(22): 15701-15705.

89. Kivela, A., Parkkila, S., Saarnio, J., Karttunen, T.J., Kivela, J., Parkkila, A.K., Waheed, A., Sly, W.S., Grubb, J.H., Shah, G., Tureci, O., and Rajaniemi, H., *Expression of a novel transmembrane carbonic anhydrase isozyme XII in normal human gut and colorectal tumors.* Am J Pathol, 2000. **156**(2): 577-584.

90. Tureci, O., Sahin, U., Vollmar, E., Siemer, S., Gottert, E., Seitz, G., Parkkila, A.K., Shah, G.N., Grubb, J.H., Pfreundschuh, M., and Sly, W.S., *Human carbonic anhydrase XII: cDNA cloning, expression, and chromosomal localization of a carbonic anhydrase gene that is overexpressed in some renal cell cancers.* Proc Natl Acad Sci U S A, 1998. **95**(13): 7608-7613.

91. Maren, T.H., *Carbonic anhydrase: chemistry, physiology, and inhibition.* Physiol Rev, 1967. **47**(4): 595-781.

92. Dodgson, S.J. and Forster, R.E., 2nd, *Inhibition of CA V decreases glucose synthesis from pyruvate.* Arch Biochem Biophys, 1986. **251**(1): 198-204.

93. Dodgson, S.J. and Forster, R.E., 2nd, *Carbonic anhydrase: inhibition results in decreased urea production by hepatocytes.* J Appl Physiol, 1986. **60**(2): 646-652.

94. Sterling, D., Alvarez, B.V., and Casey, J.R., *The extracellular component of a transport metabolon: Extracellular loop 4 of the human AE1 Cl^-/HCO_3^- exchanger binds carbonic anhydrase IV.* J Biol Chem, 2002. **277**: 25239-25246.

95. Wistrand, P.J., *Carbonic anhydrase III in liver and muscle of male rats purification and properties.* Ups J Med Sci, 2002. **107**(2): 77-88.

96. Sender, S., Decker, B., Fenske, C.D., Sly, W.S., Carter, N.D., and Gros, G., *Localization of carbonic anhydrase IV in rat and human heart muscle.* J Histochem Cytochem, 1998. **46**(7): 855-861.

97. Geers, C., Kruger, D., Siffert, W., Schmid, A., Bruns, W., and Gros, G., *Carbonic anhydrase in skeletal and cardiac muscle from rabbit and rat.* Biochem J, 1992. **282**(Pt 1): 165-171.

98. Scheibe, R.J., Gros, G., Parkkila, S., Waheed, A., Grubb, J.H., Shah, G.N., Sly, W.S., and Wetzel, P., *Expression of Membrane-bound Carbonic Anhydrases IV, IX, and XIV in the Mouse Heart.* J Histochem Cytochem, 2006: Epub ahead of print.

99. Schwartz, G.J., Kittelberger, A.M., Barnhart, D.A., and Vijayakumar, S., *Carbonic anhydrase IV is expressed in H^+-secreting cells of rabbit kidney.* Am. J. Physiol., 2000. **278**(6): F894-904.

100. Supuran, C.T., Scozzafava, A., and Casini, A., *Carbonic anhydrase inhibitors.* Medicinal Research Reviews, 2003. **23**: 146-189.

101. Stams, T. and Christianson, D.W., *X-ray crystallographic studies of mammalian carbonic anhydrase isozymes.*, in *The Carbonic Andydrases - New*

Horizons, W.R. Chegwidden, Y. Edwards, and N. Carter, Editors. 2000, Birkhauser Verlag: Basel. 159-174.

102. Lindskog, S. and Silverman, D.N., *The catalytic mechanism of mammalian carbonic anhydrases*, in *The Carbonic Anhydrases - New Horizons*, W.R. Chegwidden, Y. Edwards, and N. Carter, Editors. 2000, Birkhauser Verlag: Basel. 175-196.

103. Christianson, D.W. and Fierke, C.A., *Carbonic anhydrase: evolution of the zinc binding site by natrue and by design.* Accounts of Chemical Research, 1996. **29**: 331-339.

104. Bertini, I., Mangani, S., Scozzafava, A., and Supuran, C.T., *Carbonic anhydrase: An insight into the zinc binding site and into the active cavity through metal substitution.* Structure and Bonding, 1982. **48**: 45-92.

105. Supuran, C.T., Scozzafava, A., and Conway, J., *Carbonic Anhydrase: Its Inhibitors and Activators.* CRC Enzyme Inhibitors and Activators, ed. H.J. Smith and C. Simons. 2004, Cardiff, UK: CRC Press: 363.

106. Eriksson, A.E., Jones, T.A., and Liljas, A., *Refined structure of human carbonic anhydrase II at 2.0 A resolution.* Proteins, 1988. **4**(4): 274-282.

107. Vince, J.W., Carlsson, U., and Reithmeier, R.A., *Localization of the Cl^-/HCO_3^- anion exchanger binding site to the amino-terminal region of carbonic anhydrase II.* Biochemistry, 2000. **39**(44): 13344-13349.

108. Sterling, D., Reithmeier, R.A., and Casey, J.R., *A Transport Metabolon. Functional Interaction of Carbonic Anhydrase II and Chloride/Bicarbonate Exchangers.* J Biol Chem, 2001. **276**(51): 47886-47894.

109. Briganti, F., Mangani, S., Orioli, P., Scozzafava, A., Vernaglione, G., and Supuran, C.T., *Carbonic anhydrase activators: X-ray crystallographic and*

spectroscopic investigations for the interaction of isozymes I and II with histamine. Biochemistry, 1997. **36**(34): 10384-10392.

110. Alper, S.L., *Genetic diseases of acid-base transporters.* Annu Rev Physiol, 2002. **64**: 899-923.

111. DeCoursey, T.E., *Hypothesis: do voltage-gated H^+ channels in alveolar epithelial cells contribute to CO_2 elimination by the lung?* Am J Physiol Cell Physiol, 2000. **278**(1): C1-C10.

112. Roth, D.E., Venta, P.J., Tashian, R.E., and Sly, W.S., *Molecular basis of human carbonic anhydrase II deficiency.* Proc Natl Acad Sci U S A, 1992. **89**(5): 1804-1808.

113. Rousselle, A.V. and Heymann, D., *Osteoclastic acidification pathways during bone resorption.* Bone, 2002. **30**(4): 533-540.

114. Sun, M.K. and Alkon, D.L., *Carbonic anhydrase gating of attention: memory therapy and enhancement.* Trends Pharmacol Sci, 2002. **23**(2): 83-89.

115. Scozzafava, A. and Supuran, C.T., *Carbonic anhydrase activators: Human isozyme II is strongly activated by oligopeptides incorporating the carboxyterminal sequence of the bicarbonate anion exchanger AE1.* Bioorg Med Chem Lett, 2002. **12**(8): 1177-1180.

116. Reithmeier, R.A.F., *A membrane metabolon linking carbonic anhydrase with chloride/bicarbonate anion exchangers.* Blood cells, Molecules and Diseases, 2001. **27**: 85-89.

117. Sterling, D., Reithmeier, R.A.F., and Casey, J.R., *Carbonic anhydrase: in the driver's seat for bicarbonate transport.* J. of the Pancreas, 2001. **2**: 165-170.

118. Sterling, D., Brown, N., Supuran, C.T., and Casey, J.R., *The functional and physical relationship between the downregulated in adenoma bicarbonate transporter and carbonic anhydrase II.* Am. J. Physiol., 2002. **283**: C1522-1529.

119. Aronsson, G., Martensson, L.G., Carlsson, U., and Jonsson, B.H., *Folding and stability of the N-terminus of human carbonic anhydrase II.* Biochemistry, 1995. **34**(7): 2153-2162.

120. Dahl, N.K., Jiang, L., Chernova, M.N., Stuart-Tilley, A.K., Shmukler, B.E., and Alper, S.L., *Deficient HCO_3^- transport in an AE1 mutant with normal Cl^- transport can be rescued by carbonic anhydrase II presented on an adjacent AE1 protomer.* J Biol Chem, 2003. **21**: 44949-44958.

121. Alvarez, B., Loiselle, F.B., C.T., S., Schwartz, G.J., and Casey, J.R., *Direct extracellular interaction between carbonic anhydrase IV and the NBC1 Na^+/HCO_3^- co-transporter.* Biochemistry, 2003. **42**: 2321-2329.

122. Gross, E., Pushkin, A., Abuladze, N., Fedotoff, O., and Kurtz, I., *Regulation of the sodium bicarbonate cotransporter kNBC1 function: role of Asp(986), Asp(988) and kNBC1-carbonic anhydrase II binding.* J Physiol, 2002. **544**(Pt 3): 679-685.

123. Loiselle, F.B., Alvarez, B.V., and Casey, J.R., *Regulation of the Human NBC3 Na^+/HCO_3^- co-transporter by Carbonic Anhydrase II and Protein Kinase A.* Am. J. Physiol., 2004. **286**(6): 307-317.

124. Loiselle, F.B., Jaschke, P., and Casey, J.R., *Structural and Functional Characterization of the Human NBC3 Sodium/Bicarbonate Co-transporter Carboxyl-Terminal Cytoplasmic Domain.* Mol. Mem. Biol., 2003. **20**: 307-317.

125. Shandro, H.J. and Casey, J.R., *Plasma Membrane Cl^-/HCO_3^- Exchange Proteins,* in *Chloride Movements Across Cellular Membranes.* 2006, *In Press.*

126. Pushkin, A. and Kurtz, I., *SLC4 base (HCO_3^-, CO_3^{2-}) transporters: classification, function, structure, genetic diseases, and knockout models.* Am J Physiol Renal Physiol, 2006. **290**(3): F580-599.

127. Bajaj, G. and Quan, A., *Renal tubular acidosis and deafness: report of a large family.* Am J Kidney Dis, 1996. **27**(6): 880-882.

128. Bentur, L., Alon, U., Mandel, H., Pery, M., and Berant, M., *Familial distal renal tubular acidosis with neurosensory deafness: early nephrocalcinosis.* Am J Nephrol, 1989. **9**(6): 470-474.

129. Karet, F.E., Finberg, K.E., Nelson, R.D., Nayir, A., Mocan, H., Sanjad, S.A., Rodriguez-Soriano, J., Santos, F., Cremers, C.W., Di Pietro, A., Hoffbrand, B.I., Winiarski, J., Bakkaloglu, A., Ozen, S., Dusunsel, R., Goodyer, P., Hulton, S.A., Wu, D.K., Skvorak, A.B., Morton, C.C., Cunningham, M.J., Jha, V., and Lifton, R.P., *Mutations in the gene encoding B1 subunit of H^+-ATPase cause renal tubular acidosis with sensorineural deafness.* Nat Genet, 1999. **21**(1): 84-90.

130. Cordat, E., Kittanakom, S., Yenchitsomanus, P.T., Li, J., Du, K., Lukacs, G.L., and Reithmeier, R.A., *Dominant and Recessive Distal Renal Tubular Acidosis Mutations of Kidney Anion Exchanger 1 Induce Distinct Trafficking Defects in MDCK Cells.* Traffic, 2006. **7**(2): 117-128.

131. Tanphaichitr, V.S., Sumboonnanonda, A., Ideguchi, H., Shayakul, C., Brugnara, C., Takao, M., Veerakul, G., and Alper, S.L., *Novel AE1 mutations in recessive distal renal tubular acidosis. Loss-of-function is rescued by glycophorin A.* J Clin Invest, 1998. **102**(12): 2173-2179.

132. Ribeiro, M.L., Alloisio, N., Almeida, H., Gomes, C., Texier, P., Lemos, C., Mimoso, G., Morle, L., Bey-Cabet, F., Rudigoz, R.C., Delaunay, J., and

Tamagnini, G., *Severe hereditary spherocytosis and distal renal tubular acidosis associated with the total absence of band 3.* Blood, 2000. **96**(4): 1602-1604.

133. http://www.nlm.nih.gov/medlineplus/ency/article/000493.htm, *Medline Plus; Medical Encyclopedia.* 2006, U.S. National Library of Medicine and the National Institute of Health.

134. Soleimani, M. and Burnham, C.E., *Physiologic and molecular aspects of the Na^+:HCO_3^- cotransporter in health and disease processes.* Kidney Int., 2000. **57**(2): 371-384.

135. Li, H.C., Szigligeti, P., Worrell, R.T., Matthews, J.B., Conforti, L., and Soleimani, M., *Missense mutations in Na^+:HCO_3^- cotransporter NBC1 show abnormal trafficking in polarized kidney cells: a basis of proximal renal tubular acidosis.* Am J Physiol Renal Physiol, 2005. **289**(1): F61-71.

136. Peters, T.A., Monnens, L.A., Cremers, C.W., and Curfs, J.H., *Genetic disorders of transporters/channels in the inner ear and their relation to the kidney.* Pediatr Nephrol, 2004. **19**(11): 1194-1201.

137. Bok, D., Galbraith, G., Lopez, I., Woodruff, M., Nusinowitz, S., BeltrandelRio, H., Huang, W., Zhao, S., Geske, R., Montgomery, C., Van Sligtenhorst, I., Friddle, C., Platt, K., Sparks, M.J., Pushkin, A., Abuladze, N., Ishiyama, A., Dukkipati, R., Liu, W., and Kurtz, I., *Blindness and auditory impairment caused by loss of the sodium bicarbonate cotransporter NBC3.* Nat Genet, 2003. **34**(3): 313-319.

138. Reiners, J., Nagel-Wolfrum, K., Jurgens, K., Marker, T., and Wolfrum, U., *Molecular basis of human Usher syndrome: deciphering the meshes of the Usher protein network provides insights into the pathomechanisms of the Usher disease.* Exp Eye Res, 2006. **83**(1): 97-119.

139. Reiners, J., van Wijk, E., Marker, T., Zimmermann, U., Jurgens, K., te Brinke, H., Overlack, N., Roepman, R., Knipper, M., Kremer, H., and Wolfrum, U., *Scaffold protein harmonin (USH1C) provides molecular links between Usher syndrome type 1 and type 2.* Hum Mol Genet, 2005. **14**(24): 3933-3943.

140. Donner, K., Hemila, S., Kalamkarov, G., Koskelainen, A., Pogozheva, I., and Rebrik, T., *Sulfhydryl binding reagents increase the conductivity of the light-sensitive channel and inhibit phototransduction in retinal rods.* Exp Eye Res, 1990. **51**(1): 97-105.

141. Yang, Z., Alvarez, B.V., Chakarova, C., Jiang, L., Karan, G., Frederick, J.M., Zhao, Y., Sauve, Y., Li, X., Zrenner, E., Wissinger, B., Hollander, A.I., Katz, B., Baehr, W., Cremers, F.P., Casey, J.R., Bhattacharya, S.S., and Zhang, K., *Mutant carbonic anhydrase 4 impairs pH regulation and causes retinal photoreceptor degeneration.* Hum Mol Genet, 2005. **14**(2): 255-265.

142. Do, E., Ellis, D., and Noireaud, J., *Intracellular pH and intrinsic H^+ buffering capacity in normal and hypertrophied right ventricle of ferret heart.* Cardiovasc Res, 1996. **31**(5): 729-738.

143. Pucéat, M., Roche, S., and Vassort, G., *Src family tyrosine kinase regulates intracellular pH in cardiomyocytes.* J. Cell Biol., 1998. **141**(7): 1637-1646.

144. Khandoudi, N., Albadine, J., Robert, P., Krief, S., Berrebi-Bertrand, I., Martin, X., Bevensee, M.O., Boron, W.F., and Bril, A., *Inhibition of the cardiac electrogenic sodium bicarbonate cotransporter reduces ischemic injury.* Cardiovasc Res, 2001. **52**(3): 387-396.

145. Alvarez, B.V., Xia, Y., Karmazyn, M., and Casey, J.R., *Inhibition of phenylephrine-induced cardiac hypertrophy by a carbonic anhydrase inhibitor: a*

pathological pathway linking CAII, NHE1 and AE3fl. J. Mol. Cell. Cardiol., 2004. **37**(299 (Abstract)).

146. Madshus, I.H., *Regulation of intracellular pH in eukaryotic cells.* Biochem J, 1988. **250**(1): 1-8.

147. Farias, F., Morgan, P., Chiappe de Cingolani, G., and Camilion de Hurtado, M.C., *Involvement of the Na^+-independent Cl^-/HCO_3^- exchange (AE) isoform in the compensation of myocardial Na^+/H^+ isoform 1 hyperactivity in spontaneously hypertensive rats.* Can J Physiol Pharmacol, 2005. **83**(5): 397-404.

148. Linn, S.C., Askew, G.R., Menon, A.G., and Shull, G.E., *Conservation of an AE3 Cl^-/HCO_3^- exchanger cardiac-specific exon and promotor region and AE3 mRNA expression patterns in murine and human hearts.* Circ. Res., 1995. **76**: 584-591.

149. Chiappe de Cingolani, G., Morgan, P., C, M.-W., Casey, J.R., Fujinaga, J., Camilión de Hurtado, M., and Cingolani, H., *Expression of the Cl^-/HCO_3^- anion exchanger mRNA in the hypertrophied myocardium of spontaneously hypertensive rat.* Cardiovascular Research, 2001. **51**: 71-79.

150. Alvarez, B.V., Fujinaga, J., and Casey, J.R., *Molecular Basis for angiotensin II-induced increase of chloride/bicarbonate exchange in the myocardium.* Circ. Research, 2001. **89**: 1246-1253.

151. Chiappe de Cingolani, G.E., Ennis, I.L., Morgan, P.E., Alvarez, B.V., Casey, J.R., and Camilion de Hurtado, M.C., *Involvement of AE3 isoform of Na^+-independent Cl^-/HCO_3^- exchanger in myocardial pH_i recovery from intracellular alkalization.* Life Sci, 2006. **78**(26): 3018-3026.

152. Simpson, J.E., Gawenis, L.R., Walker, N.M., Boyle, K.T., and Clarke, L.L., *Chloride conductance of CFTR facilitates basal Cl^-/HCO_3^- exchange in the villous epithelium of intact murine duodenum.* Am J Physiol Gastrointest Liver Physiol, 2005. **288**(6): G1241-1251.

153. Hadorn, B., Johansen, P.G., and Anderson, C.M., *Pancreozymin secretin test of exocrine pancreatic funtion in cystic fibrosis and the significance of the result for the pathogenesis of the disease.* Can Med Assoc J, 1968. **98**(8): 377-385.

154. Steward, M.C., Ishiguro, H., and Case, R.M., *Mechanisms of bicarbonate secretion in the pancreatic duct.* Annu. Rev. Physiol., 2005. **67**: 377-409.

155. Kulczycki, L.L., Kostuch, M., and Bellanti, J.A., *A clinical perspective of cystic fibrosis and new genetic findings: relationship of CFTR mutations to genotype-phenotype manifestations.* Am J Med Genet, 2003. **116A**(3): 262-267.

156. Wine, J.J., *Cystic fibrosis: The 'bicarbonate before chloride' hypothesis.* Curr Biol, 2001. **11**(12): R463-466.

157. Poulsen, J.H. and Machen, T.E., *HCO_3^--dependent pH_i regulation in tracheal epithelial cells.* Pflugers Arch, 1996. **432**(3): 546-554.

158. Poulsen, J.H., Fischer, H., Illek, B., and Machen, T.E., *Bicarbonate conductance and pH regulatory capability of cystic fibrosis transmembrane conductance regulator.* Proc Natl Acad Sci U S A, 1994. **91**(12): 5340-5344.

159. Park, M., Ko, S.B., Choi, J.Y., Muallem, G., Thomas, P.J., Pushkin, A., Lee, M.S., Kim, J.Y., Lee, M.G., Muallem, S., and Kurtz, I., *The cystic fibrosis transmembrane conductance regulator interacts with and regulates the activity of the HCO_3^- salvage transporter human Na^+/HCO_3^- cotransport isoform 3.* J Biol Chem, 2002. **277**(52): 50503-50509.

160. Reddy, M.M. and Quinton, P.M., *Control of dynamic CFTR selectivity by glutamate and ATP in epithelial cells.* Nature, 2003. **423**(6941): 756-760.

161. Cavalheiro, E.A. and Olney, J.W., *Glutamate antagonists: deadly liaisons with cancer.* Proc Natl Acad Sci U S A, 2001. **98**(11): 5947-5948.

162. Duan, S. and Cooke, I.M., *Glutamate and GABA activate different receptors and Cl^- conductances in crab peptide-secretory neurons.* J Neurophysiol, 2000. **83**(1): 31-37.

163. Shayakul, C., Kanai, Y., Lee, W.S., Brown, D., Rothstein, J.D., and Hediger, M.A., *Localization of the high-affinity glutamate transporter EAAC1 in rat kidney.* Am J Physiol, 1997. **273**(6 Pt 2): F1023-1029.

164. Hakuba, N., Koga, K., Gyo, K., Usami, S.I., and Tanaka, K., *Exacerbation of noise-induced hearing loss in mice lacking the glutamate transporter GLAST.* J Neurosci, 2000. **20**(23): 8750-8753.

165. Harada, T., Harada, C., Watanabe, M., Inoue, Y., Sakagawa, T., Nakayama, N., Sasaki, S., Okuyama, S., Watase, K., Wada, K., and Tanaka, K., *Functions of the two glutamate transporters GLAST and GLT-1 in the retina.* Proc Natl Acad Sci U S A, 1998. **95**(8): 4663-4666.

166. Iwanaga, T., Goto, M., and Watanabe, M., *Cellular distribution of glutamate transporters in the gastrointestinal tract of mice: an immunohistochemical and in situ hybridization approach.* Biomed Res, 2005. **26**(6): 271-278.

167. Ballatori, N., Moseley, R.H., and Boyer, J.L., *Sodium gradient-dependent L-glutamate transport is localized to the canalicular domain of liver plasma membranes. Studies in rat liver sinusoidal and canalicular membrane vesicles.* J Biol Chem, 1986. **261**(14): 6216-6221.

168. Howell, J.A., Matthews, A.D., Swanson, K.C., Harmon, D.L., and Matthews, J.C., *Molecular identification of high-affinity glutamate transporters in sheep and cattle forestomach, intestine, liver, kidney, and pancreas.* J Anim Sci, 2001. **79**(5): 1329-1336.

169. McMurtrie, H.L. and Casey, J.R., *Glutamate Regulates Bicarbonate Transport Metabolon Function.* In Preparation, 2006.

170. Fierke, C.A., Calderone, T.L., and Krebs, J.F., *Functional consequences of engineering the hydrophobic pocket of carbonic anhydrase II.* Biochemistry, 1991. **30**(46): 11054-11063.

171. Bradford, M.M., *A rapid and sensitive method for the quantitation of microgram quantities of protein utilizing the pricinple of protein-dye binding.* Anal. Biochem., 1976. **72**: 248-254.

172. Laemmli, U.K., *Cleavage of structural proteins during assembly of the head of bacteriophage T4.* Nature, 1970. **227**: 680-685.

173. Brion, L.P., Schwartz, J.H., Zavilowitz, B.J., and Schwartz, G.J., *Micro-method for the measurement of carbonic anhydrase activity in cellular homogenates.* Anal Biochem, 1988. **175**(1): 289-297.

174. Maren, T.H., *A simplified micromethod for the determination of carbonic anhydrase and its inhibitors.* J Pharmacol Exp Ther, 1960. **130**: 26-29.

175. Sato, S., Zhu, X.L., and Sly, W.S., *Carbonic anhydrase isozymes IV and II in urinary membranes from carbonic anhydrase II-deficient patients.* Proc Natl Acad Sci U S A, 1990. **87**(16): 6073-6076.

176. Sundaram, V., Rumbolo, P., Grubb, J., Strisciuglio, P., and Sly, W.S., *Carbonic anhydrase II deficiency: diagnosis and carrier detection using*

differential enzyme inhibition and inactivation. Am J Hum Genet, 1986. **38**(2): 125-136.

177. Heikkila, J.J., Kaldis, A., and Abdulle, R., *Analysis of molecular chaperones using a Xenopus oocyte protein refolding assay.* Methods Mol Biol, 2006. **322**: 213-222.

178. Kalinyak, J.E. and Taylor, J.M., *Rat glutathione S-transferase. Cloning of double-stranded cDNA and induction of its mRNA.* J Biol Chem, 1982. **257**(1): 523-530.

179. Lindahl, M., Svensson, L.A., and Liljas, A., *Metal poison inhibition of carbonic anhydrase.* Proteins, 1993. **15**(2): 177-182.

180. Yin, J., Andryski, S.E., Beuscher, A.E.t., Stevens, R.C., and Schultz, P.G., *Structural evidence for substrate strain in antibody catalysis.* Proc Natl Acad Sci U S A, 2003. **100**(3): 856-861.

181. DeLano, W.L., Ultsch, M.H., de Vos, A.M., and Wells, J.A., *Convergent solutions to binding at a protein-protein interface.* Science, 2000. **287**(5456): 1279-1283.

182. Lopez, I.A., Acuna, D., Galbraith, G., Bok, D., Ishiyama, A., Liu, W., and Kurtz, I., *Time course of auditory impairment in mice lacking the electroneutral sodium bicarbonate cotransporter NBC3 (slc4a7).* Brain Res Dev Brain Res, 2005.

183. Ho, Y.T., Purohit, A., Vicker, N., Newman, S.P., Robinson, J.J., Leese, M.P., Ganeshapillai, D., Woo, L.W., Potter, B.V., and Reed, M.J., *Inhibition of carbonic anhydrase II by steroidal and non-steroidal sulphamates.* Biochem Biophys Res Commun, 2003. **305**(4): 909-914.

184. Koch, H.P. and Larsson, H.P., *Small-scale molecular motions accomplish glutamate uptake in human glutamate transporters.* J Neurosci, 2005. **25**(7): 1730-1736.

185. King, N., Williams, H., McGivan, J.D., and Suleiman, M.S., *Characteristics of L-aspartate transport and expression of EAAC-1 in sarcolemmal vesicles and isolated cells from rat heart.* Cardiovasc Res, 2001. **52**(1): 84-94.

186. Kanai, Y. and Hediger, M.A., *Primary structure and functional characterization of a high-affinity glutamate transporter.* Nature, 1992. **360**(6403): 467-471.

187. Nakayama, T., Kawakami, H., Tanaka, K., and Nakamura, S., *Expression of three glutamate transporter subtype mRNAs in human brain regions and peripheral tissues.* Brain Res Mol Brain Res, 1996. **36**(1): 189-192.

188. Levy, L.M., Warr, O., and Attwell, D., *Stoichiometry of the glial glutamate transporter GLT-1 expressed inducibly in a Chinese hamster ovary cell line selected for low endogenous Na^+-dependent glutamate uptake.* J Neurosci, 1998. **18**(23): 9620-9628.

189. Zerangue, N. and Kavanaugh, M.P., *Flux coupling in a neuronal glutamate transporter.* Nature, 1996. **383**(6601): 634-637.

190. Camacho, A. and Massieu, L., *Role of glutamate transporters in the clearance and release of glutamate during ischemia and its relation to neuronal death.* Arch Med Res, 2006. **37**(1): 11-18.

191. Won, S.J., Kim, D.Y., and Gwag, B.J., *Cellular and molecular pathways of ischemic neuronal death.* J Biochem Mol Biol, 2002. **35**(1): 67-86.

192. Raj, D., Langford, M., Krueger, S., Shelton, M., and Welbourne, T., *Regulatory responses to an oral D-glutamate load: formation of D-pyrrolidone*

carboxylic acid in humans. Am J Physiol Endocrinol Metab, 2001. **280**(2): E214-220.

193. Dall'Asta, V., Bussolati, O., Sala, R., Parolari, A., Alamanni, F., Biglioli, P., and Gazzola, G.C., *Amino acids are compatible osmolytes for volume recovery after hypertonic shrinkage in vascular endothelial cells.* Am J Physiol, 1999. **276**(4 Pt 1): C865-872.

194. Ogata, T., *Bicarbonate secretion by rat bile duct brush cells indicated by immunohistochemical localization of CFTR, anion exchanger AE2, Na^+/HCO_3^- cotransporter, carbonic anhydrase II, Na^+/H^+ exchangers NHE1 and NHE3, H^+/K^+-ATPase, and Na^+/K^+-ATPase.* Med Mol Morphol, 2006. **39**(1): 44-48.

195. Alvarez, B.V., Xia, Y., Soliman, D., Light, P., Karmazyn, M., and Casey, J.R., *A Carbonic Anhydrase Inhibitor Prevents and Reverts Cardiomyocyte Hypertrophy.* J. Physiol., 2006(Submitted for Publication).

196. Khandoudi, N., Laville, M.P., and Bril, A., *Protective effect of the sodium/hydrogen exchange inhibitors during global low-flow ischemia.* Journal of Cardiovascular Pharmacology, 1996. **28**(4): 540-546.

197. Kahle, K.T., Gimenez, I., Hassan, H., Wilson, F.H., Wong, R.D., Forbush, B., Aronson, P.S., and Lifton, R.P., *WNK4 regulates apical and basolateral Cl- flux in extrarenal epithelia.* Proc Natl Acad Sci U S A, 2004. **101**(7): 2064-2069.

198. Xu, J., Henriksnas, J., Barone, S., Witte, D., Shull, G.E., Forte, J.G., Holm, L., and Soleimani, M., *SLC26A9 is expressed in gastric surface epithelial cells, mediates Cl^-/HCO_3^- exchange, and is inhibited by NH_4^+.* Am J Physiol Cell Physiol, 2005. **289**(2): C493-505.

199. Wheat, V.J., Shumaker, H., Burnham, C., Shull, G.E., Yankaskas, J.R., and Soleimani, M., *CFTR induces the expression of DRA along with Cl^-/HCO_3^- exchange activity in tracheal epithelial cells.* Am J Physiol Cell Physiol, 2000. **279**(1): C62-C71.